MECHANISMS UNDERLYING MUSCLE RECRUITMENT IN RESPONSE TO POSTURAL PERTURBATIONS

A Dissertation
Presented to
The Academic Faculty

by

Claire Honeycutt

In Partial Fulfillment
of the Requirements for the Degree
Doctor of Philosophy in the
School of Biomedical Engineering

Georgia Institute of Technology/ Emory University
May 2009

MECHANISMS UNDERLYING MUSCLE RECRUITMENT IN RESPONSE TO POSTURAL PERTURBATIONS

Approved by:

Dr. T. Richard, Nichols, Advisor
School of Applied Physiology
Georgia Institute of Technology

Dr. Shawn Hochman
Department of Physiology
Emory University

Dr. Thomas Burkholder
School of Applied Physiology
Georgia Institute of Technology

Dr. Lena Ting
Department of Biomedical Engineering
Georgia Institute of Technology

Dr. Timothy Cope
Department of Neuroscience,
Cell Biology, and Physiology
Wright State University

Date approved: [Month, dd, yyyy]

It can ~~not~~ be done
-Southern Railway System
(Brought to my attention by William Fletcher)

To the animals that gave their lives to improve the lives of others

ACKNOWLEDGEMENTS

My journey to here would not have been possible with out the support of many.

First and foremost, I wish to thank my advisor, Richard Nichols, who shaped my entire graduate school experience. Richard supported me through the tough times and quietly taught me how to stand on my own two feet. Moreover, he is not only a scientist that I admire but a caring, compassionate, and patient person whose skills in life I aspire to achieve.

Thanks to my committee members who have given of their time and energy to help me become a better scientist. Timothy Cope shut down his lab on two separate occasions to allow data collection that was critical to my thesis. Moreover, Tim's passionate enthusiasm for science and his support of young scientists inspired me throughout my journey. Shawn Hochman supported me on a side venture into histology and without hesitation offered of his time, lab supplies, and personnel. His straightforward and direct communication showed me the standards and where I needed to be to achieve success. As a primary figure in the posture community, Lena Ting offered her expertise and time to help me shape my own hypotheses, even when they did not agree with her own. She seems tireless in pushing me to formulate my ideas and teach me the skills a young scientist needs for success. Thomas Burkholder used his critical eye to evaluate my work and his unique perspective always advanced and improved my analysis techniques.

Thanks to the Nichols lab current and past, many of whom are the best friends I've ever had. Without these people both my scientific and personal life would have been very empty. They got up early, worked through lunch, and stayed up late helping with experiments. They taught me science, surgery, and how to survive graduate school. So to Victoria Stahl, Jinger Gottschall, Clo Huyghues-Despointes, Kyla Ross, Beven Livingston, Chris Tuthill, Andrea Burgess, and Thom Abelew, thank you. Also, many thanks to Ramaldo Martin and Katie Murinas who performed much of the preliminary work that I continued in my thesis. Finally, much appreciation to Bill Goolsby who worked tirelessly on the posture equipment to ensure that experiments were a success.

I have been immensely blessed with an incredible family who has supported and challenged me through every aspect of my life. To Mom, Dad, Mimi, Willie, Granddad, Grandmother, Laurie, Gerry, Graham, Heather, Carly, and Peyton, I would not be who I am and where I am today without your love, patience, and support. You challenge me every day to be better and stronger than I am.

To all my amazing friends who have supported me through these years and many of which have already been mentioned, much love and thanks.

Finally, I have been extremely lucky to be part of three different departments during my time at Georgia Tech and Emory. So to the Biomedical Engineering department (Georgia Tech), Physiology department (Emory), and Applied Physiology department faculty and staff many, many thanks.

TABLE OF CONTENTS

LIST OF TABLES

LIST OF FIGURES

SUMMARY

The neural and sensory mechanisms underlying appropriate muscle recruitment in response to balance challenges remains elusive. We asked whether the decerebrate cat preparation might be employed for further investigation of postural mechanisms. First, we evaluated the muscular activation patterns and three-dimensional whole limb forces generated by a modified premammillary decerebrated cat. We hypothesized that directionally appropriate muscle activation does not require the cerebral cortices. Furthermore, we hypothesized that the muscle responses would generate functionally appropriate and constrained force responses similar to those reported in the intact animal. Data confirmed both of our hypotheses and suggested important roles for the brainstem and spinal cord in mediating directionally appropriate muscular activation.

Second, we investigated how individual muscle activation is translated to functional ground reaction forces. We hypothesized that muscles are selectively activated based upon their potential counteractive endpoint force. Data demonstrated that the endpoint force generated by each muscle through stimulation was directed oppositely to the principal direction of each muscle's EMG tuning curve. Further, muscles that have variable tuning curves were found to have variable endpoint forces in the XY plane. We further hypothesized that the biomechanical constraints of individual muscle actions generate the constrained ground reaction forces created in response to support surface perturbations. We found that there was a lack of muscles with strong medial-lateral actions in the XY plane. This was further exaggerated at long stance conditions, which

corresponds to the increased force constraint present in the intact animal under the same conditions.

Third, we investigated how loss of cutaneous feedback from the footpads affects the muscle recruitment in response to support surface perturbations. We utilized our decerebrate cat model as it allows 1) isolation of the proprioceptive system (cutaneous and muscle receptor) and 2) observation of the cutaneous loss before significant compensation by the animal. We hypothesized that muscle spindles drive directionally sensitive muscle activation during postural disturbances. Therefore, we expected that loss of cutaneous feedback from the foot soles would not alter the directional properties of muscle activation. While background activity was significantly diminished, the directionally sensitive muscular activation remained intact. Due to fixation of the head, the decerebrate cat additionally does not have access to vestibular or visual inputs. Therefore, this result strongly implicates muscle receptors as the primary source of directional feedback.

Finally to confirm that muscle receptors, specifically muscle spindles, are capable of generating feedback to drive the directionally tuning, we investigated the response properties of muscle spindles to horizontal support surface perturbations in the anesthetized cat. As previously stated, we hypothesized that muscle spindles provide the feedback necessary for properly directed muscular responses. We further hypothesized that muscle spindles can relay feedback about the perturbation parameters such as velocity and the initial stance condtion. Results confirmed that muscle spindle generate

activation patterns remarkably similar to muscular activation patterns generated in the intact cat. This information, along the knowledge that cutaneous feedback does not substantially eliminate directional tuning, strongly suggests that muscle spindles contribute the critical directional feedback to drive muscular activation in response to support surface perturbations.

CHAPTER 1

INTRODUCTION

Impaired balance dramatically affects the quality of life of millions of people across the globe on a daily basis. Most neurological diseases and injuries result in balance insufficiencies that impair a patient's ability to perform the most basic tasks like standing and walking. Furthermore, falling is the leading cause of death in the elderly (CDC 2006). Before we can develop appropriate rehabilitation therapies to restore balance for these populations, we must have a clear understanding of the control mechanisms underlying normal postural control.

Traditionally, support surface perturbations have been utilized to evaluate the postural strategy employed by terrestrial animals maintain stability. Macpherson (Macpherson 1988a; b) used radial, horizontal movements of the support surface to evoke coordinated postural responses from cats trained to stand quietly on a platform. Under preferred stance conditions, each limb responded to the radial perturbations with directed forces that cluster into two diagonal XY populations extending toward and away from the center of mass of the animal. Muscle activation patterns were quantified through creation of tuning curves which compared increases and decreases in muscle activity to background and graphed the difference against perturbation direction. Muscles were found to have a principal direction of activation, but were also found to have a substantial breadth or range of directions over which the muscle was active. In general, tuning curves were found to be broadly tuned occupying 25% or more of the perturbation space and often overlapped the activation space of other muscles. Subsequent analysis of these tuning

curves demonstrated that muscles are recruited in groups or synergies (Ting and Macpherson 2005).

This postural strategy is present in naïve subjects and is independent of prior experience (Macpherson 1994b) suggesting that it is a robust and innate motor task. This strategy is also observed during alternative postural perturbations like rotations (Ting and Macpherson 2004) and is observed in humans (Henry et al. 2001). Alterations in parameters such as velocity and amplitude of perturbation result in changes in timing and amplitude of the responses, but the spatial properties of the strategy remain intact (Diener et al. 1988). While it has been suggested that these postural responses can be modeled accurately using kinematic feedback from the movements of the center of mass (Lockhart and Ting 2007), the manner in which these task-level variables are represented by the nervous system or derived from the sensory signals available remains poorly understood.

The mechanisms mediating this strategy have received considerable attention in recent decades (Allum et al. 1998; Bloem et al. 2000; Chanaud and Macpherson 1991; Deliagina et al. 2006; Diener et al. 1988; Fung and Macpherson 1995; Henry et al. 1998; Jacobs and Horak 2007; Lockhart and Ting 2007; Macpherson 1988a; b; Maurer et al. 2006; Mergner et al. 2003; Nashner 1976; Stapley et al. 2002; Torres-Oviedo et al. 2006). However, many gaps exist in our knowledge pertaining to 1) what neural structures are required to generate this strategy, 2) how biomechanics influences postural control, and 3) what sensory sources are necessary to achieve appropriate muscular activation.

Neural structures

While it is certain that each of the three major divisions of the nervous system (cortex, brainstem, and spinal cord) contribute significantly to postural control, it remains unclear what roles each of these structures play. The spinal cord is known to mediate diverse motor tasks including wiping reflexes (Poppele and Bosco 2003; Stein and Daniels-McQueen 2004) and locomotion (Edgerton et al. 2001). The wiping reflex is a goal-directed task that requires integration of limb position and desired endpoint information (Poppele et al. 2003). The isolated spinal circuits of the frog and turtle are capable of control and programming of many unique wiping actions, including choosing to use the contralateral limb when the ipsilateral limb is inappropriate (Stein 2008; Stein and Daniels-McQueen 2004). These spinalized animals can achieve the appropriate endpoint destination from unique limb configurations as well (Fukson et al. 1980), indicating that the isolated cord has access to feedback about limb kinematics and muscle actions. In addition to wiping actions, the isolated cord can mediate locomotion patterns (Edgerton et al. 2001) even demonstrating control by adjusting these patterns when external stimuli (such as loads during swing) are present (Timoszyk et al. 2002). Additionally, we know that spinal circuits participate in a variety of postural functions including stiffness regulation of muscle, joints, and limb (Nichols 1989; Nichols and Houk 1976).

Despite this evidence, the poor postural responses of spinalized animals (Fung and Macpherson 1999; Macpherson and Fung 1999a; Pratt et al. 1994) have been interpreted to indicate that spinal pathways are not adequate for appropriate muscle activation. It should be noted, however, that the spinal lesion interrupts neural communication between

forelimbs and hindlimbs, and may interfere with postural networks that depend on propriospinal pathways. Furthermore, chronic spinal injury in cats is accompanied by widespread clasp-knife inhibition (Bonasera et al. 1994; Nichols et al. 1999), increases in inhibitory neurotransmitters, and re-organization of spinal synapses (Edgerton et al. 2001), and flexor neuromuscular junction degradation (Potluri et al. 2008); all of which likely influence spinal cord functionality. Nonetheless, the spinalized animal has pronounced balance insufficiencies, which suggests that the spinal cord alone cannot mediate postural control.

The brainstem also plausibly contributes to postural control as evidenced by reports demonstrating that lower brainstem regions, specifically the ventral and dorsal tegmental fields (VTF and DTF), can excite or inhibit postural tone respectively (Mori 1987). Authors additionally used horseradish peroxidase to determine which regions were being stimulated through passing fibers. They determined that the most effective VTF stimulation sites also stimulated upper brainstem regions such as the hypothalamus and subthalamic nucleus while the most effective DTF stimulation sites corresponded with the diencephalons and the dorsal posterior and lateral hypothalamus. The upper brainstem's role in postural control appear analogous to its role in locomotion where the subthalamic nucleus controls the expression of locomotion generated by the mesenphalic locomotor region of the lower brainstem (Mori et al. 1989). The close association of the postural tone regions (VTF and DTF) to the expression of locomotion only further indicates that these two systems are likely similarly controlled. These observations imply that the upper brainstem (regions rostral to the superior colliculus) controls the expression

of the lower brainstem (regions caudal to the superior colliculus) regions associated with postural tone. However, significantly more work is required until these proposals can be properly evaluated.

Initially dismissed due to the short latency at which postural responses occur, there is growing evidence that the cortex plays a significant role in postural control. It has been proposed that the cortex participates dynamically in control of complex motor tasks requiring integration of information about global parameters, limb position, and environmental conditions (Dietz et al. 1984). This notion is corroborated by pyramidal tract (primary descending cortical neurons) recordings demonstrating that these cells are excited by contralateral limb movements (Beloozerova et al. 2005; Beloozerova et al. 2003a). Additionally, reports showing that cortical suppression can inhibit the longer latency muscle stretch responses to simulated postural disturbances (Taube et al. 2006) indicate that the cortex plays a role in scaling muscle responses at a longer latency. While these longer latency responses are likely not under exclusive control of the cortex (Schieppati and Nardone 1995), it is reasonable to assume that the longer latency responses are influenced by the cortex, in particular the somatosensory cortex (Miller and Brooks 1981). Additionally, the cortex and other supra-spinal structures plausibly are responsible for scaling and in some cases elimination of directionally inappropriate responses (Nashner 1976). Although cortical circuits influence most motor behaviors, the extent to which these circuits are required for the expression of the postural response remains unknown (Jacobs and Horak 2007). Therefore, the location of the required

neural integration and the degree to which this integration is distributed among areas in the central nervous system remain elusive.

Biomechanics

Having a clear understanding of the biomechanical environment that animals must command to maintain balance is critical to comprehending the mechanisms that underlie that control. To understand why a muscle is activated in response to a perturbation, we must know what role that muscle plays in stabilizing the body. There is evidence that muscles are activated based solely upon their mechanical advantage (Buchanan et al. 1986; Kutch et al. 2008). However, mathematical analysis of muscular activation patterns has shown that muscles appear to be activated in groups or synergies (Ting and Macpherson 2005; Torres-Oviedo et al. 2006). It is therefore possible that muscles might not be exclusively activated based upon their mechanical advantage.

It has been demonstrated that muscles of the wrist can be activated in what is assumed to be non-mechanically favorable directions (Fagg et al. 2002; Hoffman and Strick 1999). The wrist's architecture is very complex and mechanical actions difficult to ascertain. Furthermore, the wrist does not have the same utility for weight support; therefore, its musculature is likely adapted to a different set of mechanical tasks. Still, one study from the human leg also demonstrated a small deviation from a muscle's preferred direction and its mechanical action (Nozaki et al. 2005). This implies that muscles are capable of recruitment outside their mechanical advantage. This has significant implications for how the control mechanisms mediating muscular activation.

Our knowledge of the muscular actions of the hindlimbs has been mostly gleaned through morphological analysis and subsequent modeling (Burkholder and Nichols 2004; McKay et al. 2007; McKay and Ting 2008). However, model data appears to deviate from experimental data generated from the intact limb of a decerebrate cat (Burkholder and Nichols 2004; Murinas 2003). Specifically, non-sagittal forces are largely not present in model predictions. Therefore, the mechanical actions attributed to the muscles of the hindlimb remain uncertain.

Sensory sources

Sensory signals from the vestibular system, skin and muscles (Allum et al. 1998; Beloozerova et al. 2003b; Everaert et al. 2005; Macpherson and Inglis 1993; Stapley et al. 2002; Ting and Macpherson 2004) have been implicated in mediating postural responses. The relative contributions of these systems on muscle activation patterns have yet to be determined, but some progress has been made concerning the role of vestibular feedback. Vestibular loss leads to hypermetria, which destabilizes the animal (Macpherson and Inglis 1993); however, the spatial tuning properties of the responses (direction and breadth) are little affected by the lesion, suggesting that feedback from either skin or muscle (or both) contributes in a major way to directional tuning of these responses.

Some have suggested that cutaneous feedback alone could be responsible for directional muscle activation (Bloem et al. 2000; Ting and Macpherson 2004). Evidence for an important role of cutaneous feedback comes from studies showing that cutaneous inputs

can affect postural stability during unperturbed stance (Meyer et al. 2004; Roll et al. 2002). There are four types of cutaneous receptors: Merkel, Ruffini, Meissners, and Pacinian (Kandel et al. 2000). These receptors vary dramatically in their receptive field size, adaptation time, and sensitivity to pressure and vibration. The diversity in their properties indicates that these four types of receptors can encode copious amounts of feedback about the external environment. Most specifically, they have been proposed to generate feedback about the three-dimensional direction of a perturbation based upon the ratio of shear to loading forces (Ting and Macpherson 2004).

Finally, it has been proposed that feedback from muscle receptors could generate the key directional information driving appropriate muscle recruitment (Nichols et al. 1999). Two types of muscle receptors, muscle spindles and golgi tendon organs, provide length and force feedback respectively. Muscle spindle response properties have been well documented in isolated muscle (Hasan and Houk 1975; Houk et al. 1981a). Muscle spindle firing rates encode muscle length and give feedback about the rate of change of this length during perturbation. This feedback is relayed to a variety of destinations including monosynaptic stretch reflexes and disynapitc inhibition of antagonistic muscles. Furthermore, muscle spindles are known to send excitatory feedback to synergistic muscles. Force feedback mediated through the golgi tendon organs remains more elusive. However, it is certain that feedback about the current force being generated by a muscle is critical to the performance of most motor tasks. Force feedback additionally has more distributive pathways reaching across joints (Bonasera and Nichols 1996; 1994; Ross

2006; Wilmink and Nichols 2003). It is highly probable that muscle receptors are generating critical feedback to control of posture.

An obstacle in parsing the contributions of feedback from skin and muscles in intact animals is the difficulty in isolating these sensory systems. Furthermore, animals can compensate to some extent for the loss of one system by shifting the feedback weights toward the residual system, obscuring the normal balance among the various sources of sensory information (Maurer et al. 2006). In addition while the cutaneous system can be somewhat compromised using lidocaine (Meyer et al. 2004) or hypothermic anesthesia (Stal et al. 2003), there is not an appropriate and reversible intervention that exclusively affects muscle receptors of the intact system in the same way. Furthermore even if isolation of these systems was possible, we still would not have a clear understanding of how these inputs are represented in the nervous system. Single-unit studies of individual receptors in intact animals are difficult, although progress has been made using this approach. Initial studies using multi-electrode arrays indicate that appropriate spatial tuning can be observed in both cutaneous and muscle afferents (Stein et al. 2004a; Stein et al. 2004b). However, further study is needed to ascertain the role of each system.

Objectives and hypotheses

For the above reasons, we asked whether the decerebrate cat preparation might be employed for further investigation of postural mechanisms. The decerebrate cat has been utilized extensively to study many mechanisms of motor control, including motor unit recruitment (Cope and Clark 1991; Cope et al. 1997), spinal pathway organization (Houk

1979; Nichols 1989; 1999; Nichols et al. 1999; Sherrington 1898), pattern generating circuits (McCrea et al. 1995; Mori 1987; Pearson 1995; Shik et al. 1968), and integration of feedback from the vestibular system and from neck proprioceptors (Gottschall and Nichols 2007; Wilson et al. 1984; Wilson et al. 1986). In the first two chapters, we will discuss the elements of the postural response that can be generated without the presence of the cerebral cortices. In the following three chapters, we will discuss the control mechanisms governing these responses.

In chapters 2 and 3, we describe the electromyographic responses and ground reaction forces generated by the decerebrate cat when subjected to support surface perturbations. We *hypothesize* that directionally appropriate muscle activation does not require the cerebral cortices. Furthermore, we *hypothesize* that the muscle responses will generate functionally appropriate force responses that will be constrained similarly to those reported in the intact animal. Therefore, our *objectives* were 1) to establish the decerebrate cat as an appropriate model for further research into the sensory mechanisms underlying postural control and 2) to observe what elements of the postural response can be generated in the absence of the cerebral cortices.

In chapter 4, we investigate how individual muscle activation is translated to functional endpoint forces and the variability associated with that transformation. We *hypothesize* that muscles are selectively activated based upon their potential counteractive endpoint force. Our *objective* is to observe and quantify the individual muscle endpoint forces and compare those forces to the muscle activation patterns generated in the intact and

decerebrate animals in response to support surface perturbations. We further *hypothesize* that the biomechanical constraints of individual muscle actions generate the constrained ground reaction forces created in response to support surface perturbations. As muscles are active over all 360 degrees, we suspect that few muscles will have strong non-sagittal actions. Our *objective* is to quantify the alterations of individual muscle endpoint forces at different stance conditions and compare those to the alterations in force constraint strategy when intact and decerebrate cats are subjected to horizontal support surface perturbations.

In chapter 5, we investigate how loss of cutaneous feedback from the footpads affects the muscle recruitment in response to support surface perturbations. We utilized our decerebrate cat model as it allows 1) isolation of the proprioceptive (cutaneous and muscle receptor) system and 2) observation of the cutaneous loss before significant compensation by the animal. We *hypothesize* that muscle spindles drive the directionally sensitive muscle activation during postural disturbances. Therefore, we expect that loss of cutaneous feedback from the foot soles will not alter the directional properties of muscle activation. Our *objective* was to observe the influences of cutaneous dennervation on the principal direction and breadth of muscle responses.

Finally in chapter 6, we investigate the response properties of muscle spindles to examine what elements of the muscular response to support surface perturbations they can encode. As previously stated, we *hypothesize* that muscle spindles provide the feedback necessary for properly directed muscular responses. We further *hypothesize* that muscle spindle can

also relay feedback about the perturbation parameters such as velocity and the initial inter-limb spacing. Our *objectives* were 1) to quantify the muscle spindle responses to support surface perturbations from different inter-limb spacings and varying velocity conditions and 2) to compare the muscle spindle response of the intact limb to those previously reported in isolated muscle.

CHAPTER 2

ELECTROMYOGRAPHIC RESPONSES FROM THE HINDLIMB MUSCLES OF THE DECEREBRATE CAT TO HORIZONTAL SUPPORT SURFACE PERTURBATIONS

2.1 Introduction

The mechanisms underlying the ability of terrestrial animals to remain upright and maintain stability in the face of mechanical perturbations have received considerable attention in recent decades (Allum et al. 1998; Bloem et al. 2000; Chanaud and Macpherson 1991; Deliagina et al. 2006; Diener et al. 1988; Fung and Macpherson 1995; Henry et al. 1998; Jacobs and Horak 2007; Lockhart and Ting 2007; Macpherson 1988a; b; Maurer et al. 2006; Mergner et al. 2003; Nashner 1976; Stapley et al. 2002; Torres-Oviedo et al. 2006). In a classic series of studies, Macpherson (Macpherson 1988a; b) used radial, horizontal movements of a support surface to evoke coordinated postural responses from cats trained to stand quietly on a platform. Muscle activation patterns were quantified through creation of tuning curves which compared increases and decreases in muscle activity to background and graphed the difference against perturbation direction. Muscles were found to have a principal direction of activation, but were also found to have a substantial breadth or range of directions over which the muscle was active. In general, tuning curves were found to be broadly tuned occupying 25% or more of the perturbation space and often overlapped the activation space of other muscles. Subsequent analysis of these tuning curves demonstrated that muscles are recruited in groups or synergies (Ting and Macpherson 2005). However, no clear consensus has been reached detailing the important sensory mechanisms and neural structures necessary for the production of appropriate postural corrections.

A significant debate exists as to whether the neural networks in the brainstem and spinal cord can mediate the observed directional tuning, or whether circuits in cortical areas are required as well. It has been argued that isolated spinal circuits with intact musculoskeletal systems are responsible for quite sophisticated motor tasks (Edgerton et al. 2001; Stein and Daniels-McQueen 2004; Timoszyk et al. 2002) and sensorimotor transformations (Bosco and Poppele 2001; Poppele and Bosco 2003). In contrast, the poor postural responses of spinalized cats (Fung and Macpherson 1999; Macpherson and Fung 1999a; Pratt et al. 1994) have been interpreted to indicate that spinal pathways are not adequate for appropriate muscle activation. It should be noted, however, that the spinal lesion interrupts neural communication between forelimbs and hindlimbs, and may interfere with postural networks that depend on propriospinal pathways. Furthermore, chronic spinal injury in cats is accompanied by widespread clasp-knife inhibition (Bonasera et al. 1994; Nichols et al. 1999), increases in inhibitory neurotransmitters, and re-organization of spinal synapses (Edgerton et al. 2001); all of which likely influence spinal cord functionality. More recent studies suggest that spinal circuits can support postural control as long as supraspinal influences remain intact (Deliagina et al. 2008; Deliagina et al. 2006; Lyalka et al. 2005; Musienko et al. 2008). Although cortical circuits influence most motor behaviors, the extent to which these circuits are required for the expression of the postural response remains unknown (Jacobs and Horak 2007). Therefore, the location of the required neural integration and the degree to which this integration is distributed among areas in the central nervous system remain elusive.

For the above reasons, we asked whether the decerebrate cat preparation might be employed for further investigation of both the sensory and neural mechanisms employed during postural control. The decerebrate cat has been utilized extensively to study many mechanisms of motor control, including motor unit recruitment (Cope and Clark 1991; Cope et al. 1997), spinal pathway organization (Houk 1979; Nichols 1989; 1999; Nichols et al. 1999; Sherrington 1898), pattern generating circuits (McCrea et al. 1995; Mori 1987; Pearson 1995; Shik et al. 1968), and integration of feedback from the vestibular system and from neck proprioceptors (Gottschall and Nichols 2007; Wilson et al. 1984; Wilson et al. 1986). Our objectives were 1) to establish the decerebrate cat as an appropriate model for further research into the sensory mechanisms of postural control and 2) to observe what elements of the postural response can be generated in the absence of the cerebral cortices. We hypothesize that directionally appropriate muscle activation does not require the cerebral cortices.

We have developed a reduced preparation that exhibits directionally appropriate muscle responses in the absence of the cerebral cortices. This preparation, consisting of a modification of the premammillary decerebration, retains responsiveness to postural perturbations but does not exhibit spontaneous stepping. A description of the activation patterns of selected hindlimb muscles in response to horizontal platform perturbations is included in this paper. The data from this preparation are also compared to those obtained from intercollicular decerebrate cats, and the implications of this comparison for the role of supraspinal circuits in the expression of the force constraint strategy are

discussed. Preliminary results have been published in abstract form (Honeycutt and Nichols 2005).

2.2 Methods

Ten cats, used in accordance with the issued standards of the National Institutes of Health and the Emory Institutional Animal Care and Use Committee, will be described in the following report. Animals will be referred to by the date of the experiment (6/8, 9/7, 9/11, 9/13, 9/29, 10/8, 11/7, 12/18, 1/22, 2/23). Under isoflurane anesthesia, a trachometry was performed to monitor anesthesia levels and an IV was inserted in the external jugular vein for hydration and drug delivery. Bipolar electrodes, constructed from Teflon coated braided wire, were inserted into the belly of the medial gastrocnemius (MG), lateral gastrocnemius (LG), vastus lateralis (VL), vastus medialis (VM), semitendinosis (ST), semimebranosis (SM), gracilis (Grac), iliopsoas (Ilio), internal oblique (IO), anterior sartorius (aSart), anterior biceps femoris (aBF), posterior biceps femoris (pBF), and gluteus medius (Glut) muscles in the right hindlimb.

We used two decerebration techniques: intercollicular and a modified premammillary. The more traditional intercollicular decerebration consisted of a vertical transection through the superior colliculus. All brain material rostral to the transection was removed. The intercollicular decerebration technique did not produce consistent postural responses (see Results) so we utilized a modification of the premammillary decerebration, a preparation usually used to obtain spontaneous stepping. Following the premammillary transection and removal of all brain tissue rostral to the cut, a second, vertical transection

was made at the level of the mammillary bodies to prevent spontaneous locomotion. The resulting preparation was considerably more responsive to mechanical perturbations than animals prepared with intercollicular transections.

2.2.1 Experimental protocol

After the initial surgery, the animal was positioned using a stereotaxic frame to support the head and a sling to support the body. Additionally, a clamp was fixed at the base of the tail to support the hindquarters of the animal. The clamp did not interfere with hip rotation and allowed for a more natural hip angle and movement than fixation of the hip or spinal clamps. The sling was detached after isoflurane was removed and weight bearing was established. Anatomical measurements, collected on intact animals during standing, were used to position the hip height, head height, and paw spacing (both transverse and sagittal planes). The feet were placed over four ATI force transducers located on a support platform. The natural turnout of the foot was used for each animal. Electrical signals from the bipolar electrodes were passed through a preamplifier, with a gain of 200 (overall gain of 1000) and bandpass filter from 10Hz - 1150Hz. Electromyographic (EMG) data from the electrodes and three dimensional force data from the transducers were collected using a LabView program designed specifically for this project.

Once the animal was completely removed from anesthesia, the support surface was translated in 16 different, horizontal directions using two motors: rotational and linear. The rotational motor positioned the linear motor for the perturbation. This technique

ensured a linear perturbation. Support surface translations were delivered in random order. In all but one case, the support surface was perturbed 4cm over 400ms with an acceleration of .5 (m/s^2). In one animal (6/8), the platform was moved 8cm over 400ms. The perturbation parameters were chosen based upon previous studies in intact cats for comparison purposes. Unique to the decerebrate cat, the animal's head and tail were in a fixed position. Thus the limbs were perturbed, held at the extended position for 1000ms and then returned 4cm over 400ms to the initial position. In one animal (10/8), the hold position was only 500ms.

2.2.2 Data analysis and quantification

EMG data were notch filtered for 60Hz noise, demeaned, high passed at 30Hz (to remove movement artifacts), and rectified. EMG data were additionally averaged across three trials for figures; however statistical analysis was completed one 1 trial of 16 directions individually (see proceeded paragraph). EMG data were compiled only for trials where muscle responses were present in all 16 directions. Typically this was achieved within 5-10 minutes after removal from anesthesia; however trials were taken for several hours to ensure no deviation in muscle activation. Latencies were estimated by visual inspection. An increase in firing amplitude or firing rate greater than the maximum amplitude or firing rate during the background was considered an active response. The muscle responses were evaluated during several 200ms windows during the perturbation (dynamic phase) and the hold (steady-state phase). The background mean EMG activity, from a 200ms window pre-perturbation, was subtracted from the mean EMG activity of each 200ms window. The resulting responses were graphed against perturbation

direction to create a tuning curve (see Figure 1 and 2 of Results for further description). EMG tuning curves are portrayed in two formats 1) radial and 2) linear. Tuning curves were normalized to maximum activation before quantification. Inhibitory responses were normalized to maximum excitation to maintain individual muscle scale.

In order to quantify the tuning curves, the breadth and principal direction were calculated for each muscle response. The breadth of the response was quantified by calculating the area under the normalized excitatory and inhibitory tuning curves. A large breadth represents a muscle that is active over many perturbation directions. The principal direction represents the maximum direction of activation. To determine the principal direction, muscle responses from each direction were converted to a vector and x and y components were averaged to find the primary vector or principal direction of the response. The principal direction represents the average direction of all directional muscle activity. Statistical comparison of means of principal direction and breadth at different time epochs were completed with a two-tailed T-test of equal variance. F-tests were used to confirm equal variance and lillifore tests used to confirm normalized distributions in samples with more than 4 observations. In the rare case that the populations exhibited non-normalized distributions a Kolmogorov-Smirnov test, which does not assume normalized distribution, was utilized. In the rare case that the F-test indicated an unequal variance, a T-test of unequal variance was performed. In order to be included in statistical analysis, the muscle must have responded in a minimum of three trials for the full set of 16 directions in each animal. Degrees of freedom for statistical significance were adjusted appropriately based upon the number of observations in each

muscle (see Tables for observation numbers). T-tests were preformed at a .95 confidence interval or p-value of .05.

2.3 Results

2.3.1 Summary

In 8 of 9 modified premammillary decerebrate cat preparations tuned muscular responses were evoked in response to support surface perturbations. These responses were demonstrated in a diverse set of muscles, whose tuning curves span all 360 degrees of the perturbation space. The dynamic (0-400ms) response, either excitatory or inhibitory, remained through the steady-state (400-1400ms) time period. Quantification of these later time periods demonstrated no alteration in principal direction or breadth of tuning. Additionally animals transected at the intercollicular level rarely respond to perturbation (3 out of 28 animals); however when responses were present they were tuned similarly to the modified premammillary and intact animal.

2.3.2 Modified premammillary preparation

The muscles of the decerebrate cat responded to horizontal support surface perturbations with varying amounts of excitation or inhibition. Figure 2.1 shows the raw (3 trials averaged) EMG traces for each of the 16 directions of perturbation for the guteus mdius muscle (10/8 experiment). EMG traces are depicted in order of perturbation direction starting with trace 1 at 0 degrees (lateral direction) and proceeding counter-clockwise. Perturbation direction angles are shown graphically in Figure 2.2A. Excitation and inhibition in all muscles occurred at latencies ranging from 20-30ms (Figure 2.1). As can

be seen from traces 3-8 (Figure 2.1), activity generally increased in firing frequency during the ramp. In the case of inhibitory responses (traces 11-16), firing frequently ceased during the ramp. Some traces showed little excitation or inhibition and appear to be transition phases between the two states. Quantification of these changes in muscle activity within tuning curve creation is demonstrated in Figure 2.2.

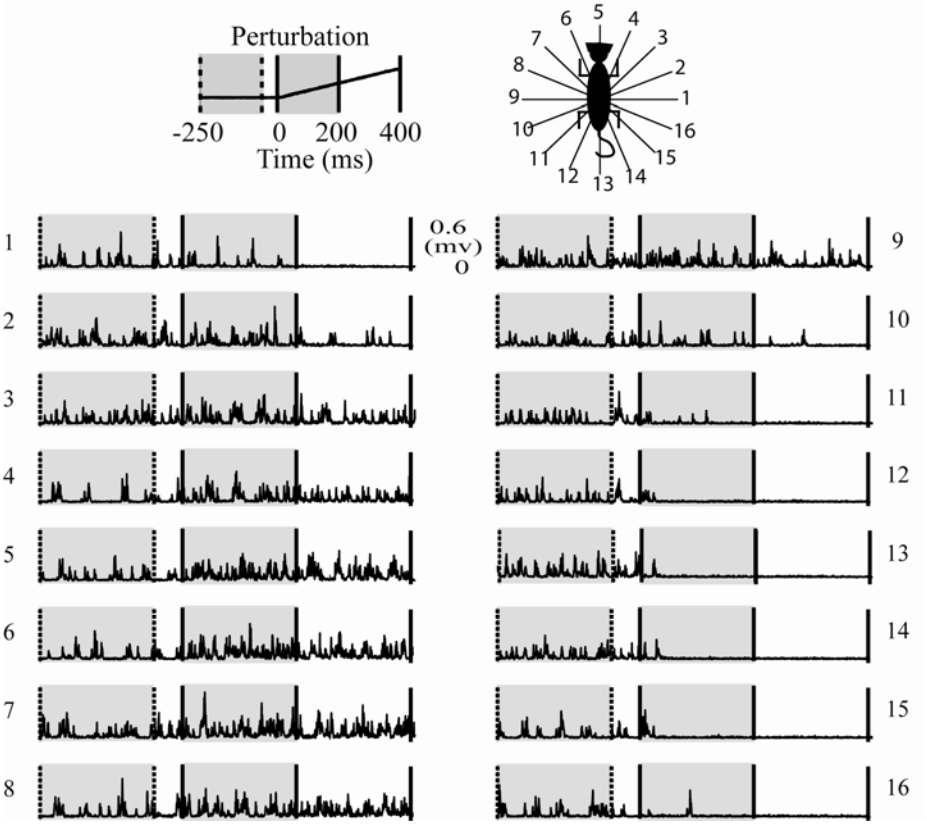

Figure 2.1: Raw EMG traces from a representative Gluteus Medius muscle. Shows the raw (3 trials averaged) EMG traces for each of the 16 directions of perturbation for the Gluteus Medius muscle (10/8 experiment). EMG tuning curves are created from a comparison of the EMG activity during the first 200 ms (solid lines) and 200ms of background activity (dashed lines). EMG traces are depicted in order of perturbation direction starting with trace 1 at 0 degrees (lateral direction) and proceeding counter-clockwise. Perturbation direction angles are shown graphically in Figure 2.2A. Excitation (depicted in traces 4-8) demonstrates an increased activity that holds constant through the ramp while decreased activity (depicted in traces 12-16) typically terminates firing with only occasional spiking occurring. Some traces show little excitation or inhibition (traces 9-11 and 1-3) and appear to be transition phases between the two states.

The muscles of the decerebrate cat produced broad tuning curves usually encompassing up to 25 percent of the perturbation space. The raw traces depicted in Figure 2.1 were quantified by comparing the initial mean response (0-200ms) to mean background activity. The change in mean activity was then graphed against perturbation direction to give a visual representation of what directions cause muscle activation or inhibition. The time period (0-200ms) was chosen for comparison to intact animal data (Macpherson 1988b). The excitatory and inhibitory tuning curves of the gluteus medius muscle (10/8 expt) are depicted in two formats radial (B) and linear (C) in Figure 2.2. All tuning curves (see Figure 2.3 also) appear broad in nature demonstrating a graded and smooth increase to maximum *activation* and then a smooth decrease to a maximum *inhibition*. Therefore, muscles show a steady rise in activation until a maximum is reached rather than being turned on and off in a switch-like behavior. While active or inhibited over multiple directions, each muscle tuning curve had a principal direction where it is most active or most inhibited. We quantified both the principal direction of each tuning curve along with the breadth. The linear tuning curve in Figure 2.2C shows the quantified principal direction of the excitatory tuning curve (arrow) along with the regions used for quantification of the breadth (shaded).

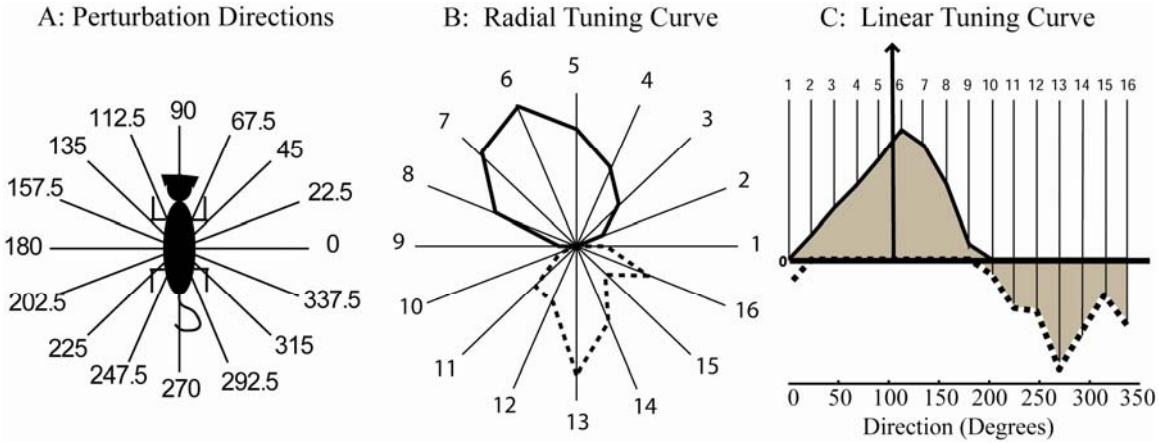

Figure 2.2: Tuning curve quantification. Shows the perturbation direction angle assignments (A) that are used for quantification of perturbation direction. Additionally, the Gluteus Medius muscle (10/8 expt.) tuning curve is shown in radial (B) and the more space efficient linear (C) format. Numbers in B and C correspond to the traces numbers in Figure 1. Solid lines in both curves represent increases in EMG activity as compared to background, while dashed represent decreases in EMG activity. The principal direction of this tuning curve is shown as an arrow at 107 degrees (C). The regions used for breadth quantification are shaded. These shaded areas are integrated after the tuning curves are normalized to maximum activation (see methods).

Tuning curves were obtained from a wide variety of muscles in the decerebrate cat. Figure 2.3 displays the typical radial tuning curves of all surveyed muscles. These tuning curves are arranged based upon the excitatory principal direction starting at 0 degrees (lateral direction) and continuing counter-clockwise. While the tuning curves span all 360 degrees of perturbation space, none of the muscles surveyed had a principal exclusively in the lateral direction (0 degrees). Inhibitory tuning curves are often present and are generally directed oppositely to the excitatory tuning curves (Table 2.1). However on an individual muscle basis, inhibitory principal directions can be as much as 25-30 degrees away from directional opposition (180 degrees difference from excitatory principal direction). More typically however, these inhibitory responses are within 10-15 degrees of 180 degrees. For quantification, inhibitory tuning curves are normalized to maximum activation of each muscle. All muscles (with the exception of pBF) demonstrated inhibitory tuning; however not all muscles demonstrated inhibitory tuning

in all experiments since inhibitory tuning curves are limited by the presence of background activity.

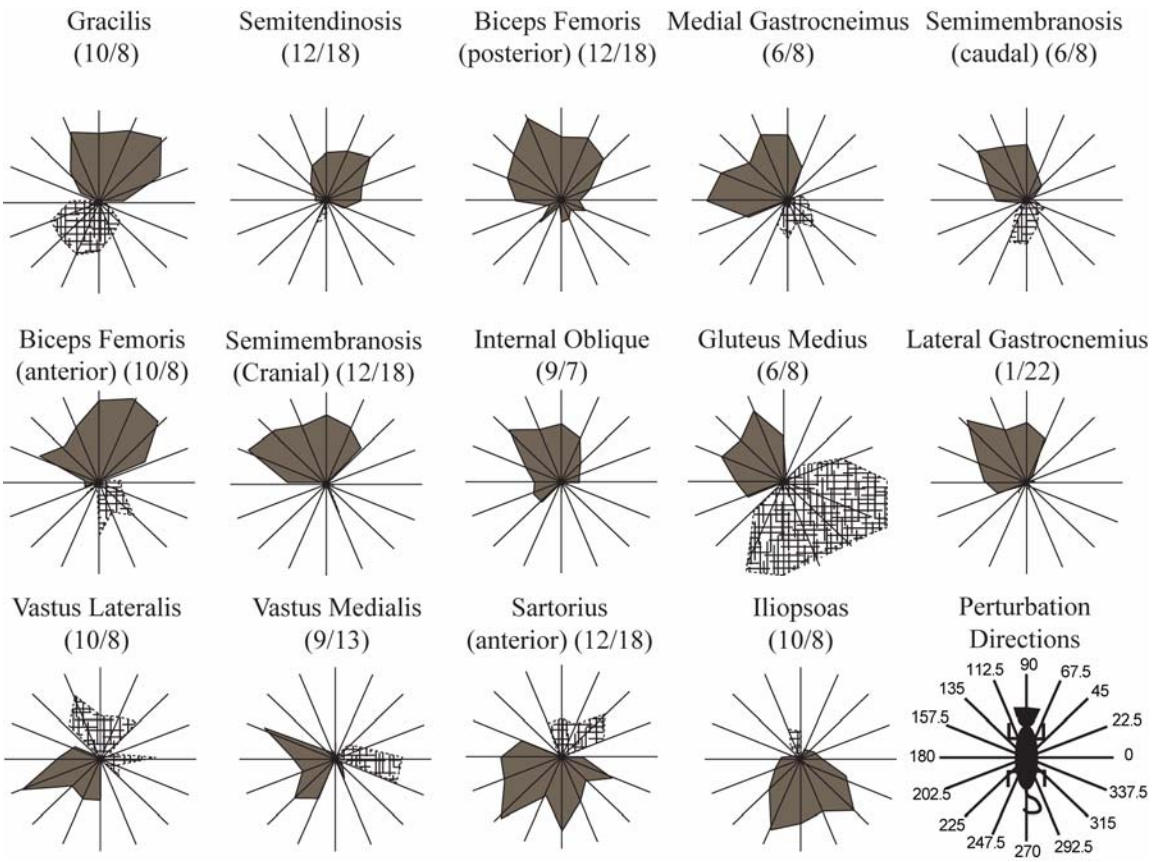

Figure 2.3: The decerebrate generates tuning curves in a wide variety of muscles. Depicts example radial tuning curves for all surveyed muscles. Solid shaded tuning curves represent increased activity from background while hash-marked tuning curves represent decreased activity. Tuning curves are arranged according to principal direction starting at 0 degrees (lateral side of the animal) and continuing counter-clockwise. Note that the muscles of the decerebrate cat produce tuning curves that span all 360 degrees of perturbation space.

Quantification of principal directions revealed that some muscles are highly consistent across experiments while others demonstrate more variability. Table 2.1 displays the quantification of the excitatory and inhibitory tuning curve's principal directions and breadths for all muscles surveyed. Muscles are in order based upon the excitatory tuning curve principal direction to correspond to Figure 2.3. The excitatory principal directions ranged from 69 to 274 degrees which again demonstrates the lack of principal direction in

the lateral (0 degrees) direction. The inhibitory principal direction range was more broad representing 3.5 to 330 degrees; however there is a lack in the medial direction from 107 to 258 degrees. Some muscles, such as Grac, ST, LG, and Illio, appeared to have very consistent excitatory principal directions (small standard deviations) while others, such as MG, VL, and VM, had significant principal direction variance across experiments. Inhibitory principal directions on average demonstrated larger variance across experiments than excitatory principal directions (Glut, VL, and VM being the exceptions). Furthermore, there were similar levels of variance for the excitatory and inhibitory directions in some muscles (MG, SM:caudal) but not in others (Grac, Ilio, LG). \

Table 2.1: Quantification of principal direction and breadth of tuning curves evaluated from 0-200ms in the modified premammillary decerebrate animal.

	Excitatory Response			Inhibitory Response		
	Prin. Dir.	*Breadth*	*N(e)*	*Prin. Dir.*	*Breadth*	*N(i)*
Gracilis	69 (3.4)	7.7 (2.5)	3	246	3.7	1
Semitendinosis	74 (8)	6.5 (1.4)	6	258 (12)	.6 (1.9)	3
posterior Biceps Femoris	91 (11)	8.2 (.8)	5	--	--	--
Medial Gastrocnemius	105 (40)	6.5 (1.8)	5	296 (56)	2.9 (1.9)	3
Semimembranosis (caudal)	106 (15)	5.9 (1.4)	5	276 (25)	1.8 (1.0)	4
anterior Biceps Femoris	112 (19)	6.8 (.8)	4	282 (20)	1.6 (1.0)	2
Semimembranosis (cranial)	114	5.3	1	277	.69	1
Interal Oblique	118	5.9	1	302	.32	1
Gluteus Medius	121 (14)	5.1 (.7)	6	307 (13)	2.5 (3.4)	6
Lateral Gastrocnemius	128 (8.9)	6.7 (1.8)	3	298 (21)	.76 (.3)	2
Vastus Lateralis	195 (33)	3.7 (1.7)	3	37 (24)	2.9 (1.8)	3
Vastus Medialis	216 (23)	5.5 (1.3)	4	3.5 (4.0)	1.4 (1.6)	4
anterior Sartorius	246	6.1	1	64	2.6	1
Iliopsoas	274 (4.6)	4.9 (.5)	3	107 (18)	1.6 (1.5)	3

Depicts the quantification measures for all tuning curves across experiments for 0-200ms. Prin. Dir. = Principal Direction, N(e) = number of excitatory curves, and N(i) = number of inhibitory curves. Standard deviations are depicted in parentheses. Muscles are arranged based upon principal direction starting at 0 degrees (lateral side of the animal) and continuing counter-clockwise. Both excitatory and inhibitory regions were quantified when present.

Quantification of breadth demonstrated that a large excitatory breadth does not correlate to a large inhibitory breadth. The largest average excitatory breadths were present in the

Grac, LG, pBF, and aBF muscles while the smallest were in the VL, Ilio, and Glut muscles (Table 2.1). The largest average inhibitory tuning curve breadths, however, were different from their excitatory counterparts. The largest inhibitory breadths were present in VL and MG and the smallest were in IO, cSM, and ST. Again, inhibitory tuning curves are limited by the presence of background activity. Therefore, it is expected that the largest inhibitory breadths were found in the anti-gravity muscles that are typically spontaneously active in these preparations.

2.3.3 Dynamic vs. steady-state

Excitation and inhibition seen during the perturbation (dynamic: 0-400ms) continued through the platform hold (steady-state: 400-1400ms). Figure 2.4 presents the muscle responses during the ramp and hold of muscles near their principal direction of excitation and inhibition. The first gray box marks the forward perturbation and the second gray box the backward (or return) perturbation. The increase of EMG activity during the dynamic response persists through the steady-state period with little adaptation in firing rate or amplitude. Inhibition generally persists through steady-state. However, some adaptation (or return of firing) was noted in a few cases (aBF, MG, IO in Figure 2.4). The magnitudes of these responses varied between muscles and experiments; however the generalized response was a burst of activity or inhibition during the initial perturbation that was usually held constant through the hold.

Despite subtle variability in response magnitudes, quantification of tuning curves throughout both the dynamic and steady-state phase showed that tuning remained

constant through time epoch. The data in Figure 2.5 illustrated the tuning curves for two time bins during the dynamic (0-200, 200-400ms) and steady state (500-700, 700-900ms) time periods. In order to compare amplitude shifts that might occur through the time epochs, tuning curves were normalized to the maximum activation of the first time epoch. All tuning curves generally demonstrated the same gradual rise in activation until a maximum is reached that was described in Figure 2.3. While there were subtle differences in the tuning with slight increases or decreases in inhibition or breadth alterations, the overall tuning remained the same. Principal directions and breadth during the last time period (700-900ms) were further quantified and reported in Table 2.2.

Quantification for the dynamic (0-200ms, Table 2.1) and steady-state (700-900ms, Table 2.2) responses showed no statistical difference in the principal direction and breadth across the time epochs. F-tests and T-tests were preformed comparing principal direction and breadth (excitatory and inhibitory) for the dynamic (0-200ms) and steady-state (700-900ms) time epochs. Tests were completed on muscles where at least 2 animals generated responses. Lillifore test confirmed all populations, except the SM muscle's breadth, were normally distributed. F-tests confirmed equal variance across all principal directions and breadths except in two cases (Ilio inhibition breadth, Grac excitation breadth). In these cases, a T-test of unequal variance was performed. All tests (T-tests of equal and unequal variance, and the Kolmogorov-Smirnov) confirmed no statistical difference between the principal direction and breadths of all muscles between the 0-200ms and the 700-900ms epochs. T-tests were performed with a 95 percent confidence interval (p-value of .05).

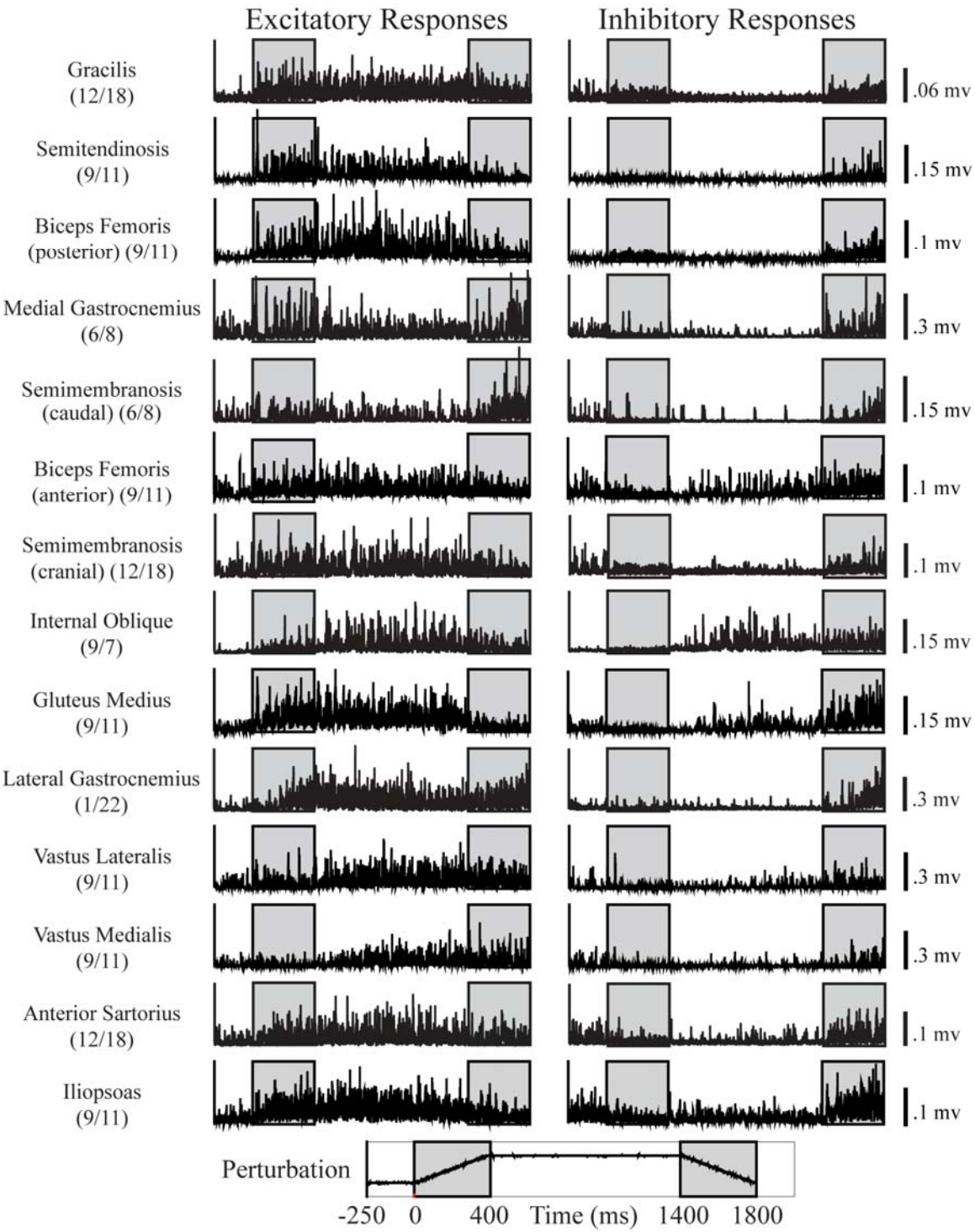

Figure 2.4: Raw traces for all surveyed muscles during the forward, hold, and return perturbation. Displays the full EMG trace for each muscle surveyed near their principal direction of excitation (Left) and inhibition (right). These directions were chosen to illustrate the most significant excitatory and inhibitory responses from each muscle. The first gray box represents the forward translation and the second the backward (or return) perturbation.

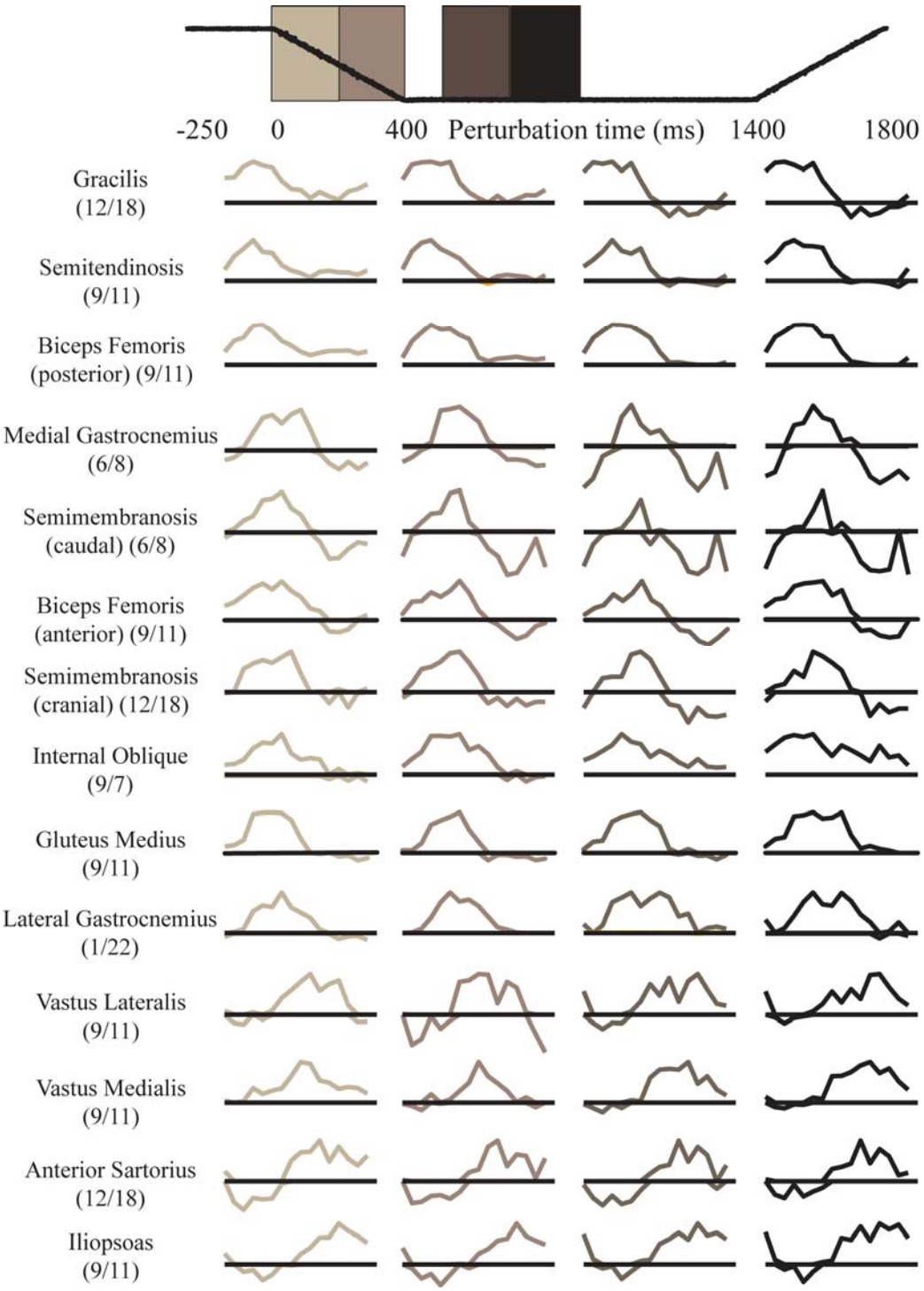

Figure 2.5: Principal direction and breadth are maintained through both dynamic and steady-state time epochs. Demonstrates the linear tuning curves for two time bins during the dynamic (0-200, 200-400ms) and steady state (500-700, 700-900ms) time periods. Linear tuning curves represented here are from the same data set as seen in Figure 4 for comparision to raw EMG traces. In order to compare amplitude shifts that might occur through the time epochs, tuning curves were normalized to the maximum activation of the first time epoch. While there are subtle differences in the tuning with slight increases or decreases in inhibition or breadth alterations, the overall tuning remain the same. Most notable changes are seen in Grac which shows a decreased breadth during the steady-state time period. Quantification of these regions is further reported in Table 2.

Table 2.2: Quantification of principal direction and breadth of tuning curves evaluated from 700-900ms in the modified premammillary decerebrate animal.

	Excitatory response			Inhibitory Response		
	Prin. Dir.	*Breadth*	*N(e)*	*Prin. Dir.*	*Breadth*	*N(i)*
Gracilis	67 (13)	6.4 (.4)	3	250 (4.7)	1.9 (2.2)	3
Semitendinosis	80 (18)	6.1 (2.8)	6	266 (16)	1 (.9)	5
posterior Biceps Femoris	100 (9.7)	6.3 (2.8)	5	269 (22)	.9 (1.0)	4
Medial Gastrocnemius	93 (26)	5.9 (2.6)	5	269 (49)	2.2 (2.6)	5
Semimembranosis (caudal)	102 (22)	5.5 (3.4)	5	269 (38)	2.9 (2.6)	4
anterior Biceps Femoris	119 (30)	5.1 (1.2)	4	284 (22)	3.4 (2.9)	4
Semimembranosis (cranial)	122	4.5	1	295	2.5	1
Interal Oblique	92	10	1	--	--	--
Gluteus Medius	135 (15)	6.8 (2.3)	6	310 (16)	3.3 (3.8)	4
Lateral Gastrocnemius	134 (17)	4.7 (2.8)	3	306 (36)	3.4 (4.1)	3
Vastus Lateralis	237 (20)	4.4 (1.5)	3	48 (19)	6.3 (9.5)	3
Vastus Medialis	232 (10)	5 (1.2)	4	43 (10)	2.2 (3.4)	4
anterior Sartorius	244	4.3	1	71	1.6	1
Iliopsoas	277 (7.5)	6.3 (1.4)	3	109 (24)	.6 (.4)	3

Displays the principal direction (Prin. Dir.), Breadth, and number of excitatory (N(e)) and inhibitory (N(i)) responses for all muscle during the steady-state (700-900ms) response. Standard deviations are in parentheses. Data are presented in the same format for comparison to Table 1 which quantifies the dynamic phase of the response (0-200ms).

2.3.4 Intercollicular preparation

Tuning curves were rarely obtained (3 out of 28 animals) from the muscles in the intercollicular decerebrate cat; however when present these curves were of similar direction and breadth to those of the modified premammillary preparation. Figure 2.6 shows example tuning curves and raw EMG from animals that demonstrated quantifiable EMG responses to horizontal perturbation. With the exception of the Grac muscle, all muscles that gave responses were extensor muscles. Raw EMG was similar in expression to that of the modified premammillary preparation; however the magnitude of the response was decreased from the modified preparation. Tuning curves were similar in expression (both principal direction and breadth) to the modified premammillary preparation. Table 2.3 displays the quantification of all tuning curves that were produced. The principal directions were comparable to those reported in the modified

premammillary animals; although the variability of the LG muscle was slightly increased. The breadths demonstrate more variation than the modified premammillary preparation. This is likely because breadths were difficult to accurately compute due to the decreased magnitude of the responses. Nevertheless, Glut shows an increased average breadth while VM and MG show decreased breadths compared to the modified premammillary preparation. In conclusion with the exception of small differences in breadth, tuning curves obtained from the intercollicular preparation were remarkably similar to those observed in the modified premammillary preparation.

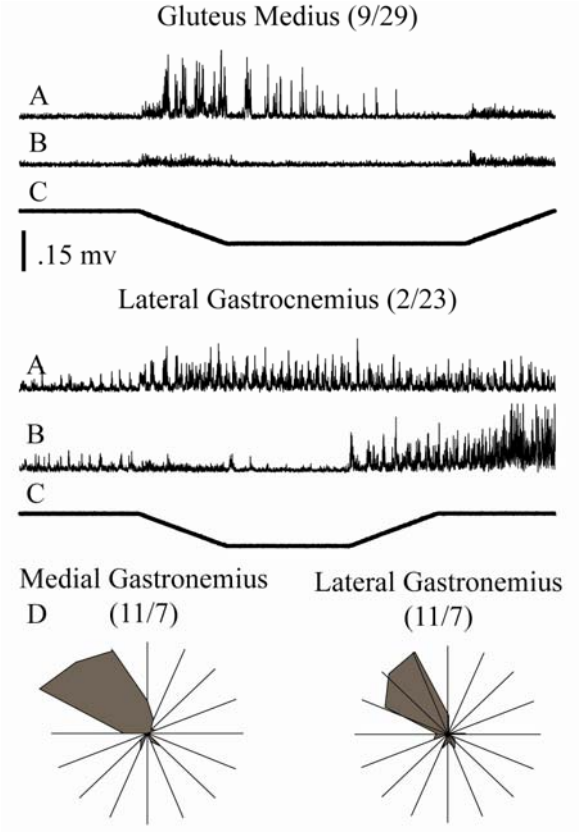

Figure 2.6: Raw EMG and tuning curves from the intercollicular decerebrate cat. Shows example traces of raw (3 averaged traces) EMG (A, B) and radial tuning curves (C) from the intercollicular preparations. The top trace of each raw EMG trace (A) is from the maximal excitatory direction and the bottom traces (B) if of the most inhibitory direction. The perturbation is depicted in the last trace (C). The raw EMG and radial tuning is remarkably similar to that of the modified premammillary preparation.

Further quantification is reported in Table 3. Intercollicular responses were rare with only 3 out of 23 animals giving quantifiable EMG activation in response to translation.

Table 2.3: Quantification of principal direction and breadth of tuning curves evaluated from 0-200ms in the intercollicular decerebrate animal.

	Excitatory response			Inhibitory Response		
	Prin. Dir.	*Breadth*	*N(e)*	*Prin. Dir.*	*Breadth*	*N(i)*
Lateral Gastrocnemius	126 (27)	5.6 (1.8)	3	261	.7	1
Gluteus Medius	116 (38)	7.1 (2.5)	2	--	--	--
Gracilis	62	7.9	1	--	--	--
Vastus Medialis	236	2.1	1	24	1.3	1
Medial Gastrocnemius	136	3.8	1	--	--	--

Displays the quantification for all muscles that gave EMG responses to translation for the intercollicular preparations. The principal directions are comparable to those reported in the modified premammillary animals; although the variability of the LG muscle is slightly increased. The breadths demonstrate more variation from the modified premammillary preparation. Glut shows an increased breadth from the modified preparation while VM and MG show decreased breadths.

2.4 Discussion

2.4.1 Summary

We have obtained active responses from 14 muscles in the right hindlimb of unanesthetized decerebrate cats in response to horizontal platform perturbations. These animals had not undergone training on the task prior to the terminal experiment. These responses could be evoked in a small proportion of those animals prepared with intercollicular decerebration and in nearly all animals subjected to premammillary transection modified by an additional transection near the subthalamic nucleus to eliminate spontaneous locomotion. The electromyographic responses obtained from the right hindlimb of each animal during the radial ramp-and-hold perturbations resembled those obtained by other researchers in intact animals both in direction and breadth. The responses were characterized by excitatory and inhibitory tuning curves that varied little in breadth and direction between the dynamic and static phases of the perturbations. The presence of appropriately tuned responses implicates a strong role for the brainstem and

spinal cord in generating the direction of muscle responses to postural perturbation. The development of this decerebrate cat preparation will allow us the ability to further investigate the role of various sensory system mechanisms underlying responses to postural disturbances.

2.4.1 Comparison to studies of intact animals

The excitatory and inhibitory tuning curves obtained in these studies were comparable in principal direction and breadth to those obtained in intact animals (Macpherson 1988b; Torres-Oviedo et al. 2006). Despite methodological differences including electrode placement and limb choice, the excitatory tuning curves for Grac, aBF, LG and VM (Figure 3) correspond to the tuning curves of the same muscles obtained in intact animals (Macpherson 1988b). Furthermore, the principal direction for pBF is shifted laterally to the principal direction of aBF (Tables 1 and 2), as is the case for the intact animal (Chanaud and Macpherson 1991). The variability (standard deviation) present in direction and breadth (Table 1) is also similar when evaluating the tuning curves reported in the literature (Chanaud and Macpherson 1991; Macpherson 1988b; Torres-Oviedo et al. 2006). In addition, both excitatory and inhibitory responses are present in the decerebrate cat as reported in Macpherson's original work in the intact animal (Macpherson 1988b).

Our primary objective was to determine if the decerebrate animal could be employed for further investigation of postural mechanisms. The decerebrate cat has been utilized extensively to study many mechanisms of motor control, including motor unit recruitment recruitment (Cope and Clark 1991; Cope et al. 1997), spinal pathway

organization (Houk 1979; Nichols 1989; 1999; Nichols et al. 1999; Sherrington 1898), pattern generating circuits (McCrea et al. 1995; Mori 1987; Pearson 1995; Shik et al. 1968), and integration of feedback from the vestibular system and from neck proprioceptors (Gottschall and Nichols 2007; Wilson et al. 1984; Wilson et al. 1986). The observation that the muscles of the decerebrate cat can produce appropriately directed tuning suggests that this preparation is appropriate to further evaluate the sensory mechanisms and neural substrates driving these responses.

2.4.2 Sensory Mechanisms

By choosing to fix the decerebrate animal's head in a stereotaxic frame and performing ramp and hold perturbations, we were able to evaluate the muscle responses without the influence of vestibular and visual feedback. In the experiments of Macpherson (Macpherson 1994a; 1988b), animals stabilized themselves over the moving platform so as to restore the original relationship of the center of mass to the placement of the four paws. Vestibular inputs are utilized under these conditions as demonstrated by balance insufficiencies and improperly scaled muscle responses following vestibular loss (Macpherson and Inglis 1993; Thomson et al. 1991). Macpherson and Inglis, however, also reported that these animals were capable of producing appropriately directed muscular responses which argues that the direction of these responses does not require vestibular input. Knowing that the decerebrate cat can also produce appropriately tuned muscular responses in the absence of visual and vestibular feedback supports this notion and further implies a critical role for cutaneous and muscle receptors in the production of appropriately directed muscle activation.

We favor the hypothesis that muscle receptors, specifically muscle spindles, provide the directional tuning for these muscle responses (Nichols et al. 1999). Supporting evidence comes from muscle spindle recordings in the anesthetized animal which display similarly directed tuned responses to their muscle of origin in response to limb perturbations of the same parameters (Honeycutt et al. 2007). In addition, reinnervated muscles , which have a surgically induced loss of muscle receptor feedback, do not exhibit a quantifiable excitatory response to postural perturbations in the anaesthetized modified premammillary decerebrate cat (Honeycutt et al. 2008). These reinnervated muscles remain functionally intact, capable of force production, and demonstrate appropriate motor unit recruitment (Abelew et al. 2000; Cope and Clark 1993; Haftel et al. 2005). Accordingly, muscle spindles are likely furnishing important directional information to the nervous system regarding postural perturbations. Nevertheless, there is considerable evidence that cutaneous feedback potently contributes to postural control (Kavounoudias et al. 2001; 1998; Maurer et al. 2001; Meyer et al. 2004; Roll et al. 2002; Stal et al. 2003; Stapley et al. 2002; Ting and Macpherson 2004). This new decerebrate preparation is being used in ongoing studies to evaluate the relative contributions of these two sources of sensory feedback. Our findings indicate that directional tuning is unaffected by loss of cutaneous feedback of the foot soles in the decerebrate cat (unpublished results).

Excitatory and inhibitory directional tuning may have differing control mechanisms. We noted that inhibitory tuning curves, while generally directed oppositely to excitatory tuning curves, could be as much as 30 degrees off from complete numerical opposition

(180 degrees). In addition, data show that muscles with highest excitatory principal direction variability did not correlate to muscles with the highest inhibitory tuning curve variability. While this may be a result of the distorting affects of changes in background activity, it could also indicate that mechanisms driving excitatory responses are distinctive from those driving inhibitory responses. We suggest that antagonistic muscles, which have well studied reciprocal inhibition, may contribute significantly to the directionality of inhibitory responses since torque exerted by antagonistic muscles can depart from direct opposition to the agonist (Lawrence 1999).

2.4.3 Central Mechanisms

There is substantial evidence that the cortex (Adkin et al. 2006; Beloozerova et al. 2005; Beloozerova et al. 2003a; Jacobs and Horak 2007; Taube et al. 2006), brainstem (Deliagina et al. 2008; Deliagina et al. 2006; Mori 1987; Mori et al. 1989; Musienko et al. 2008), and spinal cord (Bosco and Poppele 2001; Lyalka et al. 2005; Stein 2008) all contribute to postural control. Classical literature illustrates that the decerebrate cat generates several postural tasks including the righting reflex (Magnus 1926) suggesting a strong role for brainstem and spinal cord circuits. Yet, more recent evidence alludes to a role for the cortex in unpredictable postural disturbances (Adkin et al. 2006; Jacobs and Horak 2007). It is plausible that these structures exist within a hierarchical framework in which each unit is responsible for increasingly complex integration of sensory and environmental information. We therefore propose based upon this report and data from the spinalized animal that the directionally selective muscle tuning comes from the lowest levels of this hierarchy.

Our data demonstrating that robust and directionally appropriate muscle activation is present without the cerebral cortices strongly argues that the spinal cord and brainstem are responsible for the directional information driving appropriate muscular responses to horizontal perturbations. Yet, the knowledge the aBF, aSart, Glut, RF, and VM muscles of the spinalized cat generate appropriately directed muscular responses (Macpherson and Fung 1999b) further implies that the brainstem is not required for directional tuning. While directionally appropriate, responses were not of sufficient strength or duration to generate the necessary force to oppose the perturbation. This is likely the result of the clasp-knife inhibition condition, where even small muscular force production is quickly followed by rapid inhibition (Nichols and Cope 2001), and not due to the insufficiencies of the spinal cord circuitry. We know that spinal cord participates in a variety of postural functions including stiffness regulation of muscle, joints, and limb (Nichols 1989; Nichols and Houk 1976). Furthermore, the spinal cord is known to mediate diverse motor tasks including wiping actions (Poppele and Bosco 2003; Stein and Daniels-McQueen 2004) and locomotion (Edgerton et al. 2001). Based upon these considerations, we hypothesize that the spinal cord contains the circuitry required for directionally appropriate muscle activation.

A role for the upper brainstem in mediating these responses come from our data showing that the muscular responses of the modified premammillary decerebrate cat are considerably more robust and present in a larger set of muscles than either the intercollicular or spinalized animal. When muscular responses were present in either the

modified premammillary or intercollicular animal, they always generated similarly tuned responses to one another and the intact animal. However, 88.9% of animals prepared with the modified premammillary decerebration were able to generate muscular responses compared to only 11.7% of intercollicular decerebrated animals implying an important role for the upper brainstem in controlling the expression of the tuned responses generated by the lower circuitry. This notion is corroborated by reports demonstrating that simultaneous stimulation of upper and lower brainstem regions enhance the lower brainstem effects on postural tone (Mori 1987). It has been clearly demonstrated that lower brainstem regions, specifically the ventral and dorsal tegmental fields (VTF and DTF), can excite or inhibit postural tone respectively (Mori 1987). Mori et al. additionally used horseradish peroxidase to determine which regions, stimulated through their passing axons, enhanced the VTF and DTF effects. They determined that the most effective VTF stimulation sites also stimulated upper brainstem regions such as the hypothalamus and subthalamic nucleus while the most effective DTF stimulation sites corresponded with the diencephalan and the dorsal posterior and lateral hypothalamus. The upper brainstem's role in postural control appear analogous to its role in locomotion where the subthalamic nucleus controls the expression of locomotion generated by the mesephalic locomotor region of the lower brainstem (Mori et al. 1989). The close association of the postural tone regions (VTF and DTF) to the expression of locomotion only further indicates that these two systems are likely similarly controlled. These observations strongly imply that the upper brainstem controls the expression of the lower brainstem regions associated with postural tone.

CHAPTER 3

GROUND REACTION FORCES FROM THE HINDLIMB MUSCLES OF THE DECEREBRATE CAT TO HORIZONTAL SUPPORT SURFACE PERTURBATIONS

3.1 Introduction

Classically radial, horizontal support surface perturbations have been utilized to examine postural control and stability (Henry et al. 1998; Macpherson 1988a; b). Interestingly, cats respond with ground reaction forces that cluster into two diagonal XY (horizontal plane) populations extending toward and away from the center of mass of the subject (Macpherson 1988a). The constrained appearance of the forces, deemed the "force constraint strategy," was in opposition to the expected radial trajectory of forces expanding equally in all directions. Still, this clustering of forces is robust in humans and cats demonstrating its presence in naïve subjects, during support surface rotation, and volitional reaching tasks in humans (Henry et al. 1998; Macpherson 1994b; Torres-Oviedo et al. 2006). However, the strategy does demonstrate alterations in its constraint characteristics with stance condition, width of stance in human and distance between forelimbs and hindlimbs in cat (Henry et al. 2001; Torres-Oviedo et al. 2006). In shorter stance conditions, the force constraint dissipates and a more radial force trajectory is achieved. While at longer stance conditions, both humans and cats demonstrate a more constrained strategy with forces in the rostral/caudal directions achieving larger magnitudes than those in the medial/lateral dimension.

These constrained force trajectories are associated with directionally selective muscle activation patterns (Henry et al. 1998; Macpherson 1988b). Muscular activity during

support surface displacements is quantified using tuning curves, which compare increases or decreases in activity to background activation and graph the resultant against perturbation direction. The tuning curves of both humans and cats demonstrate that muscles have a principal direction of activation and are generally active over about 25 percent of the perturbation space. This selective directional activation is conserved across stance conditions; however the amplitude of the response does appear to vary in some muscles (Henry et al. 2001; Torres-Oviedo et al. 2006). We have previously demonstrated that cats decerebrated using a modified premammillary technique consistently generate similarly tuned muscular responses (Chapter 2). Furthermore, while perturbations rarely elicited a muscular response in the intercollicular decerebrate cat, when responses were present they were also directionally appropriate. This in conjunction with reports that the spinalized animal can also produce appropriately directed muscle activation patterns (Macpherson and Fung 1999b) led us to hypothesize that the spinal cord mediates the directionally specific muscle activation in response to support surface perturbation.

However, while the spinalized animal was able to produce appropriately tuned responses, these responses were not of the proper strength or duration to generate appropriately directed and constrained ground reaction forces (Macpherson and Fung 1999b). Although this is likely partially the result of the chronic spinalization which results in increases in inhibitory neurotransmitters, newly formed synapses (Edgerton et al. 2001), flexor neuromuscular junction degradation (Potluri et al. 2008), and clasp-knife inhibition (Bonasera et al. 1994; Nichols et al. 1999), it also implies that the spinal cord may require

supraspinal structures for either appropriate activation strength or mediation of the resposnes. Therefore, we wished to use the decerebrate model and to ask whether the muscular responses produced in this preparation were of sufficient strength to forcefully oppose the perturbation in a functionally significant fashion. Since we were able to elicit active responses from both the modified premammillary and intercollicular decerebrate preparations, we could additionally evaluate what influence the higher brainstem structures (rostral to the superior colliculus) have on force generation. We hypothesize that the brainstem provides the necessary support to the spinal structures to generate functional relevant force responses and therefore expect that these preparations will generate forces constrained similarly to the intact animal.

Our objectives were to 1) quantify the force responses and constraint characteristics of both the modified premammillary and intercollicular decerebrated cats and 2) further demonstrate the appropriateness of the decerebrate cat as a model to investigate the neural and sensory mechanisms underlying postural control. The force constraint characteristics of both the modified premammillary and intercollicular decerebrate cat will be shown and statistically compared. In addition, the force trajectories from different stance conditions in the modified premammillary animal will be discussed and statistically compared. These results have been previously presented in abstract form (Honeycutt and Nichols 2006).

3.2 Methods

3.2.1 Set-up

The same ten cats previously described in Chapter 2 were used in accordance with the issued standards of the National Institutes of Health and the Emory Institutional Animal Care and Use Committee. Animals will be referred to by the date of the experiment. Under isoflurane anesthesia, a trachometry was performed to monitor anesthesia levels and an IV was inserted in the external jugular vein for hydration and drug delivery. Animals were decerebrated using two techniques: intercollicular and a modified premammillary.

The more traditional intercollicular decerebration consisted of a vertical transection through the superior colliculus. All brain material rostral to the transection was removed. The modified premammillary technique, previously described in Chapter 2, modifies the premammillary decerebration (traditional locomotion preparation) to decrease the spontaneous locomotion but preserve the postural tone. Following the premammillary transection and removal of all brain tissue rostral to the cut, a second, vertical transection was made at the level of the mammillary bodies to prevent spontaneous locomotion. The resulting preparation was considerably more responsive to mechanical perturbations than animals prepared with intercollicular transections.

The animal's head was fixed in a stereotaxic frame and its tail secured through a mechanical clamp at the base of the tail. Fixation of the tail instead of the hip gave a large range of motion for the animals' hindquarters and allowed for natural hip placement.

Thus, these animals had full flexibility with hip rotation. They were only limited slightly by height and side to side movements. The toe pads of all four limbs were fixed with glue and tape to the force transducers. All force transducers were oriented the same such that positive X was rightward, positive Y was rostral, and positive Z was upward. The natural turnout of the foot was used for each animal. The large, central pad of the foot was not secured allowing natural movement of the foot during perturbations. Intact animal kinematics determined the natural stance placement of the toe approximately one centimeter behind the greater trochanter in the saggittal plane. Depending on animal size this placement resulted in a 28 – 32cm distance between the center of the forelimb and hindlimb transducers. The center of right and left forelimb and hindlimb transducers were 7cm apart. In three experiments (6/8, 1/22, 9/7), forces were evaluated at two additional stance conditions that altered the inter-limb spacing (distance between forelimbs and hindlimbs). Both hindlimbs were moved 5cm forward or 4cm backward from the natural inter-limb spacing and perturbations were completed from the new stance condition.

3.2.2 Perturbations

Once the animal was decerebrated, positioned, and removed completely from anesthesia, the support surface was translated in 16 different, horizontal directions using two motors: rotational and linear. In some experiments force data were taken under two conditions: active and anesthetized. Muscle tone and activity was monitored in the anesthetized condition to ensure that the animal was not responsive. Active data was only quantified once the animal had achieved active muscular responses (visualized through EMG

recordings) in all 16 directions. In all but two cases, the support surface was perturbed 4cm over 400ms with an acceleration of .5 (m/s^2). In the 6/8 experiment the platform was moved 8cm over 400ms and in 11/7 experiment the platform was moved 4cm over 150ms. The perturbation parameters were chosen based upon previous studies in intact cats (Macpherson) for comparison purposes. Unique to the decerebrate cat, the animal's head and tail were in a fixed position. Thus the limbs were perturbed, held at the extended position for 1000ms and then returned 4cm over 400ms to the initial position. In the 10/8 experiment the hold was 500ms and in the 11/7 and 2/23 experiment the hold was 3000ms.

3.2.3 Force data analysis and quantification

Force data from the horizontal plane (X: medial-laterial, Y: rostral-caudal) were analyzed for the purposes of this report. Trials that included stepping behavior or where the foot was lifted from the force transducer were excluded from analysis. Force data were demeaned and low passed at 30Hz. The change in force per ms was calculated by finding the area under the force curve for 100ms time intervals and dividing by 100ms. The initial time period evaluated was 50-150ms. This time interval was chosen because it eliminates the inertial properties associated with the motors during the first 50ms and it corresponds to the automatic postural response reported in intact animals (Macpherson 1988a; b). Additional time intervals were analyzed to evaluate the extended force responses past the typical automatic postural response time period. To visualize and further quantify the force constraint, the average change in force for all perturbation directions was graphed from origin (see Figure 3.3).

The constraint or clustering of the force responses was further quantified using principal direction and stiffness ellipses. Principal directions were calculated by first separating the two populations based upon their squared Euclidean distance from one another using the MATLAB function *kmeans*. The principal direction of each population was then calculated by averaging the remaining force vectors and determining the direction of the resultant vector. Stiffness ellipses were derived by dividing the 16 force vectors by the distance traveled in the x and y directions appropriately. The shape of the ellipse was calculated by dividing the minor axis by the major axis. A shape close to 1 represents a circle or non constrained force responses, while a shape close to 0 represents a line or highly constrained force responses. Figure 3.1 shows example principal direction and shape quantifications along with the perturbation directions.

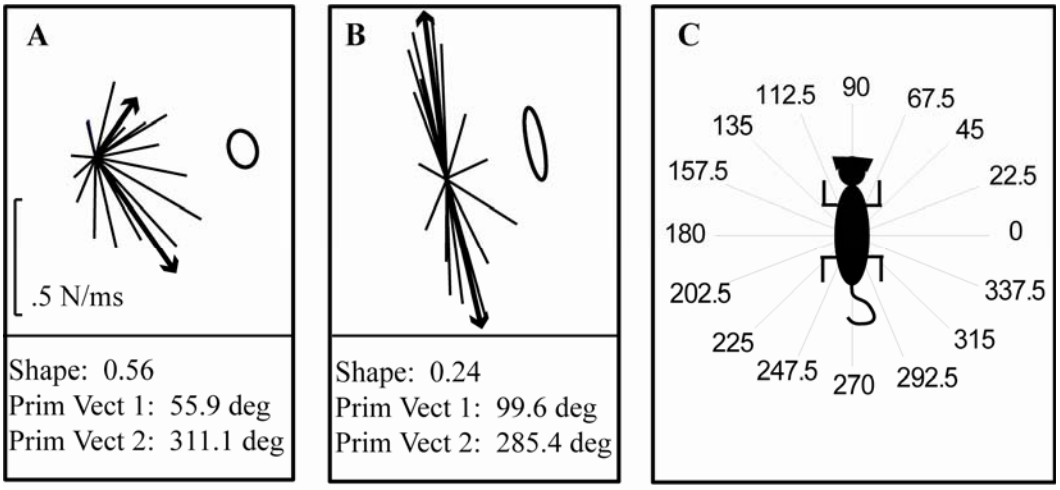

Figure 3.1: Principal direction, shape, and perturbation direction description. demonstrates the key variables used for quantifying the force responses. Each X and Y force curve is integrated for 100ms time windows and divided by 100 to get the average change in force per ms. The resultant XY vector is then graphed originating at zero. The black lines represent the force traces for the left forelimb (LF) and right hindlimb (RH) from the 6/8 experiment. The heavier and arrowed black lines represent the two primary vectors calculated through the cluster analysis. The stiffness ellipses calculated for these force traces are shown to the right. The shape, used to quantify force constraint, is a ratio of the minor axis to the major axis where 1 represents a circle and 0 represents a line. The principal directions and shapes evaluated for these two force strategies are presented below the figure.

Shape and principal directions were statistically compared during different time epochs, inter-limb spacing, and decerebration techniques. Shape and principal directions were calculated for each full set of 16 directions under each condition. A minimum of three trials (full sets of 16) were required before statistics were computed. There was one exception, which was the 9/7 long stance condition. Statistics were computed on only 2 trials. The variance was determined to be equivalent in all cases using an F-test. Therefore, a two-tailed t-test for independent variables of equal variance was used to determine if there were statistical differences between shapes and principal directions under each condition.

3.3 Results

Raw force traces demonstrate that the decerebrate cat generally produces greater maximum force in the rostral/caudal direction than in the medial/lateral direction. Figure 3.2 shows representative raw, filtered force traces from a premammillary decerebrated animal (6/8 experiment). The solid vertical line indicates perturbation initiation while the dashed line indicates perturbation termination. The force responses of Figure 3.2 illustrate the typical slow increase of force through the dynamic phase of the perturbation, which find a maximum that is maintained during the steady-state hold phase. X forces (medial/lateral) in all animals generally found a maximum around .5 N, while Y forces (rostral/caudal) typically could reach 1.5N. Decerebrated animals occasionally produced Z forces as large as 10N, however more typically the maximum Z force responses were between 2 and 2.5N during the perturbation. Finally, Figure 3.2 portrays a shaded region that represents the initial analysis time period (50-150ms) used to calculate the average

change in force. The average change in force is graphed originating at zero for further analysis of the force constraint and its principal directions.

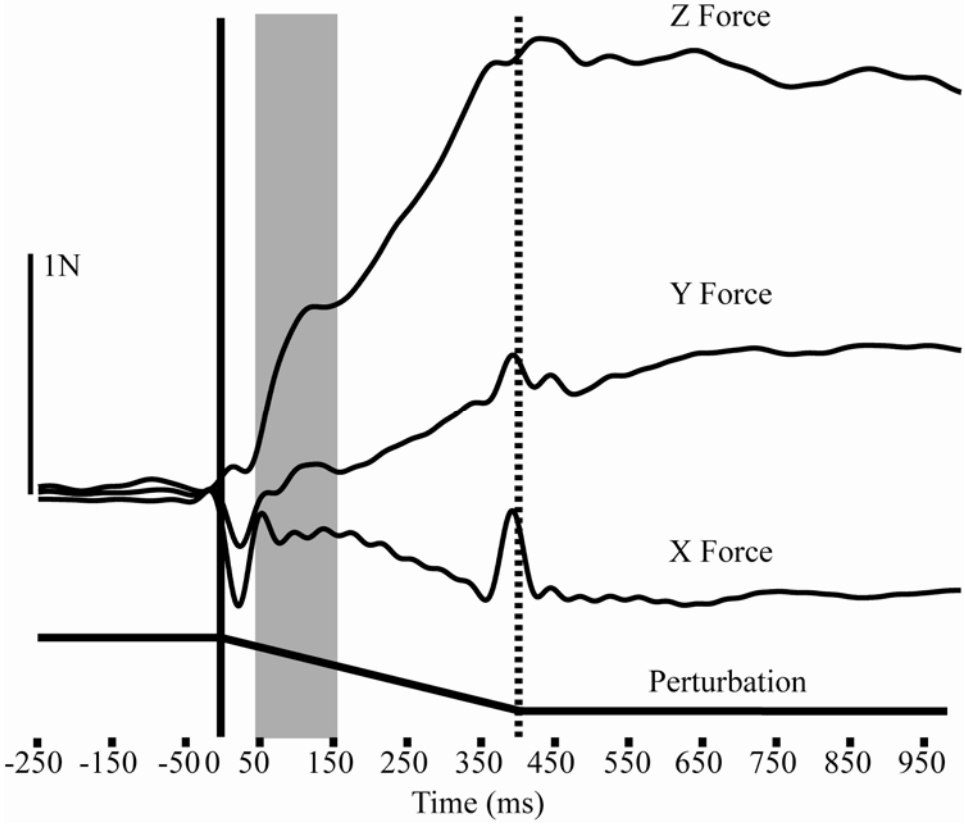

Figure 3.2: Representative raw force traces during a support surface perturbation. Depicts raw force traces (demeaned and low passed at 30Hz) for one perturbation direction of the 6/8 experiment. Perturbation initiation and termination are denoted with a solid and dashed line respectively. Forces are quantified over a 100ms time windows. The first time period evaluated is marked by a gray box and begins 50ms after perturbation initiation to avoid the inertial properties of the initial perturbation. For quantification of these responses, each force curve is integrated individually for all 16 directions.

Animals decerebrated at the premammillary level more consistently produce muscular responses to perturbation (88.9%) than intercollicular decerebrated animals (11.7%); however the force responses associated with these muscular responses were remarkably similar. Figure 3.3 shows representative active force responses from two animals decerebrated at the premammillary (B) and intercollicular (C) level. Force responses of the anesthetized premammillary animal are also depicted (A). These force responses were mostly radial in nature although a slight constraint appears to be present. In

comparison, the active responses of both the premammillary and intercollicular animals are larger in amplitude and more constrained with larger rostral-caudal forces than medial-lateral forces. The rostral-caudal forces were additionally offset from the Y axis and demonstrated a 2-13 degree inward turn toward the center of the animal. The knowledge that the active responses were distinct and larger than those of the anesthetized animal demonstrated that these animals were generating significant force in response to the support surface movement.

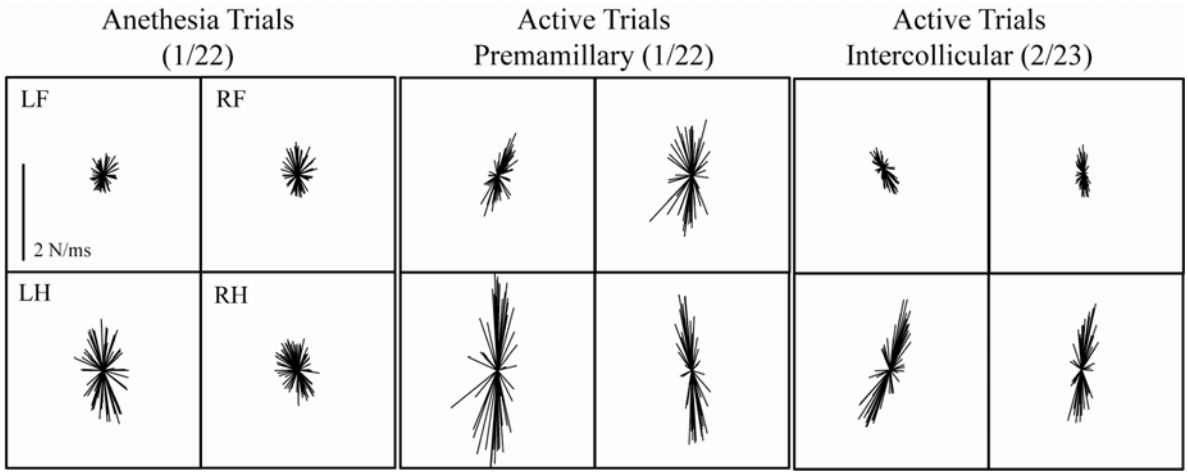

Figure 3.3: Representative horizontal plane force projections from the modified premammillary (active and anesthetized) and intercollicular decerebrate animal. Depicts the typical XY force projections of the modified premammillary decerebrate cat (1/22 expt.) under anesthesia and after the animal was removed from isoflurane (active). Forces projections were evaluated during a window of 50-150ms after perturbation initiation and graphed originating from zero. The anesthesia trials are less constrained and smaller in amplitude than the modified premammillary animals. The modified premammillary animals demonstrate a force constraint or clustering where the forces in the rostral-caudal dimension are larger than those in the medial-lateral dimension. It is noted that the force responses of the animal under anesthesia demonstrate a more subtle but present force constraint.

Animals decerebrated at the premammillary and intercollicular decerebration levels produced statistically equivalent shapes in all four limbs. Figure 3.4 illustrates the quantification of the force constraint of all four limb force responses attained in animals decerebrated at the premammillary (black) and intercollicular (white) level. The intercollicular preparation generally has slightly smaller force responses and slightly

more constrained forces (except in the RH) but none of the differences, shape (A) or principal direction (B: rostral, C: caudal), are statistically significant.

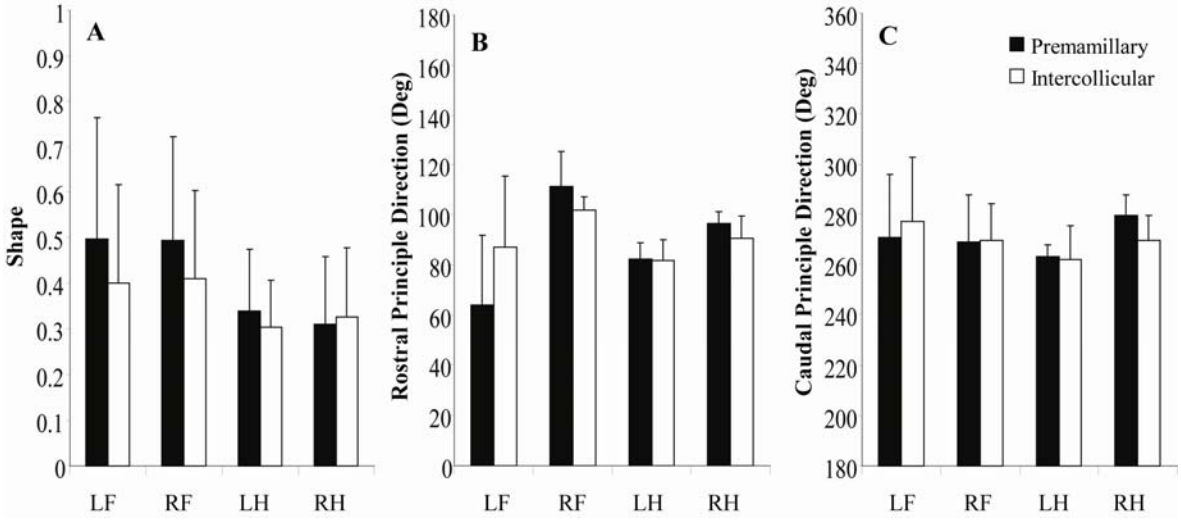

Figure 3.4: Principal direction and shape quantification for the modified premammillary and intercollicular decerebrate cat. Principal direction and shape were quantified for all four limbs (left forelimb: LH, right forelimb: RF, left hindlimb: LH, and right hindlimb: RH) in all animals that generated active muscular responses. The black columns represent the mean and standard deviation calculated from the 7 modified premammillary decerebrated animals while the white columns represent the mean and standard deviation from the 3 intercollicular decerebrated animals. All principal directions and shape quantifications were found to be statistically equivalent between the two types of preparations.

Although animals decerebrated at the premammillary and intercollicular levels produce constrained forces in all four limbs, the hindlimbs show more constrained shapes and less variable principal directions (Figure 3.4). Hindlimbs were generally more constrained in both decerebrate preparations than forelimbs with average shape values ranging .30 - .34 compared to average forelimb shape values that ranged .40 - .50. The force constraint in the hindlimbs was also more consistent with standard deviations less than .15 while forelimbs showed higher variability ranging from .19 - .27. This same trend was present in principal directions with hindlimbs presenting small standard deviations less than 14 degrees while the forelimbs were more variable generally showing standard deviations greater than 20 degrees. In addition to the consistent nature of the hindlimb responses,

the principal directions were almost mirror images of one another. The left hindlimb generated principal directions of 82 and -96, while the right hindlimb produced principal directions of 96 and -80. This demonstrates a strong symmetry between the hindlimb force responses.

Time epoch affected the magnitude of the force responses but had little effect on shape and principal direction. Figure 3.5 depicts the representative right hindlimb force responses from one experiment taken at four different time epochs. The first two time periods are during the beginning and end of the dynamic or perturbation phase (50-150ms, 250-350ms) while the second two time periods are during the steady-state or hold period (600-700ms, 900-1000ms). The data from three experiments (Figure 3.5) were further quantified (shape and principal direction) and reported in Table 3.1. The first two panels of Figure 3.5A shows that the force responses increase in amplitude through the dynamic phase reaching a maximum that is maintained through the steady-state hold period. These amplitude shifts are also seen in the raw force traces depicted in Figure 3.1. The second time period of the hold phase does demonstrate a slight adaptation with forces slightly smaller during this phase than the first time period of the hold.

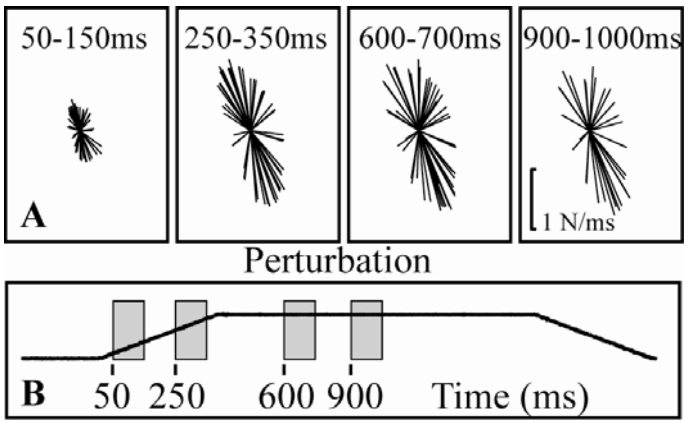

Figure 3.5: Horizontal force trajectories during different time epochs. Depicts representative force traces of the right hindlimb (9/7) during 4 time periods: 50-150ms, 250-350ms, 600-700ms, and 900-1000ms. All forces were graphed on the same scale across experiments and conditions. The force constraint or shape appears to be maintained through the time periods. However, the amplitude is affected by time. Shape and principal directions were further quantified for this and 2 additional experiments and are presented in Table 3.1.

Table 3.1: Principal direction and shape for 4 different time epochs in 3 representative experiments.

9/11/2007

Time (ms)	*Shape*	*Pos Prim Vect*	*Neg Prim Vect*
50 - 150	.36 (.07)	92.4 (2.8)	-99.6 (9.1)
250 - 350	.37 (.33)	92.4 (1.5)	-98.2 (8.3)
600 - 700	.33 (.08)	89.6 (2.0)	-94.1 (13.3)
900 - 1100	.34 (.08)	89.4 (1.9)	-94.7 (11.6)

10/8/2007

Time (ms)	*Shape*	*Pos Prim Vect*	*Neg Prim Vect*
50 - 150	.28 (.02)	91.5 (2.9)	-87.1 (1.8)
250 - 350	.35 (.03)	90.2 (0.6)	-91.1 (1.3)
600 - 700	.29 (.03)	93.1 (1.3)	89.1 (3.7)
900 - 1100	.28 (.04)	90.2 (1.3)	-90.6 (1.6)

9/7/2007

Time (ms)	*Shape*	*Pos Prim Vect*	*Neg Prim Vect*
50 - 150	.37 (.03)	101.8 (4.2)	-70.3 (3.8)
250 - 350	.32 (.01)	103.1 (1.3)	-71.0 (2.4)
600 - 700	.36 (.01)	95.9 (2.2)	-68.9 (3.1)
900 - 1100	.37 (.01)	92.8 (0.6)	-68.9 (3.1)

The mean and standard deviation of the shape and principal direction of the right hindlimb was evaluated over four time windows (50-150ms, 250-350ms, 600-700ms, and 900-1000ms) in three experiments (9/11, 10/8, 9/7).

While the amplitude of the force responses was altered by time epoch, the shape and principal direction were affected minimally across all time epochs. T-tests confirmed that principal directions were statistically equivalent in all three experiments. Furthermore, the shape indices for all time epochs were found to be statistically

equivalent to the first time epoch except the second time epoch of the dynamic phase in the 10/8 and 9/7 experiments. Although these two were shown to be statistically difference, neither represented greater than an 11% difference from the initial time epoch.

The premammillary decerebrate cat demonstrates an increasing force constraint as quantified by shape as stance condition is lengthened. Figure 3.6A shows the force responses for the 6/8 experiment under all three stance conditions: short, natural, and long. The short force trajectories appear more radial while the natural and long conditions show increasing force constraint. Figure 3.6 (B-D) depicts the quantification across experiments of the shape and principal directions for each of the three stance conditions. The shape values were the most affected by stance condition (Figure 3.6A). While the 6/8 experiment showed the most dramatic change in shape from .56 at the shorter stance to .14 at the longer stance, all of the experiment show decreasing shape values. Shape values from each experiment were statistically different from short to long stance and shapes from natural to long were highly significantly different (6/8) or showed a trend towards significance (9/7, 1/22). However, only the 6/8 experiment demonstrated highly significant differences between the short and natural condition. All of the rostral principal directions were found to be statistically the same in each experiment. The caudal principal directions showed some significant differences across conditions but the percent difference was not greater than 9 percent indicating the shifts were only slight.

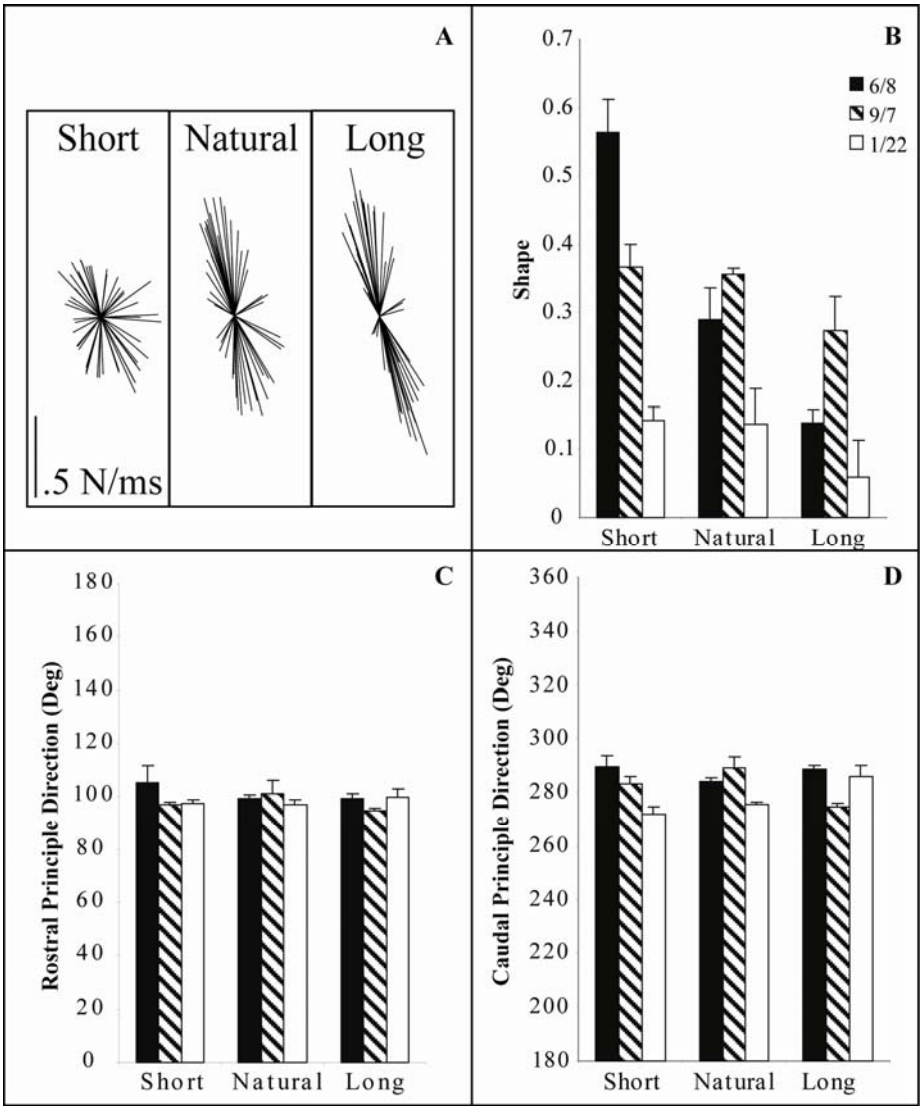

Figure 3.6: Shape of the force responses is most affected by changes in stance condition. Depicts the Right Hindlimb force trajectors for three different inter-limb spacing conditions (6/8 expt.). Both hindlimbs were moved 3cm forward (short) and backward (long) from natural stance and perturbations reapplied and forces reevaluated. While the 6/8 experiment shows the most dramatic change in shape from .56 at the shorter stance to .14 at the longer stance, all of the experiment show decreasing shape values. Principal directions are less affected by changes in inter-limb spacing; however some statistical significance did occur although they did not represent changes greater than 9 percent difference.

3.4 Discussion

3.4.1 Comparison to the intact animal

Our objectives were to 1) quantify the force responses and constraint characteristics of both the modified premammillary and intercollicular decerebrated cats and 2) to further

demonstrate the appropriateness of the decerebrate cat as a model to investigate the neural and sensory mechanisms underlying postural control. Both the modified premammillary and intercollicular decerebrate animals produced constrained force responses (i.e. the force constraint strategy) that closely resemble those reported in the intact animal in all four limbs; however active force responses were observed more frequently in the premammillary preparation. Our previous report established that the decerebrate cat preparation can produce appropriately directed muscle activation patterns to support surface perturbation. These muscle responses are similar both in direction and breadth (range of directions) to those reported in the intact animal. Even though the decerebrate cat preparation was fixed at the head and tail limiting its mobility to fully compensate for the postural disturbance, these preparations produced whole body active responses which show all four limbs generating forces that cluster into two XY plane populations similarly described in the intact animal. Also the decerebrate animal, like the intact animal, showed a stronger force constraint (lower shape) in the hindlimbs than the forelimbs. Furthermore, the decerebrate animal demonstrates the characteristic dependence on stance condition producing less clustered responses as inter-limb spacing is decreased. This indicates that the decerebrate cat's muscular responses are associated with functionally significant force responses.

The only distinction from the intact animal noted was the smaller variability of principal direction in our preparations. The decerebrate cat consistently produces an inward rotation of the force constraint varying from 2-13 degrees off the rostral/caudal axis. Conversely, the intact animal generates more variable inward rotations ranging from

small rotations of 5-10 degrees [(Macpherson and Fung 1999b): ctrl data; (Ting and Macpherson 2004): prior experience] to large rotations of almost 45 degrees (Macpherson 1994b; 1988a). The cause for the increased variability in the intact animal is not apparent. It is possible that the constraints brought by our methodological design limits the directionality of the force constraint. Indeed, our method affords more rigorous control of the kinesthetic conditions such as toe placement 1cm behind the greater trochanter, sagittal and frontal plane paw spacing, hip height, and foot turnout. The intact animal has more flexibility to choose and adjust its limb configuration. There are also likely biomechanical discrepancies between the animals such as weight, height, and morphological composition that certainly impact the force constraint rotation. Regardless, the inward rotation demonstrated in the decerebrate cat is well within the range of observed principal directions of the intact animal. Therefore, we believe that the decerebrate cat is an appropriate model to investigate the sensory and neural mechanisms underlying the postural response.

3.4.2 Central Mechanisms

We have previously hypothesized that the circuits in the spinal cord are responsible for the directional tuning of muscle responses but not necessarily the magnitude (Chapter 2). This is corroborated not only by our evidence that the decerebrate cat produces appropriately directed muscular responses without the influence of the cerebral cortices but also the observation that spinalized animals do so as well without the influence of the any supra-spinal structures (Macpherson and Fung 1999b). Still, while it is likely that the spinal cord supports directional tuning, the muscle responses of the spinalized animal are

not of sufficient strength or duration to oppose the perturbation. These animals do not exhibit the force constraint strategy and moreover they can rarely remain upright when challenged with support surface movement. As noted previously (Chapter 2), chronic spinal injury in cats is accompanied by widespread clasp-knife inhibition (Bonasera et al. 1994; Nichols et al. 1999), increases in inhibitory neurotransmitters, and re-organization of spinal synapses (Edgerton et al. 2001); all of which likely influence spinal cord functionality and prevent expression of the force constraint strategy.

It has been previously suggested that spinal circuits could support postural control as long as some supraspinal influences remain intact (Deliagina et al. 2008; Deliagina et al. 2006; Lyalka et al. 2005; Musienko et al. 2008). This proposal is corroborated by reports demonstrating that lower brainstem regions, specifically the ventral and dorsal tegmental fields (VTF and DTF), can excite or inhibit postural tone respectively (Mori 1987). These authors additionally used horseradish peroxidase to determine which regions were being stimulated through passing fibers. They determined that the most effective VTF stimulation sites also stimulated upper brainstem regions such as the hypothalamus and subthalamic nucleus while the most effective DTF stimulation sites corresponded with the diencephalon and the dorsal posterior and lateral hypothalamus. The upper brainstem's role in postural control appear analogous to its role in locomotion where the subthalamic nucleus controls the expression of locomotion generated by the mesenphalic locomotor region of the lower brainstem (Mori et al. 1989). The close association of the postural tone regions (VTF and DTF) to the expression of locomotion further indicates that these two systems are likely similarly controlled. These observations strongly imply

that the upper brainstem (regions rostral to the superior colliculus) controls the expression of the lower brainstem (regions caudal to the superior colliculus) regions associated with postural tone.

Our data from two levels of brainstem transection support this notion of upper brainstem support of lower brainstem regions. Intercollicular and premammillary decerebrated animals produce statistically indistinguishable force results implying that the upper brainstem is not required for appropriate force responses. Yet, intercollicular animals rarely were able to elicit muscular responses to support surface perturbation. Furthermore, the intercollicular animals' responsiveness to perturbations was typically transient lasting only a few minutes compared to the several hours of in the modified premammillary animals. In conclusion, we hypothesize that the postural response attributes of directional tuning and activation strength are housed within a hierarchical framework located in the brainstem and spinal cord regions. The spinal cord likely mediates directional tuning of muscles while lower brainstem regions modulate the strength of those responses. Finally, the upper brainstem mediates the excitability of at least the lower brainstem and likely the spinal cord as well allowing for robust and continuing responses.

3.4.3 Origins of the force constraint

Two hypotheses about the appearance of the force constraint strategy: 1) it results from supraspinal processing within the brainstem or 2) it results from the mechanical capabilities of the limb musculature. While these hypotheses are not mutually exclusive,

we suggest that the latter makes the more significant contributions. The fixture of the head and the tail of the cat allow us to observe the forces without the inertial influences of body movement. The inertial influences of the limbs, as observed during anesthesia trials, are mostly radial in nature and do not demonstrate a strong force constraint. This implies that the ground reaction forces generated by muscular activation are exclusively responsible for the constrained appearance of the forces in the decerebrate animal. Generally, the non-sagittal actions of the hindlimb musculature are not as strong as the rostral/caudal actions. Therefore, the force generating power of the hindlimb musculature is in the rostral/caudal dimension. This is substantiated by empirical model results demonstrating that the feasible force set, the calculated maximum force that the limb musculature can exert in all directions, is constrained in a similar fashion to the force constraint strategy (McKay et al. 2007). These considerations suggest that the biomechanical constraints of the limb contribute strongly to appearance of the force constraint strategy.

CHAPTER 4

MECHANICAL ACTIONS OF THE CAT HINDLIMB MUSCULATURE AS ASSESSED BY INTRAMUSCULAR STIMULATION: IMPLICATIONS FOR POSTURAL CONTROL

4.1 Introduction

Humans and cats are known to respond to horizontal support surface perturbations with directionally selective muscle recruitment (Henry et al. 1998; Macpherson 1988b). While muscles have a principal direction where maximal activation is achieved, they are also activated broadly over many perturbation directions. The directional sensitivity of these tuning curves is highly robust remaining unaffected by alterations in stance condition (distance between forelimbs and hindlimbs) (Torres-Oviedo et al. 2006) and perturbation parameters (velocity and amplitude) (Diener et al. 1988). While most muscles demonstrate directionally consistent activation within a subject some muscles, such as the rectus femoris (RF), sartorius (Sart), and tibialis anterior (TA) muscles, are uniquely more variable in direction across trials and have broader activation patterns (Macpherson 1988b). Data from the decerebrate cat also indicates that the medial gastrocnemius (MG), vastus medialis (VM), and vastus lateralis (VL) muscles show variability in principal direction across animals (Chapter 2). It is unclear if these muscles are responding distinctly due to differing control mechanisms or unique mechanical environments. Before we can evaluate these two notions, we must have a clear picture of how individual muscle activation is translated to functional endpoint forces and the variability of that transformation.

We know that cats and humans generate whole limb force responses that are constrained in appearance when subjected to support surface perturbation (Henry et al. 2001; Macpherson 1988a). While initially hypothesized that forces would project equally in all directions, similar to the activation patterns observed, data from the intact (Macpherson 1988a) and decerebrate cat (Chapter 3) demonstrate that forces cluster into two rostral-caudally directed XY (horizontal plane) force populations. There is a noted absence of strong non-sagittal forces. Still, this force constraint is robust in humans and cats demonstrating its presence in naïve subjects (Macpherson 1994b), during support surface rotation (Ting and Macpherson 2004; Torres-Oviedo et al. 2006), and volitional reaching tasks in humans (unpublished observationsLeonard et al. 2009). This constrained strategy is surprising as muscles are activated in all 360 degrees of the perturbation space. Furthermore, the constraint characteristics are altered with changes in inter-limb spacing (distance between hindlimbs and forelimbs), while the directionality of the muscle activation patterns remains unaffected (Macpherson 1994a).

We *hypothesize* that the biomechanical constraints of individual muscle actions generate the constrained forces. As muscles are active over all 360 degrees, we suspect that few muscles will have strong non-sagittal actions. Our objective was to quantify the alterations of individual muscle endpoint forces at different stance conditions (inter-limb spacing) and compare to the alterations in force constraint strategy when intact and decerebrate cats are subjected to horizontal support surface perturbations. We further *hypothesize* that muscles are selectively activated based upon their potential counteractive endpoint force. We therefore expect that 1) tuning curves will be directed oppositely

(180 degrees) from the muscle endpoint ground reaction force and 2) muscles that exhibit variable tuning curves (RF, TA, Sart, MG, VL, and VM) will exhibit variability in their horizontal plane (XY) ground reaction forces as well. Our second objective was to observe and quantify the individual muscle endpoint forces and compare those forces to the muscle activation patterns generated in the intact and decerebrate animals in response to support surface perturbations. Our quantification of the three dimensional endpoint forces expanded upon preliminary work (Murinas 2003) and provided insight into the mechanical actions of the muscles surveyed which has not been done experimentally. We compared our experimental results with those obtained with a three dimensional hindlimb model (Burkholder and Nichols 2004).

4.2 Methods

4.2.1 Experimental set-up

Eleven adult cats (3.6kg to 6.4kg) were used in this study. Animal care was in accordance with the National Institutes of Health and the Emory Institutional Animal Care and Use Committee. Under isoflurane anesthesia, a trachometry was performed to monitor anesthesia levels and an IV was inserted in the external jugular vein for hydration and drug delivery. Intramuscular (IM) stimulation electrodes were implanted into the vastus medialis (VM), vastus lateralis (VL), rectus femoris (RF), medial gastrocnemius (MG), lateral gastrocnemius (LG), tibialis anterior (TA), biceps femoris (anterior: aBF, middle: mBF, posterior: pBF), semitendinosus (ST) semimembranosus (cranial: cSM), caudofemoralis (CF), gluteus medius (Glut), gracilic (Grac), sartorius (anterior: aSart, medial: mSart), and iliopsoas (IL) muscles. Electrode placement was

verified at the conclusion of all experiments and detailed notes recorded about the placement. Electrodes were constructed from Teflon coated, braided, stainless steel wire and were suitable for both electromyography (EMG) recordings and intramuscular (IM) stimulation.

Animals were decerebrated at the precollicular level with the removal of both cerebral cortices and all brain material rostral to the superior colliculus. The precollicular decerebration produced adequate background tone in the hindlimb musculature to achieve natural leg kinematics without producing the stepping or postural behaviors typical of the more rostral decerebrations. The animal's head was fixed in a stereotaxic frame and its tail secured through a mechanical clamp at the base of the tail. Fixation of the tail allowed for more natural rotation of the hip as opposed to hip fixation with pins. A sling was used to support the animal's torso and to ensure a proper back alignment. The toe pads of all four limbs were fixed with glue and tape to four ATI force transducers instrumented to record three dimensional ground reaction forces and torques. The large, central pad of the foot was not secured to allow natural movement of the foot at longer stance conditions. Based upon recorded intact animal kinematics, we placed the toe approximately one centimeter behind the greater trochanter for natural stance conditions.

IM stimulation was taken under 5 different stance conditions (inter-limb spacing): shortest (SS), short (S), natural (N), long (L), and longest (LL). Both the right and left hindlimbs were moved rostrally from the natural stance 5 and 8cm for S and SS conditions and caudally 4 and 7cm for the L and LL conditions. The reproducibility of

this protocol was tested by repositioning the legs again after a complete data set. Statistics confirmed no statistical difference in angle or magnitude between these trials (see Data analysis for description of angle and magnitude).

4.2.2 IM stimulation protocol

After proper positioning the decerebrate animal, five trials of IM stimulation were applied to each muscle individually under each limb condition. A four pulse chain stimulation at 200Hz over 20ms was used to produce a twitch contraction in each muscle. This protocol, used previously in the intact (Pratt 1995) and decerebrate animal (Murinas 2003), creates a significant contraction of the muscle for reproducible force outputs but not so strong as to significantly alter limb kinematics to a non naturalistic configuration. The stimulation amplitude was chosen to be three times the threshold at which each muscle begins to contract. Stimulation amplitude increases were found to create a sinusoidal response that levels out at approximately two times threshold. We chose three times threshold to ensure that we were firmly in the plateau region for reproducible results. IM stimulation electrodes were also suitable for EMG recordings which were used to ensure that stimulation was isolated to the test muscle.

4.2.3 Data analysis

Force data were analyzed at 35ms, a time when forces were large enough to be reliably measured but before the influences of force and length pathways could alter the muscle's force output. Figure 4.1 shows all three dimensions of the raw force traces for one IM stimulation trial of the biceps femoris (anterior) muscle. The vertical line represents

35ms. This figure also shows the coordinate system used for evaluation of these responses: rostral (+Y), lateral (+X), dorsal (+Z).

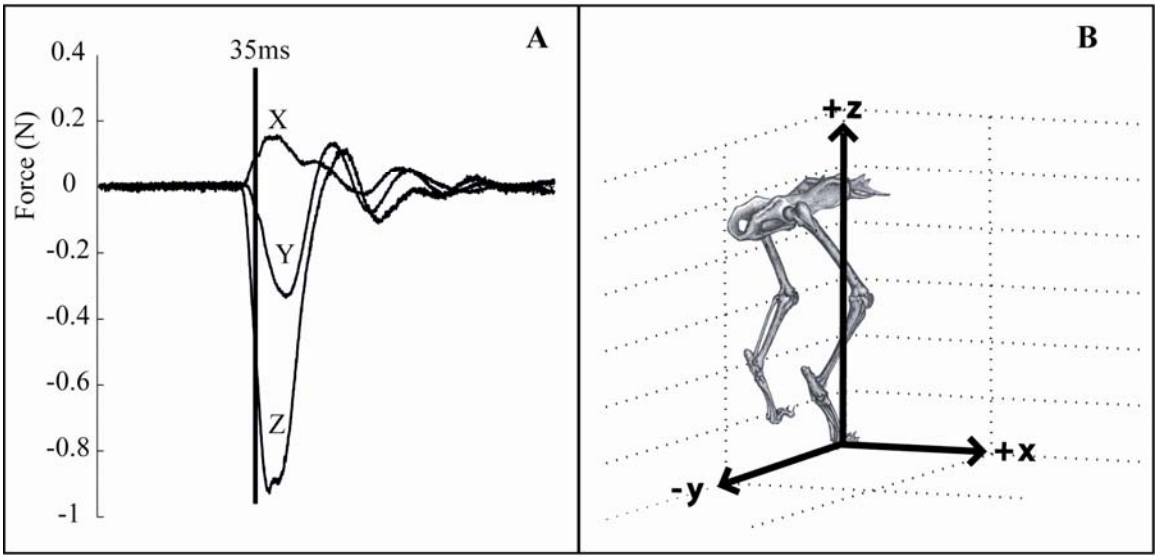

Figure 4.1: Raw IM stimulation forces and axis assignment. Shows the raw force traces for a representative anterior biceps femoris muscle during the 9/29 experiment (A). The black line marks 35ms after stimulation, the time that IM stimulation forces were analyzed. The axes are also defined in this figure (B): lateral (+x), rostral (+Y), and dorsal (+Z). All data were collected in the **RIGHT** hindlimb.

The magnitudes of the three dimensional force vectors were variable across experiments as electrodes differed in conductance. Therefore, in order to compare results across experiments, we normalized each three dimensional force vector to 1N. We evaluated the data in two planes XY (horizontal plane) and YZ (sagittal plane). In each plane, we report a magnitude and an angle of the response. The magnitude reported is the projected normalized vector of 1N onto each of the two planes. Therefore, the XY magnitude is the XY component of the normalized force vector. In the horizontal (XY) plane "0" corresponded to the +X axis, while in the sagittal plane "0" corresponded to the +Y axis. Occasionally, the angle of the force vector varied across the 0 degree angle. In these cases, angles in the bottom, right quadrant were converted to negative numbers. This alteration allowed for appropriate standard deviations representing the true variance of

the muscle force. Forces (magnitude and angle) were calculated for each plane (XY and YZ) for all 5 stance conditions (SS, S, N, L, and LL).

4.2.4 Statistics

A two-way ANOVA was performed on the 5 stance conditions in each plane. The mean angles and magnitudes (projection of normalized vector) of each muscle were averaged across experiments for each of the 5 conditions. The two-way ANOVA, completed using Statistica, was chosen as it allowed us to pull out both the cat and position effect. This ensured that statistical differences in angle or magnitude were not affected by the variance generated by the inter-animal differences. If the ANOVA reported statistical differences in the position condition, a Tukey HSD was utilized to compute statistical differences for all pairwise comparisons. These results were then depicted graphically in Figures 4.4 – 4.7.

4.3 Results

4.3.1 Natural Stance

IM stimulation produced highly consistent results in all three planes with most muscles demonstrating consistent angles and magnitudes; however some muscles (VM, RF, TA, and mSart) were more variable in angle across experiments. Results were compiled for all three planes; however we will focus on the XY and YZ plane data for the purposes of this report. Within an experiment, all muscles produced consistent angles with standard deviations lower than 10 degrees in all planes except TA (expt 3), ST (expt 3), and mSart (expt 1, 2) in the XY plane; IL (expt 10) in the YZ plane. Across experiments, most

muscles showed angle standard deviations less than 20 degrees. Notable exceptions included VM, RF, and TA (XY plane) and mSart (YZ plane), which demonstrated larger variability across experiments. Magnitude measurements showed little variability, within each experiment, with standard deviations less than .10 except ST (XY plane, expt 3) and IL (YZ plane, expt 10). Magnitude variability across experiments was less than .20 except aBF, mSart, IL in the XY plane, which showed higher variability across experiments. The YZ plane showed extremely low variability in magnitudes across experiments with all standard deviations less than .1. In general both angles and magnitudes were more consistent in the YZ plane across experiments than those values reported in the XY plane.

Results demonstrate that most muscles produce only small actions in the XY plane and there is a lack of muscles with strong force actions in the medial-lateral direction. Averaged angle and magnitude data is presented in graphical form in Figure 4.2 and values are reported in Table 4.1. Through examination of average magnitudes pBF, Grac, and aSart have the most significant actions in the XY plane with magnitudes exceeding .7; while VM, TA, RF, and VL have limited actions in the XY plane with magnitudes less than .25. Interestingly, VM, RF, and TA also showed large angle standard deviations across experiments suggesting that their weak actions in this plane contribute to that variability. In comparison to the YZ plane (Figure 4.3), it appears that muscles do not have strong actions in the XY plane, particularly in the medial-lateral directions. The muscles that do exhibit responses in this dimension have small

magnitudes. Muscles appear to have stronger actions in the rostral-caudal direction with a slight counter-clockwise turn.

Table 4.1: Quantification of XY and YZ angles and projected normalized magnitude.

	XY Mag	*XY Angle*	*YZ Mag*	*YZ Angle*
Vastus Medialis	.13 (.03)	55 (26)	.998 (.001)	276 (3)
Vastus Lateralis	.28 (.07)	52 (12)	.985 (.008)	283 (4)
Rectus Femoris	.24 (.16)	52 (53)	.995 (.001)	281 (12)
Medial Gastrocnemius	.58 (.11)	282 (6)	.990 (.008)	235 (8)
Lateral Gastrocnemius	.60 (.12)	271 (4)	.985 (.034)	234 (10)
Tibialis Anterior	.26 (.08)	199 (31)	.973 (.019)	96 (8)
Biceps Femoris (anterior)	.41 (.21)	321 (13)	.942 (.066)	252 (15)
Biceps Femoris (middle)	.60 (.17)	311 (5)	.908 (.069)	240 (10)
Biceps Femoris (posterior)	.70 (.09)	283 (7)	.982 (.015)	134 (6)
Semitendinosus	.69 (.07)	261 (9)	.979 (.018)	134 (3)
Semimembranosus (cranial)	.60 (.17)	271 (6)	.998 (.003)	232 (12)
Caudofemoralis	.62 (.09)	338 (4)	.806 (.073)	253 (2)
Gluteus Medius	.52 (.10)	343 (7)	.865 (.061)	260 (3)
Gracilis	.77 (.07)	245 (6)	.944 (.030)	138 (7)
Sartorius (anterior)	.95 (.08)	90 (7)	.993 (.006)	14 (12)
Sartorius (medial)	.76 (.15	130 (19)	.888 (.050)	47 (21)
Iliopsoas	.32 (.19)	79 (14)	.993 (.010)	288 (11)

Values in parentheses are standard deviations

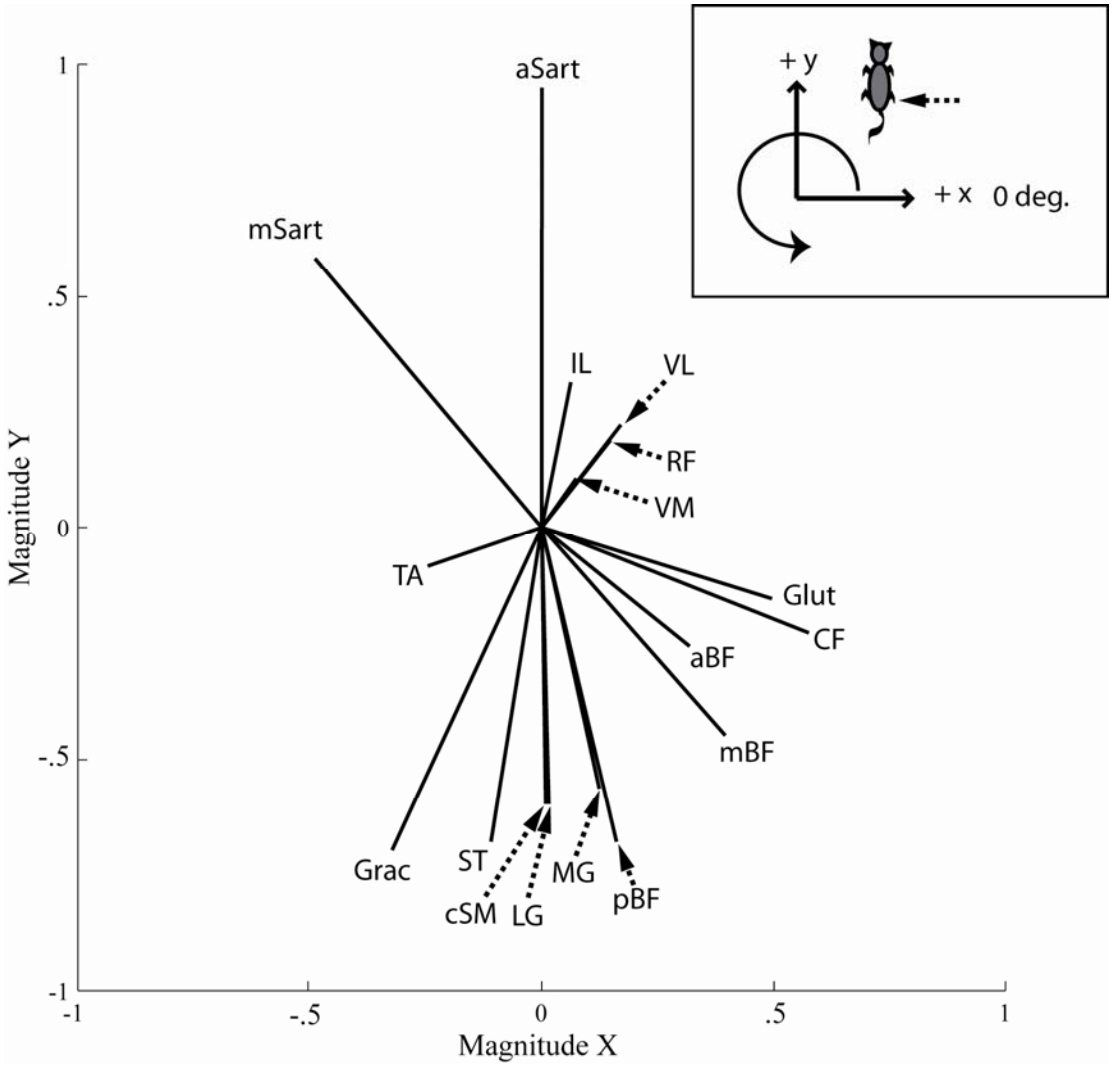

Figure 4.2: Projected normalized magnitudes in the XY plane. Shows the average projected XY force of the normalized IM stimulation vector for all muscles surveyed. Data was collected in the Right hindlimb. It is noted that most muscles have strong sagittal actions.

The YZ plane shows the most significant muscle actions with most muscles having a magnitude over .9. Figure 4.3 depicts the average angle and magnitude for all muscles in the YZ plane, while values are reported in Table 4.1. Magnitudes are high in this plane with all muscles except CF, Glut, and IL showing average magnitudes over .9. VM, RF, cSM, and LG all have magnitudes .99 and higher showing that their primary action is in the YZ plane. Additionally, muscles that were shown to have the least action in the XY

plane (VM, VL, RF, and TA) are shown to have large Z components with actions mostly directed ventrally or dorsally.

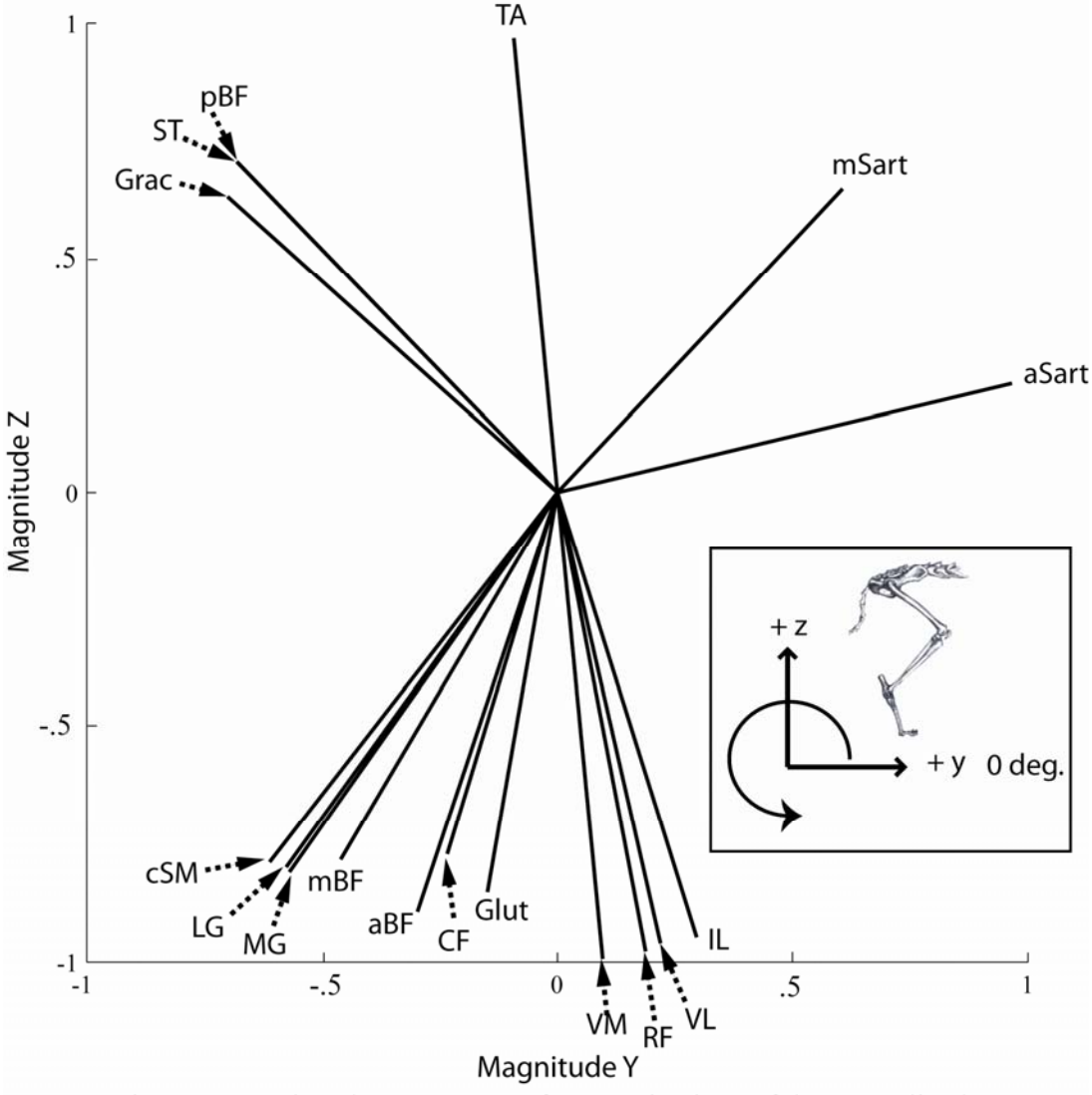

Figure 4.3: Projected normalized magnitudes in the YZ plane. Depicts the average YZ force projection of the normalized IM stimulation force data for all muscles surveyed. Muscles were shown to have large actions in the YZ plane.

4.3.2 Individual muscle actions

The RF and TA muscles have small force actions in the XY plane and primarily act in the downward and upward (Z dimension) respectively. Both muscles demonstrate variability in their XY angles across experiments; however magnitudes are consistently small. This

indicates that their primary action is in the Z axis with RF giving a strong downward force and TA a strong upward force.

The VM and VL muscles, like the RF muscle, show strong downward (negative Z) action with small force production in the XY plane. The VL muscle on average has a stronger action in the XY plane with .28 magnitude verses the .13 magnitude average of the VM muscle. The VL muscle provide more lateral action than the VM muscle, corresponding to the anatomical insertion of the VL onto the lateral edge of the patella contrary to the VM muscle insertion medially.

The MG and LG muscles have similar actions with medium strength in the XY plane and LG acting more medially than MG. The LG muscle produces force more medially than the MG muscle which corresponds to the gastrocnemius tendon twisted insertion onto the calcaneous. The MG and LG muscles both have medium actions in the XY plane giving .58 and .6 magnitudes respectively. The LG muscle demonstrates a slightly more caudal action seen in the YZ plane giving it slightly more action in the XY plane.

The CF and Glut muscles demonstrate lateral actions while the Grac muscle pulls medially; however all give medium actions in the XY plane. The CF and Glut muscles have similar actions as predicted by their similar anatomical position but the CF muscle has a stronger action in the XY plane with magnitude of .62 compared to the Glut muscle's .52. The Grac muscle has the second highest action of the muscles surveyed in

the XY plane with a normalized magnitude of .77. It has a strong medial action and is shown to pull upward (positive Z).

The cSM and ST muscles show clear differentiation although both are predicted to have the same anatomical actions. While both muscles are described as hip extensors and knee flexors, the cSM produces a downward force while the ST muscle produces an upward force. The knee flexion action appears stronger in the ST muscle which corresponds to its more distal insertion along the tibia. The ST muscle has more action in the XY plane with a magnitude of .69 as compared to .60 for the cSM muscle. However, generally it appears that there is a good deal of differentiation in the hamstring muscle groups.

Each of the three portions of the biceps femoris muscle (aBF, mBF, and pBF) was studied and demonstrated unique actions. The regions have increasing action in the XY plane with magnitudes of .41, .60, and .70 respectively. In addition, the regions slow a shift from the lateral action of aBF to a mostly caudally directed force of pBF. However the most notable difference is present in the Z action of each portion. While the aBF and mBF portions demonstrate a downward action the pBF muscle acts to produce an upward action which likely corresponds to its distal insertion along the tibia.

The IL, aSart, and mSart muscles have similar forward directed actions but subtle differences in magnitude and Z direction. The aSart muscle has the strongest action in the XY plane with magnitude of .95. The mSart muscle has a medium action in the XY plane with a magnitude of .76 while the IL muscle has the smallest action .32.

Correspondingly, aSart has the strongest rostral action and both mSart and aSart have a slight upward action (positive Z). The IL muscle alternatively has a downward action similar to the VM and VL muscles. The IL muscle is the most laterally acting muscle while mSart acts more medially than aSart corresponding to their anatomical actions.

4.3.3 Effect of inter-limb spacing

Variability across experiments in XY angles was greater at the long conditions while variability in XY magnitudes was greater at short conditions. Figure 4.4 and 4.5 show the XY angle and magnitude responses, respectively, from muscles that generated statistical differences in either parameter. The bar graphs (top) of the figure represent the numerical value of the angle or magnitude while the lower portion graphically depicts which values were statistically different. The SS and S conditions showed the least angle variability across experiments, while the L and LL conditions were more variable in nature. VM, RF, TA, and IL (L) and VM, VL, RF, pBF, ST, and IL (LL) generated standard deviations higher than 25 degrees. In contrast, the XY magnitudes were more variable across experiments at the S and SS conditions. The mBF, CF, and Glut muscles showed standard deviations greater than .20 at the SS condition and mBF, cSM, and aSart did so at the S condition. Conversely, only aBF and mSart (L) and mSart (LL) muscles showed large standard deviations at the longer conditions.

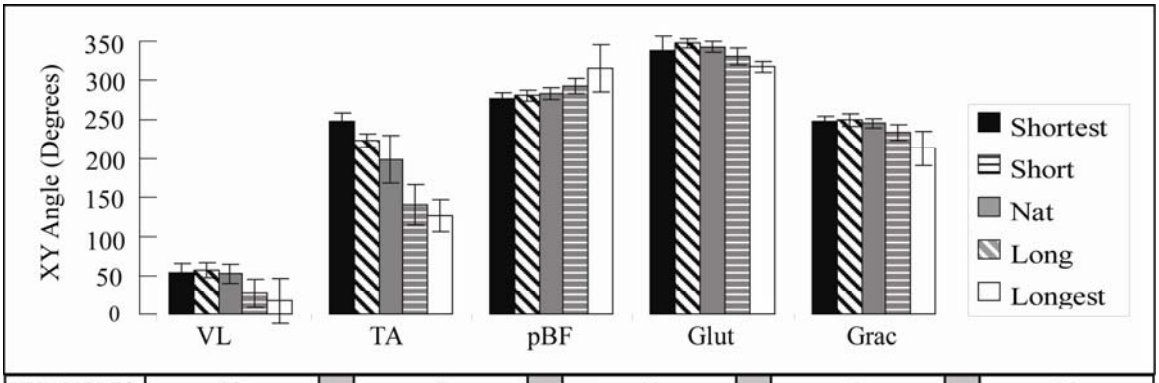

XY ANGLES	SS						S						N						L						LL				
	ss	s	n	l	ll		ss	s	n	l	ll		ss	s	n	l	ll		ss	s	n	l	ll		ss	s	n	l	ll
VL	X				■			X			■				X		■					X			■	■	■		X
TA	X		■	■	■			X		■	■		■		X	■	■		■	■	■	X			■	■	■		X
pBF	X				■			X			■				X		■					X			■	■	■		X
Glut	X							X			■				X							X				■			X
Grac	X				■			X			■				X		■					X			■	■	■		X

Figure 4.4: Graphical and statistical quantification of the XY projection's angle at different stance conditions. Shows the normalized IM stimulation force vector projected XY vector's angle at different stance conditions. Only muscles that demonstrated statistical different position affect are depicted. The numerical values and standard deviations for each muscle under each stance condition are depicted (top) along with a visual depiction of their statistical uniqueness (bottom). All conditions were compared against one another. There are 5 major column headings in capital letters (SS, S, N, L, and LL) and 5 minor column headings in lower case letters (ss, s, n, l, ll). Each box represents the comparison between that minor column condition to the major column condition. A black box demonstrates that the minor column condition is statistically different from the major column condition. An X is used when the minor column condition is compared to itself in the major column condition.

Example: The VL muscle's ll (minor column) condition was found to be statistically different from the SS, S, and N (major column) conditions; however ll (minor column) is statistically similar to the L (major column) condition.

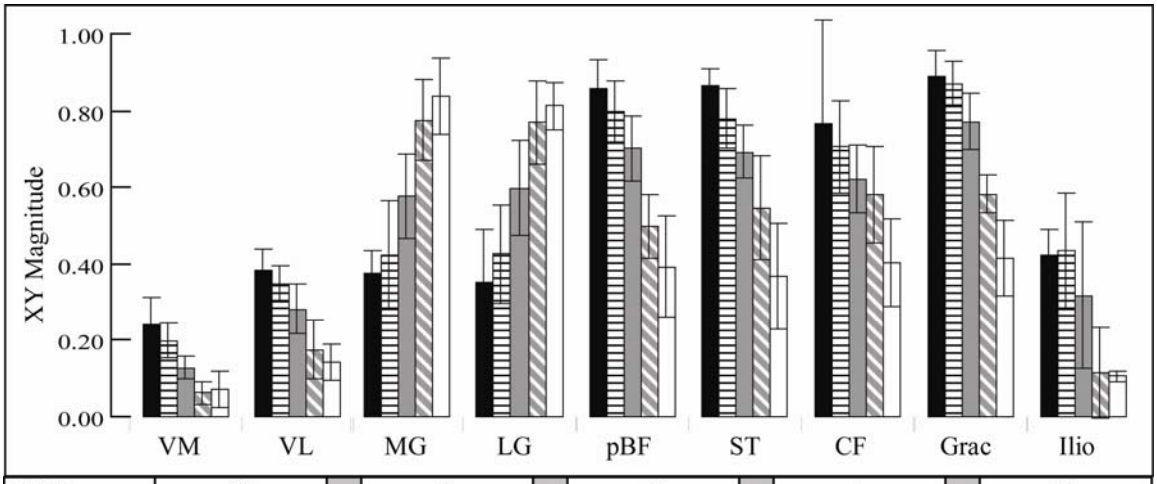

XY Mags	SS					S					N					L					LL				
	ss	s	n	l	ll	ss	s	n	l	ll	ss	s	n	l	ll	ss	s	n	l	ll	ss	s	n	l	ll
VM	X						X						X						X						X
VL	X						X						X						X						X
MG	X						X						X						X						X
LG	X						X						X						X						X
pBF	X						X						X						X						X
ST	X						X						X						X						X
CF	X						X						X						X						X
Grac	X						X						X						X						X
Ilio	X						X						X						X						X

Figure 4.5: Graphical and statistical quantification of the XY projection's magnitude at different stance conditions. Shows the normalized IM stimulation force vector's projected XY vector's magnitude at different stance conditions. Only muscles that demonstrated statistical different position affects are depicted. The top shows the numerical value and standard deviation for each muscle under each stance condition while the bottom shows a visual depiction of statistical significance (see Figure 4.4 for description).

The XY angles demonstrated little statistical difference except under the LL condition (Figure 4.4). While pBF, Glut, VL, and Grac muscles showed statistical differences, the first four conditions were statistically the same and only the LL condition was unique. The Glut muscle showed even less statistical difference with only the S and LL conditions being statistically different. The only muscle that showed statistical difference between other conditions was the TA muscle which generated statistically significant decreases in XY angle. The VL, TA, Glut, and Grac muscles showed a clockwise (decreasing angle) shift while the pBF muscle showed a counter-clockwise (increasing angle) shift in XY angle.

Alternatively, about half the muscles surveyed demonstrated statistical difference in XY magnitudes. The VL, VM, MG, LG, pBF, ST, CF, and Grac muscles all demonstrated statistically differences in the XY magnitudes. The CF muscle only showed slight differences with the LL condition. Most muscles including VM, VL, pBF, ST, CF, and Grac showed decreasing magnitude under longer conditions; however MG and LG showed increased XY magnitude at longer conditions.

Twelve muscles (VM, VL, RF, MG, LG, TA, pBF, ST, CF, Glut, Grac, Ilio) showed statistically different YZ angle shifts while only four muscles (VL, mBF, pBF, and aSart) demonstrated YZ magnitude shifts. Figure 4.6 show the angle responses for the YZ plane. All muscles that show statistically differences show a clockwise (or decreased angle) shift; however this shift is not by a consistent angle. Similarly to the XY angles, the YZ angles show more variability in the longer conditions. Only aSart (S) shows a standard deviation over 25 in the SS, S, and N conditions while LG, CF, aSart, and mSart (L) along with LG, aSart, and mSart (LL) show high standard deviations at longer stances. YZ magnitudes were very high demonstrating that most muscles have their strongest action in the Z axis. Only the CF, Glut, and mSart had magnitudes less than .90.

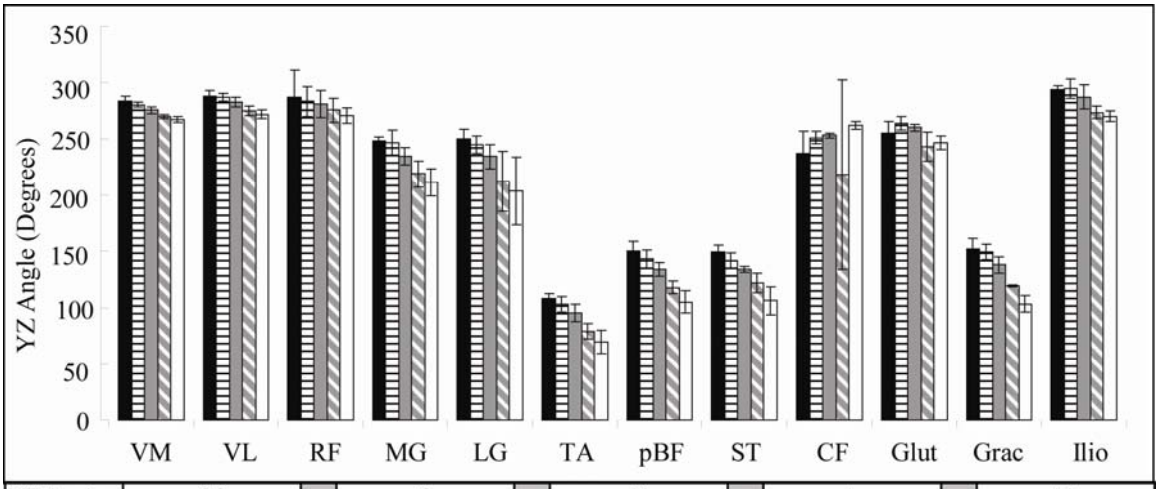

YZ Angles	SS						S						N						L						LL					
	ss	s	n	l	ll		ss	s	n	l	ll		ss	s	n	l	ll		ss	s	n	l	ll		ss	s	n	l	ll
VM	X							X							X							X							X
VL	X							X							X							X							X
RF	X							X							X							X							X
MG	X							X							X							X							X
LG	X							X							X							X							X
TA	X							X							X							X							X
pBF	X							X							X							X							X
ST	X							X							X							X							X
CF	X							X							X							X							X
Glut	X							X							X							X							X
Grac	X							X							X							X							X
Ilio	X							X							X							X							X

Figure 4.6: Graphical and statistical quantification of the YZ projection's angle at different stance conditions. Shows the normalized IM stimulation force vector's projected YZ vector's angle at different stance conditions. Only muscles that demonstrated statistical different position affects are depicted. The top shows the numerical value and standard deviation for each muscle under each stance condition while the bottom shows a visual depiction of statistical significance (see Figure 4.4 for description).

When the average force vectors for all the muscles surveyed are graphed collectively, non-sagittal forces are notably diminished at longer stance conditions. Figure 4.7 shows the average force vector for all muscles (XY plane) at each of the five stance conditions. While all of the forces appear diminished at the longer stance, the most prominent change in magnitude is represented in the non-sagittal (medial/lateral) forces. There also appears to be a convergence of several of the force trajectories such that many of them overlap at the long stance condition. In general, the longer stance conditions appear more constrained with less variation in force trajectory than the shorter stance conditions.

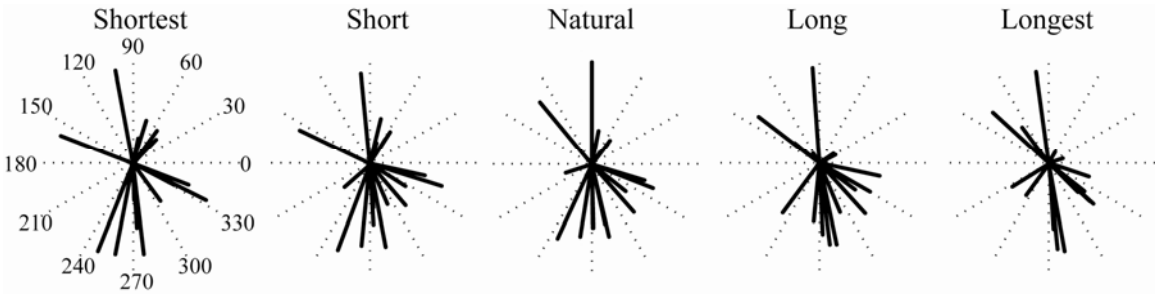

Figure 4.7: All XY force projections for each of the 5 stance conditions: Depicts the XY projections of the normalized IM stimulation vector for all muscles surveyed at different stance conditions. Note that the non-sagittal actions become smaller in magnitude at the longer stances.

4.4 Discussion

4.4.1 Summary

Under natural stance conditions, most muscles generated XY angles that had small variability; however the VM, TA, RF, and mSart muscles were found to be uniquely more variable. The VM, TA, and RF muscles were also shown to have some of the smallest magnitudes in the XY plane as their primary force generation is in the Z dimension. In comparison to the YZ plane, most muscles had small actions in the XY plane and there is a lack of muscles with strong forces in the medial-lateral direction. The lack of strong medial-lateral forces appeared to increase as stance condition was lengthened. Stance condition alteration also generated statistically significant differences in XY magnitudes (52% of muscles) and YZ angles (70% of muscles).

4.4.2 Implications for muscle recruitment

We had two expectations based upon our hypothesis that muscles are selectively activated based upon their potential counteractive endpoint force. The first was that the EMG tuning curves generated in the intact and decerebrate cat would be directed oppositely (180 degrees) from the muscle endpoint ground reaction force. Figure 4.8 presents the EMG tuning curves' principal direction and standard deviation (data from

Chapter 2) along with the IM stimulation force vector and standard deviation. Despite being collected in different animals, the EMG principal directions and the force vectors generated in response to stimulation are still oppositely directed. This supports our hypothesis by demonstrating that muscles are activated in the directions that they produce the most counteracting endpoint force. Further illustrating this point, muscles with similar mechanical actions are activated differentially based upon that individual's muscle's ability to oppose the perturbation.

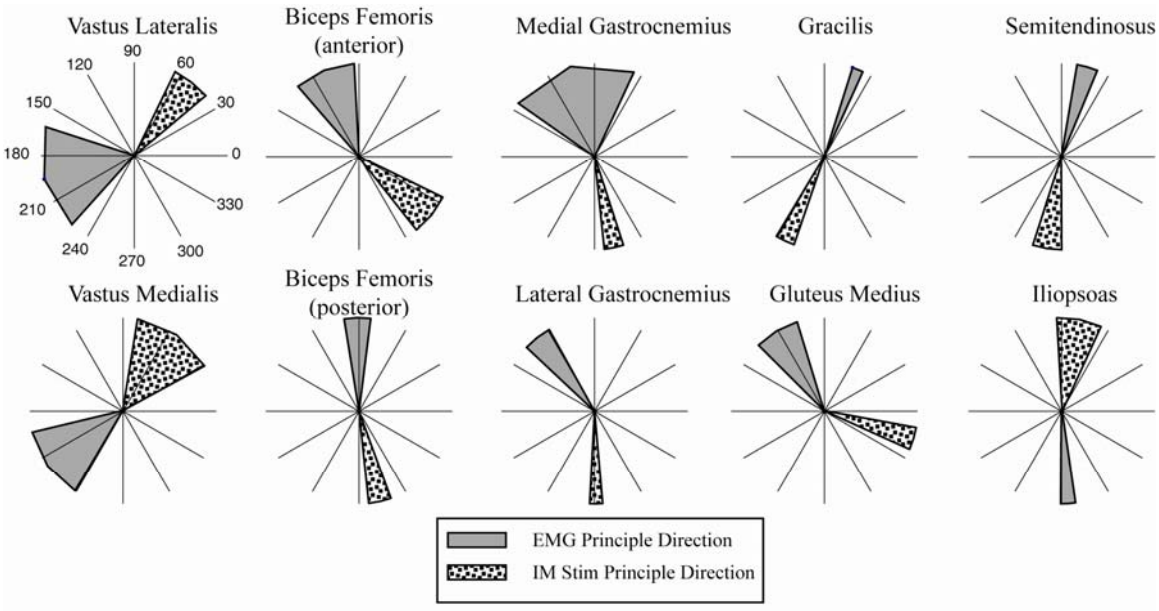

Figure 4.8: Comparison of EMG and IM stimulation principal directions. Graphs 1) the average EMG principal direction and standard deviation of the muscular responses of the decerebrate cat to horizontal support surface perturbations (gray) (data from Chapter 2) and 2) the average IM stimulation XY projection of the normalized vector (dotted).

IM stimulation force trajectories correctly predict muscle differentiation between the hamstring (aBF, mBF, pBF, cSM, and ST) and quadricep (VM and VL) muscles. The intact (Chanaud and Macpherson 1991) and decerebrate (Chapter 2) animals demonstrate that regions of the biceps femoris muscle have directionally unique EMG activation patterns. The anterior portion of biceps is activated when subjected to lateral perturbations while the middle and posterior portions show increasingly rostral activation

patterns. These regions were also found to have different endpoint forces which correspond to the directional activation of each region. The anterior portion has forces that act medially while middle and posterior biceps show increasingly more caudal force trajectories. Figure 4.8 shows the aBF and pBF EMG and IM stimulation forces demonstrating the endpoint force differentiation. The IM stimulation force trajectories also accurately predict the differentiation between the additional hamstring muscles and the quadriceps. Our data from the decerebrate cat shows that the cSM muscle is activated more laterally than the ST muscle. This is reflected in the IM stimulation endpoint forces as depicted in Figure 4.8. The VM muscle is activated more medially than the VL muscle, corresponding to the IM stimulation forces as well.

While the MG and LG muscle's EMG principal directions and IM stimulation forces are directed oppositely, their IM stimulation forces do not clearly predict the EMG activation direction. The force trajectories would imply that the MG muscle would be activated more medially during postural perturbations with LG being activated more laterally. Our report from the decerebrate cat demonstrates that on average the MG muscle is activated more laterally than the LG muscle. While the IM stimulation forces only represent a 10 degree shift in direction, we suspect this is a real result as standard deviations are low. We propose two hypotheses for why this deviation occurs: 1) the twisted insertion of the gastrocnemius tendon redirects forces to the ground and 2) LG receives most of its sensory feedback from MG (Eccles et al. 1957) which likely influences its EMG principal direction.

Previous reports of the torque generated by the muscles of the shank also report that the MG muscle has more lateral actions than the LG muscle (Lawrence et al. 1993; Lawrence 1999). This mirror refection is likely the result of the twisted insertion of the gastrocnemius tendon into the calcaneous causing a reflection of the forces generated by each portion of the gastrocnemius muscle (Crouch 1969). Three-dimensional anatomical models that account for this twisted insertion of the tendon also project the reflection of the medial and lateral portions of the gastrocnemius muscle (Burkholder and Nichols 2004). Therefore if one takes into account the anatomy, our hypothesis is upheld with the MG and LG EMG being directionally opposite to their projected IM stimulation forces.

When evaluating the principal directions of MG and LG they are much more similarly directed than the force trajectories generated through IM stimulation. The MG muscle, which has strong excitatory connections to LG, may mediate the direction of LG muscular activation during support surface perturbations. This could also explain why the IM stimulation force directions are not perfectly opposed.

Our second expectation, based upon our hypothesis, was that muscles demonstrating variable tuning curves (RF, TA, Sart, MG, VL, and VM) would generate variable ground reaction forces as well. Initial reports from the intact cat noted that the RF, TA, and Sart muscles had variable tuning curves within an animal (Macpherson 1988b). Our report demonstrates that these muscles are the most variable across animals. In the cases of RF and TA, this is likely due to their small actions in the XY plane. These muscles may be utilized as stabilizers and anti-gravity support and therefore do not have a discrete region

of activation as other muscles with more XY power. EMG data from the decerebrate cat also demonstrates that the VM and VL muscles are some of the most variable muscles across animals (Chapter 2). It also was reported that both VM and VL have small XY actions. Therefore, muscles that have poor XY actions tend to be activated more variably.

Our results, like that in the intact animal, demonstrate magnitude but not angle shifts with inter-limb spacing conditions. It has been shown in the intact cat and human that changing limb spacing can alter the amplitude of the tuning curves but has little effect of direction (Henry et al. 2001; Macpherson 1994a). Our hypothesis that muscles are recruited based upon their ability to generate counteracting force would imply that the diminishing amplitude of the muscle responses would also be seen in the IM stimulation forces. Our results demonstrate this correspondence showing that approximately half the muscles surveyed showed magnitude shifts but only a handful showed direction changes. Additionally, those that did show direction changes did so only under the LL condition. Therefore SS, S, N, and L were all statistically the same. The TA muscle did show a substantial angle shift, however, this muscle has not been reported in the intact animal so it is not possible to compare that muscle's activation pattern. We would hypothesize that it would show directional changes with inter-limb spacing alterations.

4.4.3 Sensory implications

If muscles during postural perturbations are indeed activated selectively based upon their potential counteracting endpoint point force, the sensory motor transformation must be able to represent this information. Global sensory systems, such as cutaneous and

vestibular feedback, are certainly critical for appropriate postural adjustment; however they lack selectively. Conversely, muscle receptors that give muscles specific feedback would make likely sources to relay information about the internal changes within the muscle that influence its ability to compensate for a perturbation. If a muscle is lengthened through a limb perturbation, that same muscle would generate an opposing force if contracted. Therefore muscle spindles, which give feedback on muscle length, would provide important feedback on which muscles can generate counteractive forces. We have previously demonstrated that muscle spindles produce similarly tuned and directed activation patterns to muscle activity during support surface perturbations. Furthermore, muscle spindles are known to respond not only to length changes, but also the rate of change in length (Kandel et al. 2000). As the short latency elements of muscle activation are known to change based upon the velocity of the perturbation (Diener et al. 1988), this further implies that muscle spindle feedback may be critical to establishing proper activation patterns.

4.4.4 Comparison to model results

Data from the decerebrate cat does demonstrate some alterations from model predictions. Several of the muscle forces reported by a three-dimensional anatomical model have very small non-sagittal actions (Burkholder and Nichols 2004). Our data demonstrates that many of these muscles, including the gracilis, semitendinousis, and biceps femoris muscles, have strong non-sagittal actions. While non-sagittal forces are smaller in general than those in the Y and Z dimensions, they are more substantially present than the model predicts. This observation suggests an important role for the metatarsophalangeal

joint, intrinsic musculature of the foot, and other soft tissue structures (ligaments and fascial structures) in the production of non-sagittal forces in the hindlimb as they are not present in the current model. Other deviations from model predictions include muscle actions at different stance conditions during locomotion. Previous models have assumed that the actions of the hindlimb musculature rotated with the limb (hip to toe) axis (Kaya et al. 2006). However, our results indicate that while the force vectors created through stimulation do rotate in the YZ plane as stance condition is altered, they do not show a consistent rotation across muscles. Some muscles are affected dramatically, while others show little or no rotation with stance condition. The quantitative analysis of limb axis rotation affect on the ground reaction forces of individual muscles provided by this report will provide future improvement to model assumptions of muscle ground reaction forces.

4.4.5 Force constraint strategy

Our hypothesis that the biomechanical constraints of individual muscle actions generate the constrained appearance of the force constraint strategy was upheld. The muscles surveyed appear to have a lack of force generating potential in the medial-lateral directions, which corresponds to the force constraint strategy observed in the intact and decerebrate cat. This strongly suggests that the force constraint strategy arises from the stronger rostral/caudal actions of the limb. While the limb does have non-sagittal force generation power, it seems to be smaller than that of the rostral/caudal dimension. This has been previously demonstrated in the feasible force set generated from the cat hindlimb model, which showed that the limb could generate substantially more force in the rostral/caudal direction than medial/laterally (McKay et al. 2007). Our report further

demonstrates that the mechanical actions of muscles likely contribute to the force constraint alteration at different stance conditions. We reported that the medial/lateral forces are larger at shorter stance conditions than at longer. Furthermore, there appears to be a consolidation or overlap of force trajectories at the longer stance condition.

The knowledge that mechanics are in large part responsible for the force constraint strategy as opposed to a neurally imposed constraint to limit the degrees of freedom raises some interesting questions about the control mechanisms driving these responses. Why would the limb structure be designed to have such small medial/lateral actions? When subjected to a medial/lateral perturbation the limb is more effective at generating downward force than the medial/lateral compensatory force. However, we would argue that this additional downward force is necessary for maintaining balance. When a cat or human is perturbed rostral/caudally, their limbs (hindlimb and forelimb pairs in cat) are loaded or unloaded equally. The primary force needed to counteract that perturbation is directed opposite to that perturbation. However when perturbed leftward, for example, the subject's right leg is loaded while the left leg is unloaded. Therefore, in order to maintain balance the subject must not only generate a rightward force at the feet but also generate more downward force to compensate for the additional weight of the body on the right leg. This report demonstrates that each leg can generate more lateral force than medial. Correspondingly the loaded limb (right) is also the limb that has the most counteractive force potential (laterally or leftward). Finally as having one loaded limb is more stable than no loaded limbs, medial/lateral perturbations require less medial/lateral counteractive force. When both limbs are unloaded, a larger counteractive force

(rostral/caudal) is necessary because the torque generated by gravity at the COM is larger. Therefore, the musculature is designed in such a way to generate a force constraint strategy as those are the necessary mechanical actions to maintain balance.

4.4.6 Limitations of hypothesis

Our hypothesis states that muscles are activated based upon their potential counteracting force; however this hypothesis likely does not hold for volitional tasks. It has been demonstrated that muscles of the wrist can be activated in non-mechanically favorable directions (Fagg et al. 2002; Hoffman and Strick 1999). We would argue that the wrist's architecture is very complex and mechanical actions difficult to ascertain. Furthermore, the wrist does not have the same utility for weight support; therefore, its musculature is likely adapted to a different set of mechanical tasks. Still, one study from the human leg also demonstrated a small deviation from a muscle's preferred direction and its mechanical action (Nozaki et al. 2005). However, all of these articles (including the wrist) were during volitional activation of muscles. It is likely that during a voluntary task muscles can be recruited in variety of directions that may diverge from their strict mechanical action. Co-contraction may be necessary for certain movements. Additionally, several of these articles assume a restrictive direction of mechanical action. Muscles are often made up of several compartments and certainly many motor unit populations such that a muscle's mechanical action likely can vary over several degrees during different types of motor tasks. Regardless, it is likely that that the sensory mechanisms driving this directional tuning are highly influenced by limb architecture. Therefore, our hypothesis that muscles are activated selectively based upon their potential

counteracting force likely holds the most truth under conditions where the end goal is to return to the initial starting configuration like the postural disturbance scenario.

CHAPTER 5

EFFECT OF THE LOSS OF CUTANEOUS FEEDBACK ON TUNED MSUCLE RESPONSES TO SUPPORT SURFACE PERTURBATIONS IN THE DECEREBRATE CAT

5.1 Introduction

The sensory mechanisms driving appropriate muscle activation in response to balance challenges remains poorly understood. Classically radial, horizontal support surface perturbations have been utilized to examine the nervous system's response to postural disturbances. The muscular responses and subsequent ground reaction forces were found to be remarkably similar in both human and cat. Muscular activity was quantified using tuning curves, which compare increases or decreases in activity to background activation and graphed the resultant against perturbation direction. These tuning curves demonstrated that each muscle had a principal direction of activation and was generally active over about 25 percent of the perturbation space. This indicated that muscles were discriminatory in their activation, uniquely responding to the perturbation rather than responding analogously to all perturbation directions.

Sensory signals from the vestibular system, skin and muscles (Allum et al. 1998; Beloozerova et al. 2003b; Everaert et al. 2005; Macpherson and Inglis 1993; Stapley et al. 2002; Ting and Macpherson 2004) have been implicated in mediating postural responses. The relative contributions of these systems on muscle activation patterns have yet to be determined, but some progress has been made concerning the role of vestibular feedback. Vestibular loss leads to hypermetria, which destabilizes the animal (Macpherson and Inglis 1993); however, the spatial tuning properties of the responses (direction and

breadth) are little affected by the lesion, suggesting that feedback from either skin or muscle (or both) contributes in a major way to directional tuning of these responses. Some have suggested that cutaneous feedback, specifically from the plantar surface of the foot, alone could be responsible for directional muscle activation (Bloem et al. 2000; Ting and Macpherson 2004). Evidence for an important role of cutaneous feedback comes from studies showing that cutaneous inputs can affect postural stability during unperturbed stance (Meyer et al. 2004; Roll et al. 2002). However, many support the view that feedback from muscle proprioceptors must be integrated with cutaneous inputs to achieve the observed spatial tuning (Kavounoudias et al. 2001). This notion is supported by work demonstrating that cutaneous stimulation during perturbed stance does not significantly alter muscular activation (Maurer et al. 2001). Consequently there remains a significant debate about the contribution of skin and muscle receptors in postural control.

We developed the modified premammillary decerebrate cat preparation specifically to further evaluate the sensory mechanisms driving appropriate muscle activation in responses to support surface perturbation. We have previously demonstrated that this preparation consistently generates muscle activation patterns and subsequent force trajectories typical of the intact animal. This preparation allows us the flexibility to isolate the proprioceptive (cutaneous and muscle receptors) system from other sensory influences. Specifically, fixation of the head largely precludes both visual and vestibular feedback. Therefore, the resulting muscle responses are generated mainly through feedback of skin and muscle receptors. Therefore, we can disrupt the cutaneous system

acutely and observe the system's response without 1) the influence of the vestibular and visual systems and 2) the adaptation that likely would occur if completed chronically. We have previously hypothesized that muscle receptors, specifically muscle spindles, drive the directionally appropriate muscle activation during postural disturbances. Therefore, we expect that loss of cutaneous feedback from the foot soles will not alter the directional properties of muscle activation.

5.2 Methods

5.2.1 Experimental protocol

Data from three cats, used in accordance with the issued standards of the National Institutes of Health and the Emory Institutional Animal Care and Use Committee, will be described in the following report. These three animals have been previously described in Chapters 2 and 3. Animals will be referred to by the date of the experiment (9/11, 10/8, and 6/8). Under isoflurane anesthesia, a tracheotomy was performed to monitor anesthesia levels and an IV was inserted in the external jugular vein for hydration and drug delivery. Bipolar electrodes, constructed from Teflon coated braided wire, were inserted into the medial gastrocnemius (MG), lateral gastrocnemius (LG), soleus (Sol), vastus lateralis (VL), vastus medialis (VM), semitendinosis (ST), semimebranosis (SM), gracilis (Grac), iliopsoas (Ilio), anterior biceps femoris (aBF), posterior biceps femoris (pBF), and gluteus medius (Glut) muscles.

We used a modified premammillary decerebration technique, which has been previously described in detail in Chapter 2 and 3. The technique modifies the traditional locomotion

inducing premammillary decerebration with a vertical transection near the subthalmic nucleus. This additional transection preserves postural tone and reactivity but significantly disrupts the locomotion patterns typically associated with the premammillary preparation.

After the initial surgery, the animal was positioned using a stereotaxic frame to support the head while a clamp at the based of the tail and a sling supported the body. The sling was detached after isoflurane was completely removed and weight bearing established. Anatomical measurements, collected on intact animals during standing, were used to position the hip height, head height, and paw spacing (both transverse and sagittal planes). The toe pads of all four limbs were fixed with glue and tape to four ATI force transducers. All force transducers were oriented identically such that positive X was rightward, positive Y was rostral, and positive Z was upward. The natural turnout of the foot was used for each animal. The bipolar electrodes were attached to a preamplifier, with a gain of 200 (overall gain of 1000) and bandpass filter from 10Hz - 1150Hz. Electromyographic (EMG) data from the electrodes and three dimensional force data from the transducers were collected using a LabView program designed specifically for this project.

Once the animal was removed from anesthesia, the support surface was translated in 16 different, horizontal directions using two motors: rotational and linear. The rotational motor positioned the linear motor for the perturbation. This technique ensured a linear perturbation. In experiments 9/11 and 6/8, the support surface was perturbed 8cm over

400ms with an acceleration of .5 (m/s^2). In the third animal, the platform was moved 4cm over 400ms. Previous reports indicate that the amplitude of the perturbation does not alter direction and breadth of muscular activation patterns (Diener et al. 1988). The perturbation parameters were chosen based upon previous studies in intact cats (Macpherson 1988a; b) for comparison purposes. Unique to the decerebrate cat, the animal's head and tail were in a fixed position. Thus the limbs were perturbed, held at the extended position for 1000ms and then returned 4cm over 400ms to the initial position. In one animal (10/8) the hold position was only 500ms.

5.2.2 Cutaneous dennervation

Data was collected before and after cutaneous dennervation of the foot pads. After collection of the control data, the medial side of the ankle was opened with a scalpel blade and the tibial nerve identified. The tibial nerve was then crushed repeatedly until the nerve was destroyed. Some two experiments the nerve was cut was performed to ensure that our crush technique resulted in complete dennervation. There were no statistical differences and therefore all data after crush/cut was included for statistical comparison to control. For two of the three experiments a gauze pad with lidocaine was placed over the tibial nerve before crushing to reduce the noxious stimulus of the crush. The tibial nerve innervates the foot soles (or pads of the feet) (Crouch 1969). In addition, the tibial nerve has some motor innervation of the small musculature of the foot. After tibial crush, perturbations were delivered in the same manner as during the control trials. Data were taken until the animal was no longer responsive.

5.2.3 EMG quantification

EMG data were notch filtered for 60Hz noise, demeaned, high passed at 30Hz (to remove movement artifacts), and rectified. Latencies were estimated by visual inspection of an increase in EMG magnitude or firing frequency. The muscle responses were calculated during the duration of the perturbation (400ms) by evaluating the mean EMG activity and subtracting the background mean EMG activity from a 400ms window pre-perturbation. These mean responses were graphed against perturbation direction to create a tuning curve. Tuning curves were normalized to maximum activation before quantification. When quantifying the responses, each curve was evaluated on individual trials. However, figures are a depiction of three averaged traces together.

In order to quantify the tuning curves, the breadth and principal direction were calculated for each muscle response. The breadth quantifies the responsiveness of a muscle to multiple directions. A large breadth represents a muscle that is active over many perturbation directions. The breadth of the response is calculated using the area under the normalized excitatory and inhibitory tuning curves. The principal direction represents the maximum direction of activation. To determine the principal direction, muscle responses from each direction were converted to polar coordinates using the perturbation direction as theta. Each response was then converted to a vector and x and y components were averaged to find the primary vector or principal direction of the response. The principal direction represents the average direction of all directional muscle activity. Tuning curve quantification was only computed for trials where the muscle responded for all 16 directions. Aside from visualization of raw traces, the principal direction magnitude was

used to ascertain the significance of the response. Elimination of tuning curve data was rare and its occurrence was not significantly increased after tibial nerve crush. In order to compare the tuning curves before and after tibial nerve crush, the principal direction and breadth were plotted against each other under each condition. If the ratio of the principal directions before and after crush lies along the unity line, then the principal direction was not altered substantially by the crush.

5.3.3 Force quantification

Force data from the horizontal plane (X: medial-laterial, Y: rostral-caudal) were analyzed for the purposes of this report. Trials that included stepping behavior or where the foot was lifted from the force transducer were excluded from analysis. Force data were demeaned and low passed at 30Hz. The change in force per ms was calculated by finding the area under the force curve for 100ms time intervals and dividing by 100ms. The initial time period evaluated was 50-150ms. This time interval was chosen because it eliminates the inertial properties associated with the motors during the first 50ms and it corresponds to the automatic postural response reported in intact animals (Macpherson 1988). Additional time intervals were analyzed to evaluate the extended force responses past the typical automatic postural response time period. To visualize and further quantify the force constraint, the average change in force for all perturbation directions was graphed from origin (see Figure 5.3).

The constraint or clustering of the force responses was further quantified using principal direction and stiffness ellipses. Principal directions were calculated by first separating

the two populations based upon their squared Euclidean distance from one another using the matlab function kmeans. The principal direction of each population was then calculated by averaging the remaining force vectors and determining the direction of the resultant vector. The shape of the stiffness ellipses, which quantifies the stiffness of the limb to horizontal perturbation, quantifies the amplitude of the constraint. Ellipses were derived by dividing the 16 force vectors by the distance traveled in the x and y directions appropriately. The shape of the ellipse was calculated by dividing the minor axis by the major axis. A shape close to 1 represents a circle or non constrained force responses, while a shape close to 0 represents a line or highly constrained force responses.

5.3.4 Statistics

Statistical comparison of EMG and Force parameters before and after nerve crush were completed with a two-tailed T-test of equal variance. F-tests were used to confirm equal variance and lillifore tests used to confirm normalized distributions in samples with more than 4 observations. In the rare case that the populations exhibited non-normalized distributions a Kolmogorov-Smirnov test, which does not assume normalized distribution, was utilized. In the rare case that the F-test indicated an unequal variance, a T-test of unequal variance was performed. In order to be included in statistical analysis, the muscle must have responded in a minimum of three trials for the full set of 16 directions in each animal. Degrees of freedom for statistical significance were adjusted appropriately based upon the number of observations in each muscle. T-tests were preformed at a .95 confidence interval or p-value of .05.

5.4 Results

Background muscle activity was significantly disrupted after cutaneous dennervation; however the excitatory response remained intact. Figure 5.1A depicts raw EMG traces (3 trials averaged together) of one muscle from each of the three experiments before and after tibial nerve crush. The dashed lines demarcate the perturbation initiation and termination. Control and Tibial nerve crush data are depicted on the same scale such that amplitude comparisons can be made. Cutaneous dennervation almost completely extinguished the tonic background activity of each muscle in all three experiments. However, the excitatory response to the perturbation remains intact. Every muscle studied, except one (VL: 9/11 expt), produced an excitatory response following crush. In addition, the excitatory responses occur at appropriate latencies, between 20 and 30 ms.

While the background activity and EMG response to perturbation are diminished, he difference between the EMG response and background activity remains essentially the same. Figure 5.1B shows the tuning curves (created by computing the difference between excitatory and background activity) before (solid) and after (dashed) Tibial nerve crush. The first three tuning curves (pBF, Glut, and Grac) correspond to the raw EMG traces shown in Figure 5.1A. While it was noted from the raw data that the excitatory response was smaller in amplitude, the tuning curves remain intact. Tuning curves appear to be very similar in shape, direction, and amplitude; however curves do appear to be more variable. Likely a result of the diminished amplitude, the tuning curves show more variable levels of activation instead of the smooth and graded tuning

curves seen during the control trials. Most notably in Figure 5.1B, the SM and aBF muscles demonstrate two peaks of activation which was likely a result of changing activation strength. Additional differences are noted in the pBF, ST, and Ilio muscles which show tuning curves of smaller amplitude after dennervation.

Principal direction and breadth was found to be mostly conserved after dennervation. T-test confirmed that all muscles, except Grac (10/8 expt) generated statistically equivalent principal directions before and after cutaneous dennervation. The Grac muscle of the 10/8 experiment, while statistically difference only represented a 9 degree shift in principal direction from 69 to 54 degrees indicating only a slight alteration in direction (Figure 5.1B). To further quantify the principal direction conservation, Figure 5.2A shows the mean principal direction of each muscle before and after cutaneous dennervation. The ratios lie very close to the unity line indicating a strong similarity before and after dennervation. Still while the principal directions were statistically indistinguishable, there was an increase in principal direction variability after dennervation with 68% of muscles showing larger standard deviations. Breadths were conserved but generally larger as demonstrated in most point lying above the unity line in Figure 5.2B. However statistical differences were only found in 3 out of 29 cases: MG (9/11), SM (9/11), and Glut (6/8). All three of these muscles showed an increase in breadth following dennervation. While statistically indistinguishable, many muscles did show a trend towards increasing breadth after dennervation. Finally, 86% of muscles showed an increased standard deviation in breadth after cutaneous dennervation.

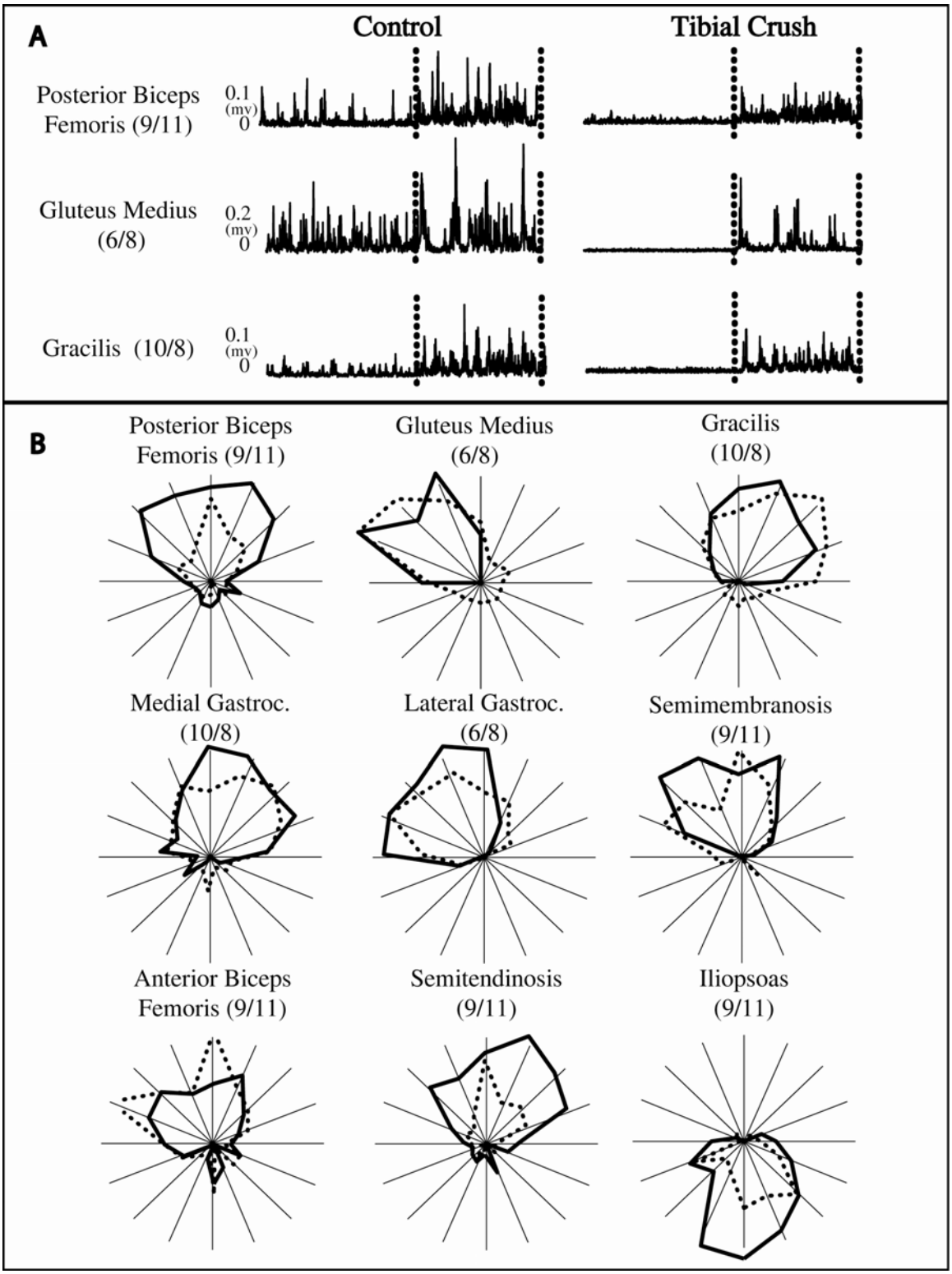

Figure 5.1: Comparison of raw EMG data and tuning curves before and after cutaneous dennervation. Shows the raw EMG traces before and after tibial nerve crush (A) along with the tuning curves under the same conditions (B)**.** The background activity in all experiments was extinguished by a strong excitatory response remains intact. Tuning curves remain intact in direction but alterations in breadth and amplitude are present.

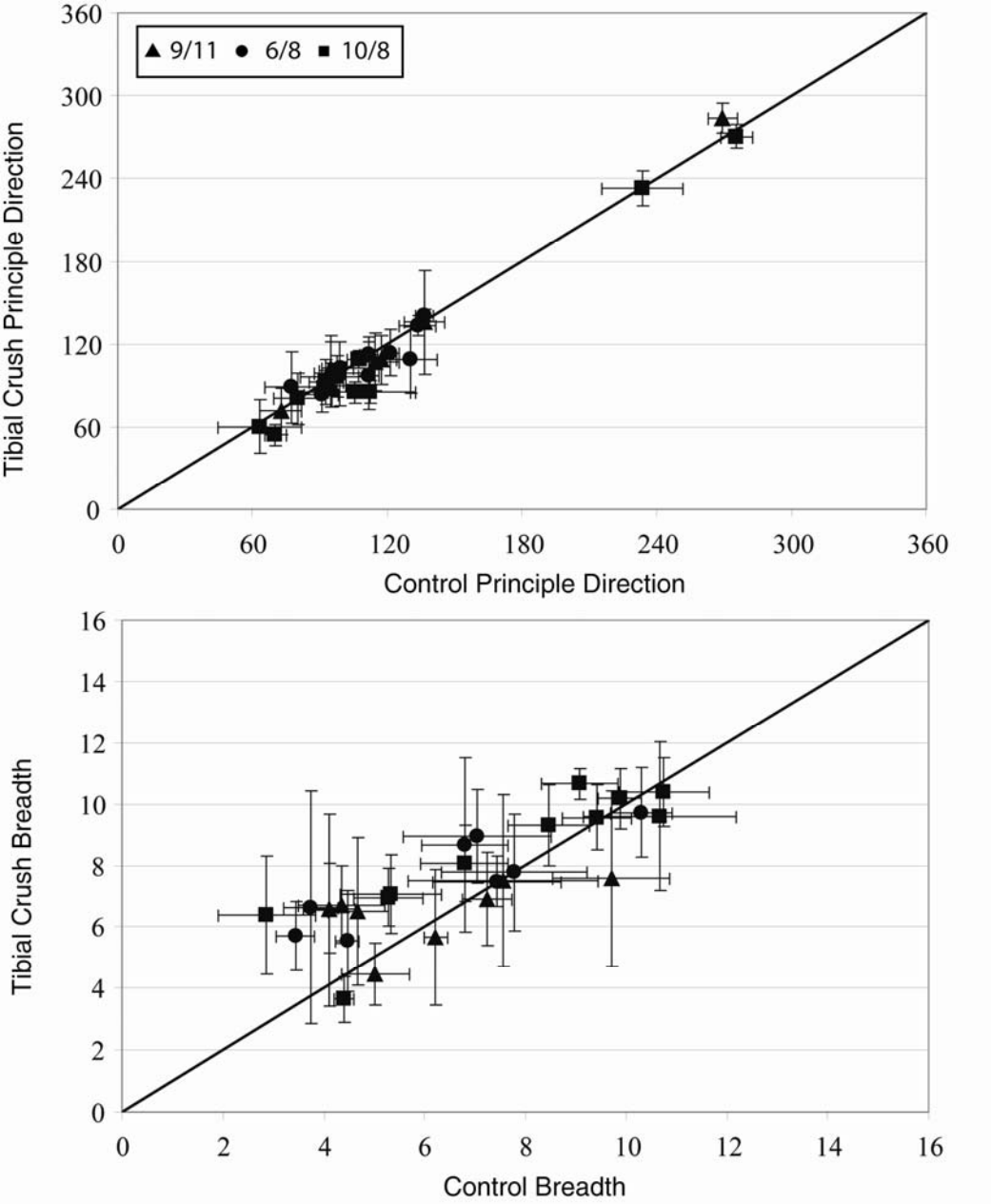

Figure 5.2: Principal direction and breadth comparison before and after cutaneous dennervation of the foot pads. Principal direction and breadth were quantified before and after the cutaneous intervention. The mean and standard deviation of the principal direction and breadth before and after intervention are depicted along with a unity line (representing a ratio of 1 between conditions) for comparison of the conditions. Principal directions were largely conserved (top) with most ratios lying near or on top of the unity line. Breadths were shown to be more variable with most muscles showing an increase in breadth after tibial crush (bottom). However, only 3 out of 29 muscles generated statistically significant differences in breadth.

Forces were generally diminished in amplitude after dennervation and showed a loss of force constraint. The diminished amplitude of the excitatory muscular response (Figure

5.1A) leads to diminished force amplitudes. However while only the right tibial nerve was crushed there was a loss force amplitude in both hindlimbs (Figure 5.3A). While the decrease in force amplitude did contribute to increased variability and alterations in the caudal force principal directions, it most notably affected the shape of the force constraint (Figure 5.3B). A statistically significant increase in shape (decrease in force constraint) of the right hindlimb was observed in all three experiments.

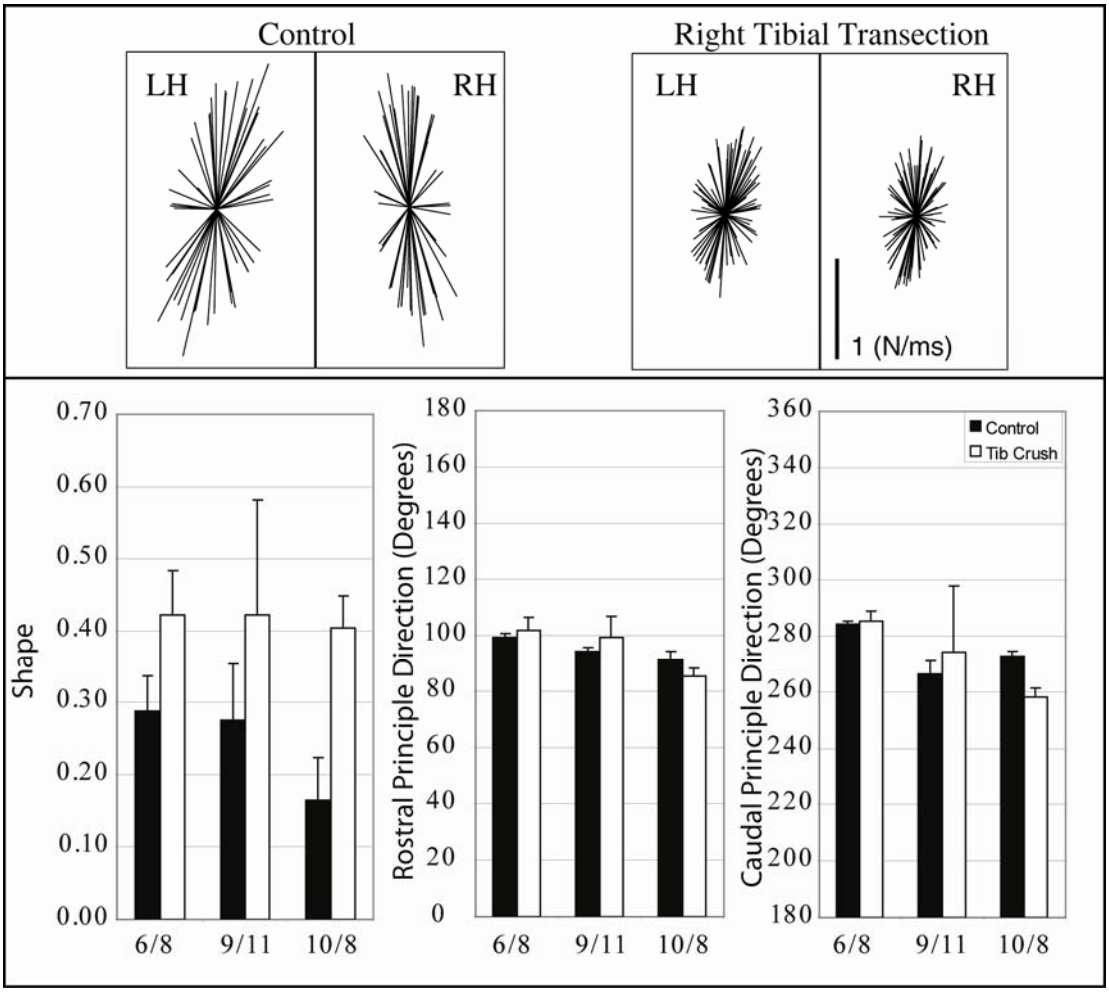

Figure 5.3: Force quantification before and after cutaneous dennervation. The horizontal force responses of the right and left hindlimb (RH, LH) for the 10/8 experiments are shown before and after cutaneous dennervation (Top). The quantification of changes in shape and principal direction for the right hindlimb in all three experiments are depicted (Below). Forces were found to be much smaller in amplitude after cutaneous dennervation and a statistically significant loss of force constraint (increase shape) was reported.

5.4 Discussion

Cutaneous feedback from the foot soles was not necessary for directionally specific muscle activation in response to horizontal support surface perturbations. All muscles surveyed, with one exception, found no statistical difference in principal direction of muscle activation after tibial nerve crush. The one exception reported a 9 degree shift in principal direction representing only a small directional shift. Further illustration of principal direction conservation is depicted in the close clustering of the ratio between control and tibial crush principal directions to the unity line (Figure 5.2A). The small standard deviations further indicate the consistency of this finding. Breadth quantification before and after tibial crush showed more differences but few that were statistically significant. Most notably, breadths appeared generally to be larger after cutaneous dennervation of the foot pads. However, there were only three examples of statistically different breadths. While breadths are more variable (even during control conditions), the ratios between control and tibial crush still held close to the unity line (see Figure 5.2B). Therefore, these results indicate that directionally specific activation remains intact after cutaneous feedback loss from the foot soles.

However, while the directional attributes of the muscle responses remain intact, the amplitude of the responses is dramatically altered affecting force generation. Most specifically background activity was almost completely eliminated. As the difference between background and excitatory responses was conserved a large decrease in excitatory response amplitude was observed. The decreased amplitude of the excitatory muscle responses was detrimental to the force generating power of the limb leading to

smaller and less constrained force responses indicating that the force constraint depends not only on a directionally appropriate response, but one of appropriate magnitude. Furthermore, force responses were globally decreased after only right hindlimb dennervation. We cannot eliminate the possibility that this global decrease in force is due to the deterioration of the preparation. We took data as long as the animal was eliciting responses; however, they generally showed a slow decline in responsiveness after dennervation. Still, this global force amplitude loss was seen in every animal suggesting that it is a real result and not due to a deterioration of the animal. Furthermore, the animal never regained background firing before the end of the experiment. Therefore, we propose that the global decrease in amplitude is likely due to the intervention of the tibial nerve crush.

The decrease in amplitude also lent itself to increased variability as demonstrated by 68% and 86% of muscles showing increased standard deviations in principal direction and breadth respectively after tibial nerve crush. This increased variability also impacts the smoothness of the tuning curve. Generally, tuning curves always appear graded in nature showing a slow increase in activation until a maximum is reached and then a slow decrease in activation. Figure 5.1B demonstrates that after cutaneous dennervation of the foot pads the tuning curves often show more variable activation levels, particularly in the 9/11 experiment. The less graded appearance of the tuning curves is not likely exclusively the result of the cutaneous dennervation but also a loss of signal, which decreases the signal to noise ratio.

5.4.1 Sensory mechanisms

These results indicate that muscle receptors provide the feedback necessary for directionally appropriate muscle activation, while cutaneous feedback likely influences the scaling of the muscular responses. As we fix the head of the decerebrate cat, the muscular responses visible are the result of feedback from the proprioceptive system. We have previously hypothesized that feedback from muscle receptors, specifically muscle spindles, drives the directional tuning in response to support surface perturbation (Honeycutt et al. 2008; Nichols et al. 1999). We have demonstrated that muscle spindles generate similarly tuned activation patterns when the right hindlimb is subjected to horizontal support surface perturbations (Honeycutt et al. 2007). The results from this paper further bolsters our results by demonstrating that cutaneous feedback is not required for directionally appropriate muscle activation. Furthermore, we have shown that muscles with surgically induced muscular receptor feedback loss have a significantly disrupted excitatory response to support surface perturbations (Honeycutt et al. 2008). While muscle receptor feedback is lost in these animal, cutaneous feedback is completely intact. This indicates that unlike muscle receptor feedback, cutaneous feedback alone cannot generate directionally appropriate muscle activation patterns.

As the tibial nerve is diverse in its innervation, this report not only suggests cutaneous feedback is unnecessary for directionally appropriate muscle activation but that the intrinsic muscles of the feet are not necessary either. Still, our data also implies an important role for either or both the cutaneous receptors in the foot pads or the intrinsic musculature of the foot in the scale of muscle activation during postural tasks. While

much information exists about the lumbrical muscles of the foot in relation to the intrinsic properties of these muscles and their spindles, little is known about their global neural connections. It is reasonable to assume that these muscles would relay important information about the external environment and could play a role in the scaling of the muscular responses that occur after postural disturbances. However, more research is required to probe their influence during postural control.

Unlike the lumbrical muscles of the foot, cutaneous receptors have documented influences on muscular activity. Previous reports that various cutaneous nerves can excite or inhibit motor unit activity during fictive locomotion (Degtyarenko et al. 1996) demonstrate the feasibility of cutaneous effects on the scale of muscular activity. This results has also been observed in the intact system as a recent report described the firing patterns of individual tibial nerves, identified as cutaneous afferents of the foot, couple with EMG output during voluntary contraction in the human (Fallon et al. 2005). While all types of cutaneous receptors showed some reflex coupling, the fast adapting I type most consistently demonstrated association with EMG activity. Furthermore, this type of modulation appears present during motor tasks such as locomotion and posture. Cutaneous reflexes are known to impact the strength of muscular activation during locomotion (Zehr and Stein 1999). Furthermore, loss of cutaneous inputs changes the amplitude of responses to perturbation but not the response itself (Bolton and Misiaszek 2007). In conclusion, the specific role of the cutaneous and lumbrical muscles remains unclear; however, this report demonstrates that the absence of these sources does not alter the directionally specific muscle activation in response to support surface perturbations.

CHAPTER 6

MUSCLE SPINDLE RESPONSES TO HORIZONTAL SUPPORT SURFACE PERTURBATIONS

6.1 Introduction

We know that intact cats and humans respond to support surface perturbations with broadly tuned, directionally sensitive muscle activation (Henry et al. 1998; Macpherson 1988a; b). The directionality of these tuning curves is highly robust appearing impervious to alterations in stance condition (Torres-Oviedo et al. 2006) and perturbation parameters such as velocity and amplitude (Diener et al. 1988). Conversely, increases in muscle activation amplitude are noted under less stable stance conditions (shorter distance between hindlimbs and forelimbs in cat) and increasing perturbation velocity (Torres-Oviedo et al. 2006). The sensory mechanisms mediating these muscle response attributes remain largely elusive.

The difficulty in isolating cutaneous and muscle receptors has lead to a multitude of hypotheses regarding the proprioceptive system's role in postural control. While some authors have suggested that lower leg proprioception is irrelevant in triggering balance corrections (Bloem et al. 2000), others have indicated that only feedback from the cutaneous receptors of the foot pads could generate the directionally sensitive muscle activation (Ting and Macpherson 2004). Still others have taken a more moderate opinion proposing that integration of proprioceptive feedback from both cutaneous and muscle receptors are required for full expression of the postural response (Kavounoudias et al. 2001).

We have previously proposed that muscle spindles could drive the directionally selective muscle activation seen in the intact animal in response to support surface perturbations (Honeycutt et al. 2007; Honeycutt et al. 2008; Nichols 1999). Much is known about the response properties of muscle spindles in isolated muscles when mechanical variables are closely controlled (Hasan and Houk 1975; Houk 1979; Houk et al. 1981a). Results from our previous studies (Chapter 4) indicate that muscles are generally activated in the directions that can generate the most counteractive force. Theoretically, the direction of a muscle's lengthening corresponds to the direction it can generate the most opposing force if contracted. Therefore, muscle spindles could encode critical feedback about the counteractive force potential of each muscle. Furthermore, the knowledge that muscle spindles show alteration in their dynamic response when subjected to perturbations from different initial starting lengths (Houk et al. 1981a; Houk et al. 1981b) suggests they could mediate the amplitude sensitivity of muscle responses at different starting stance conditions. Finally, muscle spindles are known to encode the velocity of perturbation, which is also seen in muscular responses in the intact animal (Houk et al. 1981a).

Nevertheless, without additional study, it remains uncertain if muscle spindles can generate the necessary feedback to drive appropriate muscular activation. It is not clear if the response characteristics observed in muscle spindles of isolated muscle will also be present when the stretch of a muscle is generated through whole limb support surface perturbations. Preliminary data from our lab suggests that muscle spindles generate broadly tuned activation patterns (Martin et al. 2005). Our initial objective was to expand upon this data set and observe medial gastrocnemius (MG) and biceps femoris (BF)

muscle spindle responses to support surface perturbation. Our next objectives were to 1) evaluate these same tuning curves under different initial stance conditions and 2) examine the muscle spindle response to increasing ramp velocity. Our final objective was to perform perturbations similar to those performed in isolated muscle (varying amplitude constant duration) to further examine the behavior of muscle spindles in the intact limb for comparison to data reported in isolated muscle. We hypothesize that muscle spindles will generate broadly tuned activation patterns similar to the MG and BF muscular activation patterns present when the intact or decerebrate cat is subjected to support surface perturbation. We additionally hypothesize that stance will influence the amplitude of muscle spindle tuning curves. We hypothesize that the velocity dependence, observed in the isolated muscle, will be present in the spindle response properties of the intact limb. Finally, we hypothesize that the heightened sensitivity to small perturbations observed in isolated muscle will also be present in situ.

6.2 Methods

6.2.1 Surgery

Four cats were used in accordance with the Emory and Wright State University Institutional Animal Care and Use Committees. Animals were sedated using Ketamine and then placed into an induction chamber filled with isoflurane gas until they were deeply anesthetized. After removal from the chamber, the animals were intubated for continuous, monitored administration of isoflurane gas. Additionally, an intravenous line for fluid and drug delivery along with a blood pressure transducer were inserted into the external jugular and carotid artery vessels respectively. In order to ensure deep

anesthesia, heart rate, blood pressure, oxygen and carbon dioxide saturation, temperature, and respiration rate were monitored continuously along with the withdrawal reflex.

The medial gastrocnemius and biceps femoris nerves were isolated at the knee and hip respectively and placed in nerve cuffs. The nerve sections that were related to all three portions (anterior, middle, and posterior) of the biceps femoris muscle were isolated from the nerve sections that contained the other hamstring muscles through careful dissection of the hamstring nerve. Each dissected portion was then electrically stimulated to determine its innervation. Sections of the nerve that appeared mixed or could not be conclusively identified were not included. Finally, a laminectory was performed to expose the L5-L7 dorsal roots. In one of the animals (3/20), an intercollicular decerebration was completed. However as paralyzation of the animal with pancuronim was required for data collection, all other animals were anesthetized, without decerebration, for the duration of the experiment. Data from the one afferent collected in the decerebrate animal was not substantially different from the anesthetized animals and therefore was included in all analysis.

6.2.2 Afferent identification and recording

A glass micropipette was slowly lowered into the dorsal roots (L5-L7) while either the medial gastrocnemius or biceps femoris nerve sections were rhythmically stimulated. A short conduction time between the stimulation artifact and the first action potential confirmed that the afferent was from the appropriate muscle. Specific conduction times were calculated after completion of the experiment using Spike software. Afferents were

classified as muscle spindles or golgi tendon organs based upon their firing properties. As the muscle was stimulated, ground reaction forces were collected from a force transducer located beneath the foot. Spindles were identified by their pause during contraction, while tendon organs increased firing during force generation.

6.2.3 Positioning and Perturbations

The animal's head was fixed in a stereotaxic frame while the spine and hips were secured with clamps at the L4 and L7 spinal processes. In order to achieve the most natural hip rotation, the tail was secured with duct tape and string at the base of the tail and attached to an immobile bar about the pelvis. This ensured more natural angle of the limb (as compared to data obtained in intact animals during standing: see Chapter 2 and 3). The toe pads of the hindlimb were secured with glue and tape to the surface of the perturbation platform. The large central pad of the foot was not secured to allow for more natural rotation of the metatarsophalangeal joint. The natural turnout of the foot was used to place the foot and the toe was placed 1cm behind the greater trochanter plane for the initial (natural) stance condition. This positioning was also determined through intact animal data.

Once positioned, the hindlimb was perturbed in 16 directions using two linear motors (X: rostral/caudal, Y: medial/lateral). Motor position, recorded simultaneously through the motor's encoder, was monitored closely to ensure a linear perturbation. The foot was perturbed 4cm during 400ms to be comparable to data previously collected in the intact and decerebrate animal ((Macpherson 1988b), Chapter 2). Medial gastrocnemius

afferents were subjected to further evaluation. Once a full set of 16 directions was collected, the limb was moved either 3cm rostrally or caudally from the starting stance condition (natural) and a new set of 16 direction perturbations was applied to MG afferents at the new stance condition. We then performed 4 trials of 90 degree (rostral) perturbations at different velocities (.1, .2, .4, and .8 mm/ms) constant 4cm amplitude. Finally, we performed 6 rostral perturbations at varying amplitudes (.5, .75, 1, 2, 4, 6 cm) constant duration of 400ms. These final two perturbation types were only completed in the rostral direction using 1 motor to ensure a perfectly linear perturbation at the faster speeds.

6.2.4 Data collection and tuning curve analysis

Spike software was used to collect the data which included the time of each action potential, motor position (x and y motors), and initiation of perturbation. Spike was also used to discriminate action potentials. After discrimination, the necessary data were exported to Matlab for further analysis. Instantaneous firing rate (IFR), inverse of the time of the current spike minus the time of the previous spike, was calculated for all perturbations. Tuning curve analysis was applied to the 16 direction perturbation data from the MG and BF afferents. The number of spikes that occurred during the perturbation (400ms) was calculated followed by a subtraction of the number of spikes during the same time period of background before the perturbation. The increase or decrease in activity was then graphed against perturbation direction to create a tuning curve (see Figure 6.1 – 6.4). Tuning curves were also created using the mean IFR, calculated during the same time period of 400ms and maximum IFR achieved during the

entire perturbation. Latencies were also calculated as the time when the first spike achieved greater than twice the background firing rate.

All three types of tuning curves (number of spikes, mean IFR, and max IFR) were also calculated at the different stance conditions and then further quantified with breadths and principal directions. Breadth, the area under the normalized afferent tuning curve, is a quantification of range of directions a muscle is active. A large breadth represents an afferent that is active over many perturbation directions. The principal direction represents the maximum direction of activation. In order to calculate the principal direction, afferent responses from each direction were converted to a vector and x and y components and then averaged to find the primary vector or principal direction of the response.

6.2.5 Parameter analysis

Two different parameter conditions were collected: varying amplitude constant duration and varying velocity constant amplitude. The first (varying amplitude constant duration) was quantified at 6 different time intervals. These time periods correspond to the initial dynamic (0-150ms), middle dynamic (150-300ms), last dynamic/early steady-state (300-450ms), early steady-state (450-600ms), middle steady-state (800-950), and late steady-state (1500-1650ms) phases. The mean IFR during each of these time intervals was then graphed against the mean position of the perturbation platform during the same time period (Figure 6). The second parameter condition (varying velocity constant amplitude) was quantified during short latencies 0-80ms for comparison to results obtained in the

intact animal. However as amplitude is not the same at short latencies due to the varying speed of the perturbation, we additionally calculated the firing rate at the end of the perturbation when all afferents are at the same amplitude. These values were then graphed against the velocity of the ramp perturbation to determine any correlations. It was noted that some afferents did show vibration sensitivity. However, statistical comparison of several parameters (latencies, firing rates, background firing, principal directions, breadth, etc.) did not generate significance. Therefore, all afferents were evaluated identically.

6.3 Results

6.3.1 Directionally sensitive firing

All muscle spindles, from both the MG and BF muscles, generated directionally sensitive firing. Figures 6.1 and 6.2 show typical MG and BF afferents responses to 16 different support surface perturbations. Each box represents a different direction and depicts the afferent response to the initial forward perturbation (400ms), hold (2000ms), and return perturbation (400ms). The dynamic phase, marked with dashed lines, exhibits increases in firing rate compared to background in half of the perturbation directions (22.5 -157.5 degrees). Decreases or elimination of firing is present over the opposing perturbation directions (180 – 0 degrees). Increases in firing are graded, slowly rising and falling around a maximum that is reached at 90 and 67.5 degrees for the MG and BF afferents represented in Figures 6.1 and 6.2, respectively. Opposing directions expressed either a graded decrease in firing (Figure 1) or elimination of firing (Figure 6.2). Both graded decreases and elimination of firing occurred in both MG and BF afferents.

Despite differences in latencies and firing rates, tuning curve quantification demonstrated that principal direction and breadth were almost identical across afferents. Tuning curve quantified using number of spikes, mean IFR, and max IFR were found to be almost identical. Therefore, we will discuss and depict only the number of spikes quantifications. Figure 6.3 and 6.4 show additional MG and BF muscle spindle responses (A) and tuning curves (B) from supplementary experiments. Note that the data from the 2/14 experiment were taken in the left leg so the tuning curves depict a reflection across the vertical axis. Muscle spindles were found to achieve a wide variety of different maximum firing rates with standard deviations reaching as high as 137pps (Table 6.1). Latencies were equally variable with the minimum latencies standard deviations reaching 70ms while the max IFR latency standard deviations reached 134ms (Table 6.1). This demonstrates the significant differences in the firing patterns achieved by each individual afferent. However, despite the large variability present, all muscle spindle afferents studied generated broad tuning curves with highly consistent principal directions (standard deviations less than 6.1) and breadths (standard deviations lower than 1) (Table 6.1).

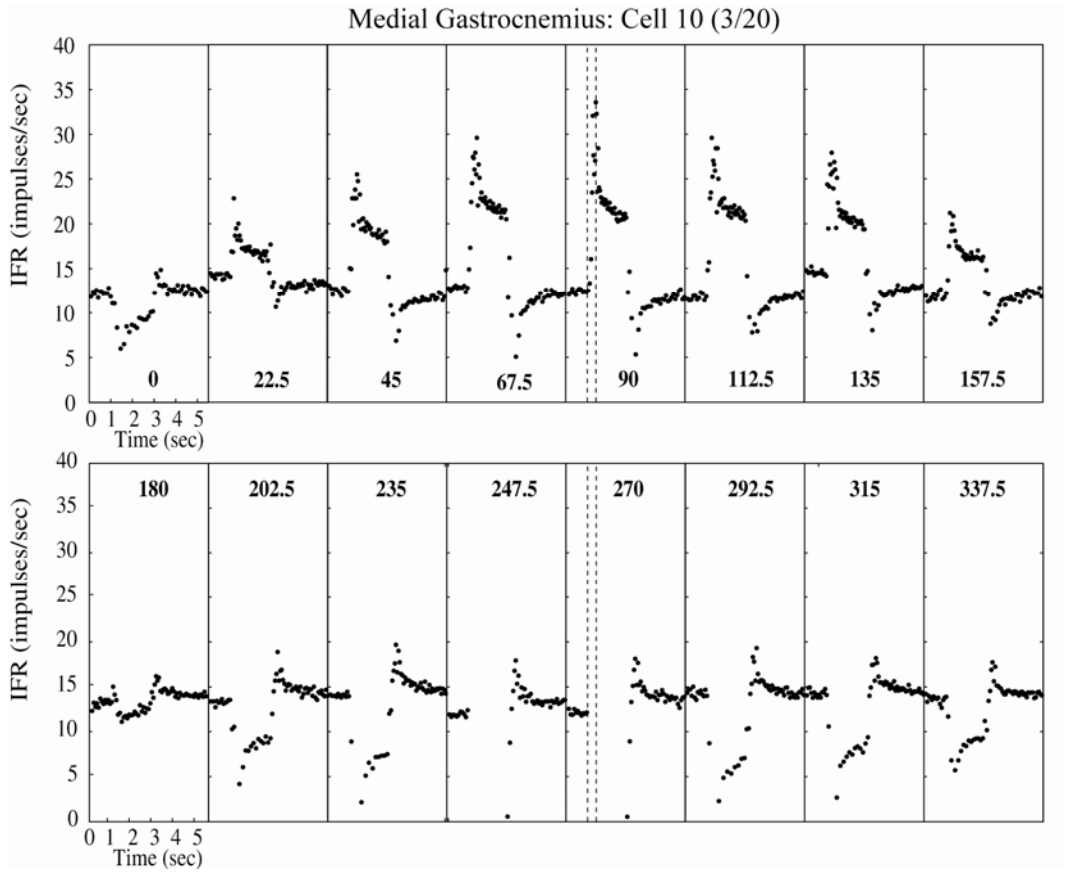

Figure 6.1: Representative MG muscle spindle responses to 16 directions of support surface perturbation. Illustrates a MG muscle spindle from the 3/20 experiment. Each box contains the forward perturbation (400ms), hold (2000ms), and return perturbation (400ms). The dashed lines in the 90 and 270 degree boxes represent the 500ms that were subsequently analyzed.

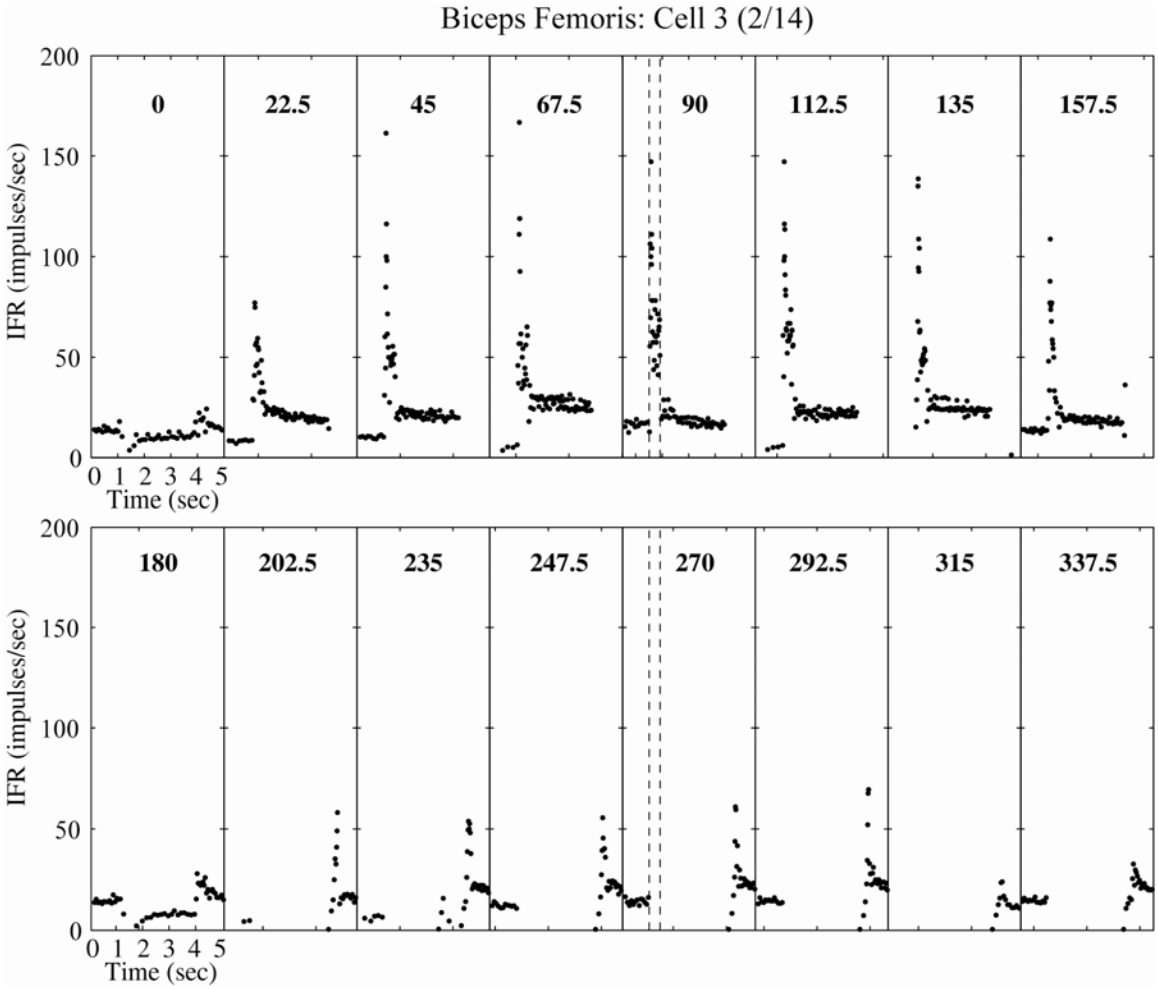

Figure 6.2: Representative BF muscle spindle responses to 16 directions of support surface perturbation. Illustrates a BF muscle spindle from the 2/14 experiment. Each box contains the forward perturbation (400ms), hold (2000ms), and return perturbation (400ms). The dashed lines in the 90 and 270 degree boxes represent the 500ms that were subsequently analyzed.

Table 6.1: Quantification of muscle spindle afferents

	Medial Gastrocnemius				*Biceps Femoris*	
	2/14/2008	***2/12/2008***	***3/22/2007***	***3/20/2007***	***2/14/2008***	***2/12/2008***
Number of Afferents	9	3	4	1	4	7
Right or Left Limb	Left	Right	Right	Right	Right	Right
Principle Direction	80 (2.9)	104 (5.8)	111 (5.2)	96	89 (6.1)	90 (5.7)
Breadth	5.1 (.3)	4.8 (.9)	4.8 (.3)	4.8	5.6 (1.0)	5.2 (.6)
Average Min Latency (ms)	35 (4)	69 (70)	65 (28)	45	45 (22)	79 (36)
Average MaxIFR (pps)	169 (60)	146 (23)	120 (19)	33	150 (36)	200 (137)
Average MaxIFR time (ms)	386 (40)	359 (51)	424 (74)	388	331 (134)	408 (10)

Standard deviations are reported in parentheses

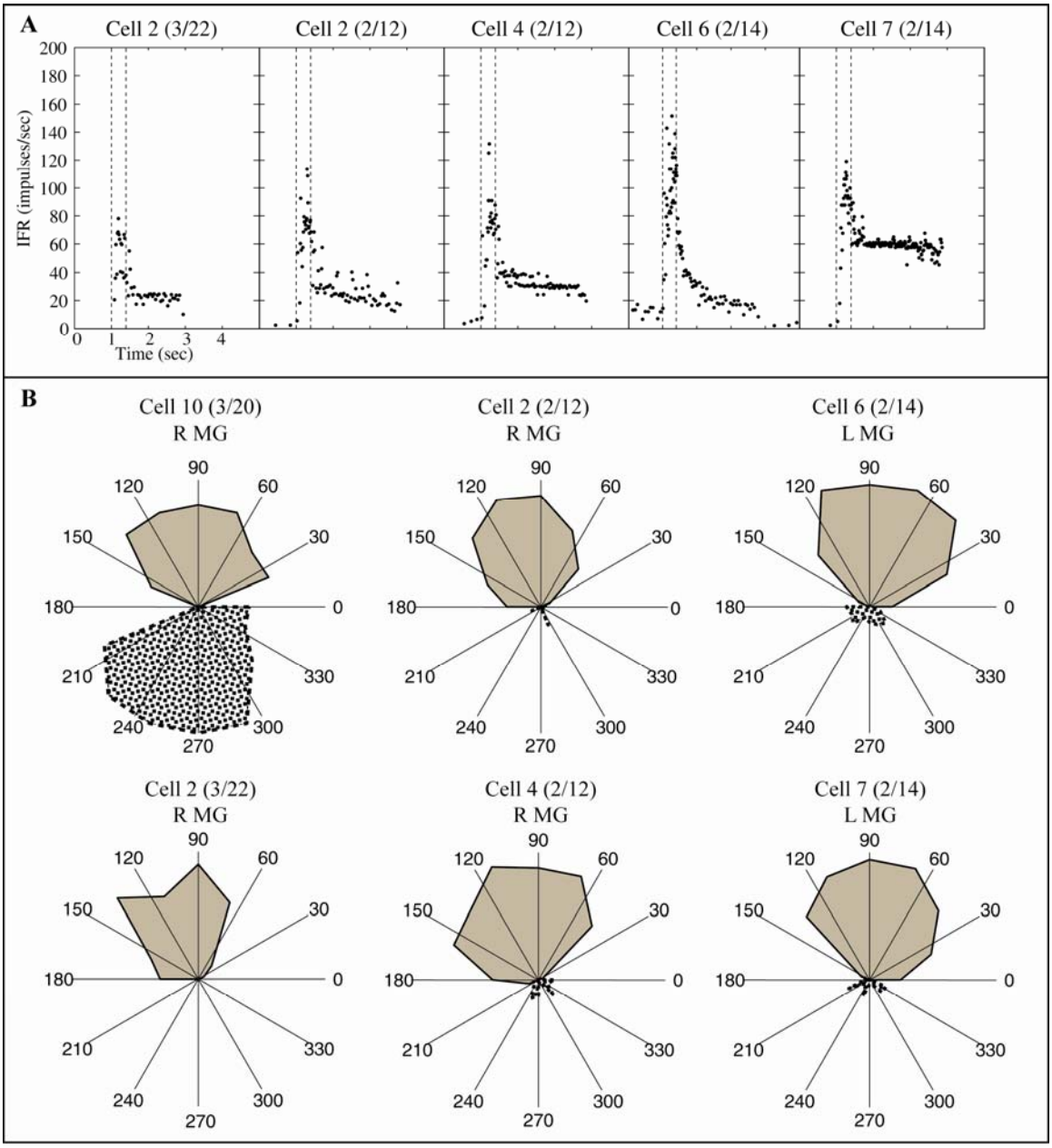

Figure 6.3: Further examples of MG muscle spindle firing along with tuning curve quantification. Shows 5 additional examples of MG muscle spindle afferent responses to 90 degree (rostral direction) support surface perturbations (A). The first 500ms, subsequently used for quantification of tuning curves, is shown with dashed lines. The tuning curves from these 5 afferents along with the afferent depicted in Figure 6.1 are shown (B). At least one example is shown from each of the 4 experiments. Tuning curves appear remarkably similar within and across experiments. Note that the 2/14 experiment data was taken from the left leg.

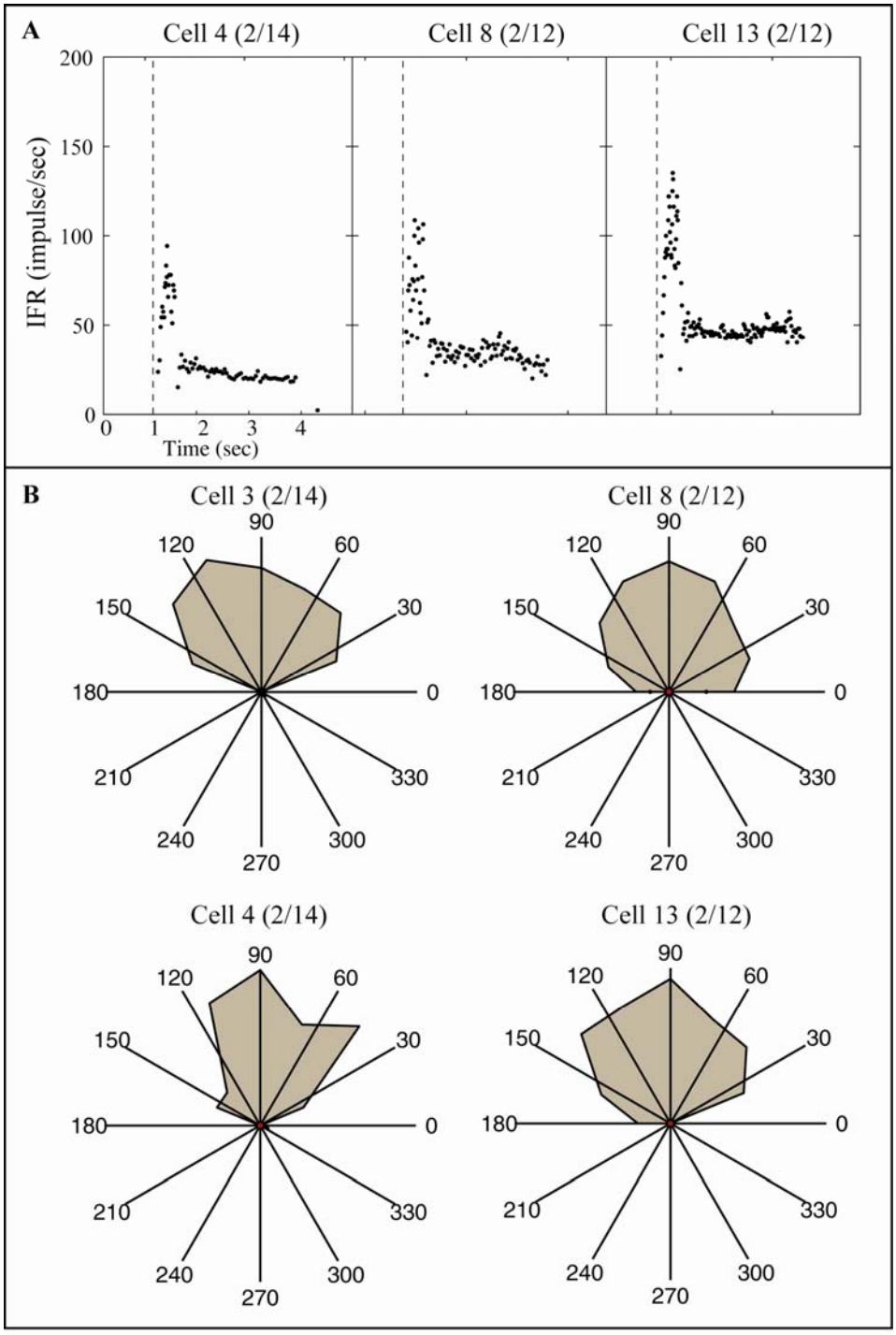

Figure 6.4: Further examples of BF muscle spindle firing along with tuning curve quantification. Shows 3 additional examples of BF muscle spindle afferent responses to 90 degree (rostral direction) support surface perturbations (A). The first 500ms, subsequently used for quantification of tuning curves, is shown with dashed lines. The tuning curves from these 5 afferents along with the afferent depicted in Figure 6.1 are shown (B). At least one example is shown from each of the 2 experiments where BF data was obtained.

The most distinguishing observation amongst the afferents studied was that about 50 percent of the afferents generated directionally sensitive steady-state firing (little or no adaptation). This occurred in both MG (Figure 6.1: Cell 10 (3/20), Figure 6.3A: Cell 4 (2/12) and Cell 7 (2/14)) and BF (Figure 6.2: Cell 3 (2/14), Figure 6.4A: Cell 13 (2/12)) afferents. The other half of the afferents demonstrated large adaptation during the steady-state phase typically returning to values almost identical or just slightly elevated about background firing. The populations, which we will designate Type 1 (large adapting) and Type 2 (small adapting), are discernable based on conduction time. Type 2 afferents have on average 0.3ms longer conduction times than Type 1 afferents. Aside from their steady-state firing and conduction time, both afferent types respond comparably. To illustrate their similarity, both types of afferents will be visually depicted under each of the future conditions.

6.3.2 Sensitivity to stance condition

Altering stance condition had little affect on principal direction or breadth of the tuning curves but background firing and maximum firing rate were affected. Figure 6.5 depicts the 90 degree response of a Type 1 (Cell 6) and Type 2 (Cell 2) afferent at each of the 3 stance conditions surveyed (A). The perturbation is marked by dashed vertical lines. Afferents were found to achieve hirer max IFRs (Figure 6.5C: Right) when perturbed from shorter stance conditions (longer muscle lengths). This trend was present in all but 3 (out of 11) afferents studied, which instead presented similar responses to perturbation regardless of the starting length of the muscle. Background firing in all afferents was found to increase at shorter stance conditions (Figure 6.5C: Left). Despite these

alterations in background and max IFR rates, the principal direction and breadth showed little change with stance condition (Figure 6.5B).

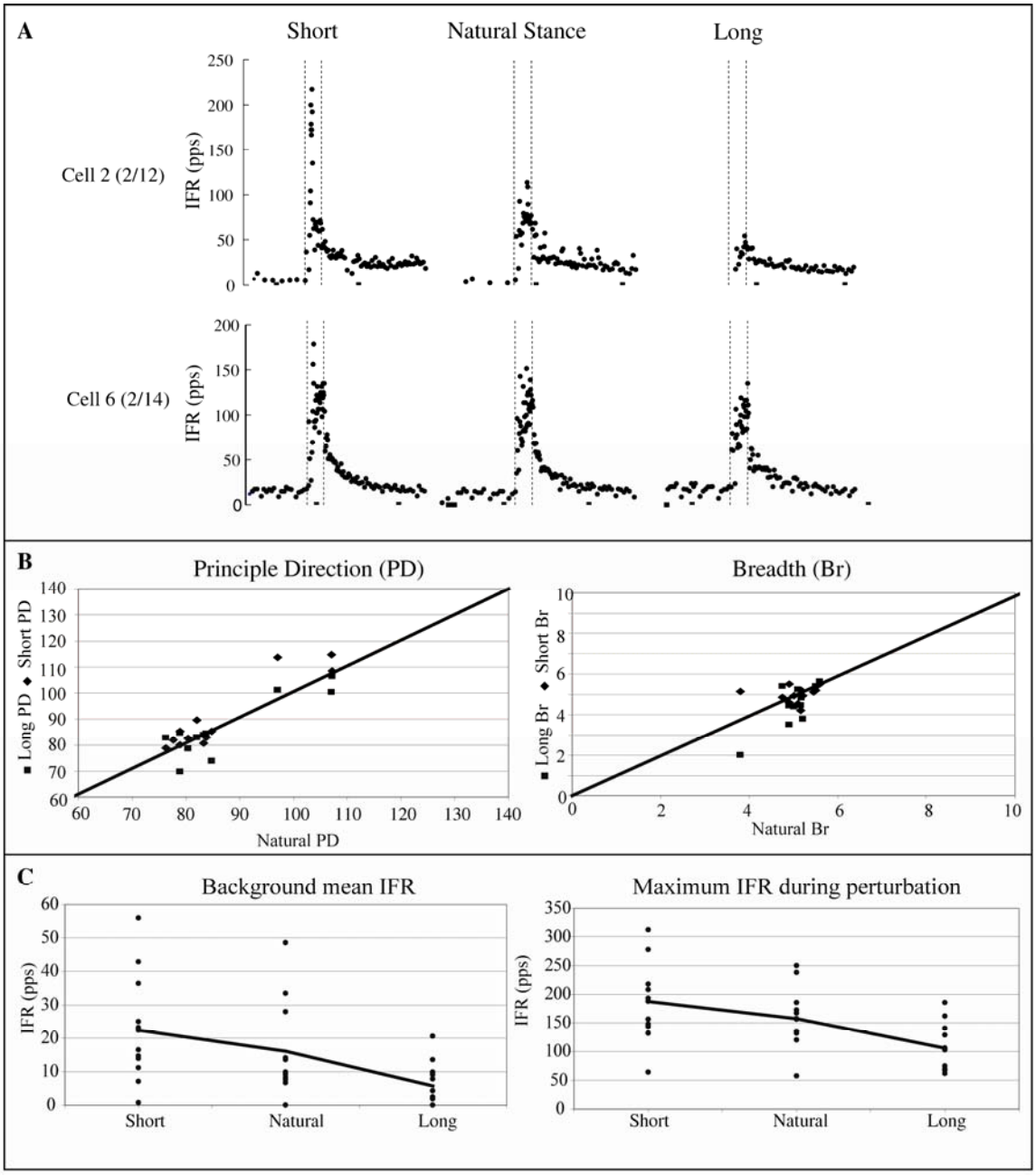

Figure 6.5: MG muscle spindle afferent response to different stance conditions. Depicts the 90 degree response of a Type 1 (Cell 6) and Type 2 (Cell 2) afferent at each of the 3 stance conditions surveyed (A). The perturbation is marked by dashed vertical lines. Tuning curve, including principal direction and breadth, were quantified for all afferents where stance condition alterations were measured. Principal directions and breadths quantified under Short and Long stance conditions are graphed against the principal directions and breadths quantified under Natural stance conditions (B). The heavy black line depicts the unity line. Values that lie along this line indicate little to no change in principal direction or breadth based upon stance condition. Background mean IFR and maximum IFR during perturbation were also quantified for all afferents studied (C). Each dot represents the value quantified for each experiment. The heavy

black line is the mean response of all afferents. All afferents showed a decreasing background mean IFR as stance condition was elongated. All but 3 afferents showed a decreasing maximum IFR during perturbation

6.3.3 Varying amplitude constant duration

MG muscle spindles appear to be more sensitive to stretch during the beginning of the dynamic phase. Figure 6.6A depicts a Type 1 (Cell 12) and Type 2 (Cell 10) afferent response to ramp and hold perturbations of increasing amplitude (.5 – 6cm) over the same duration of 400ms. Six different time periods were evaluated, which correspond to the initial dynamic (0-150ms), middle dynamic (150-300ms), last dynamic/early steady-state (300-450ms), early steady-state (450-600ms), middle steady-state (800-950), and late steady-state (1500-1650ms) phases. The mean IFR during these time periods was then graphed against the mean position of the platform. The initial time periods exhibited steeper slopes indicating increased sensitivity to perturbation. Type 1 afferents (Figure 6B: Cells 12 and 9) demonstrate decreasing slopes through all time periods, while Type 2 afferents (Figure 6.6B: Cells 10 and 8) typically level out to one slope during the early steady-state phase. Half of the cells appear to show this transition in sensitivity during later time periods demonstrating two distinct slope regions that transition around .75 – 1cm (Cells 9 and 8). However, the other half of afferents does not demonstrate this slope change (Cells 10 and 12).

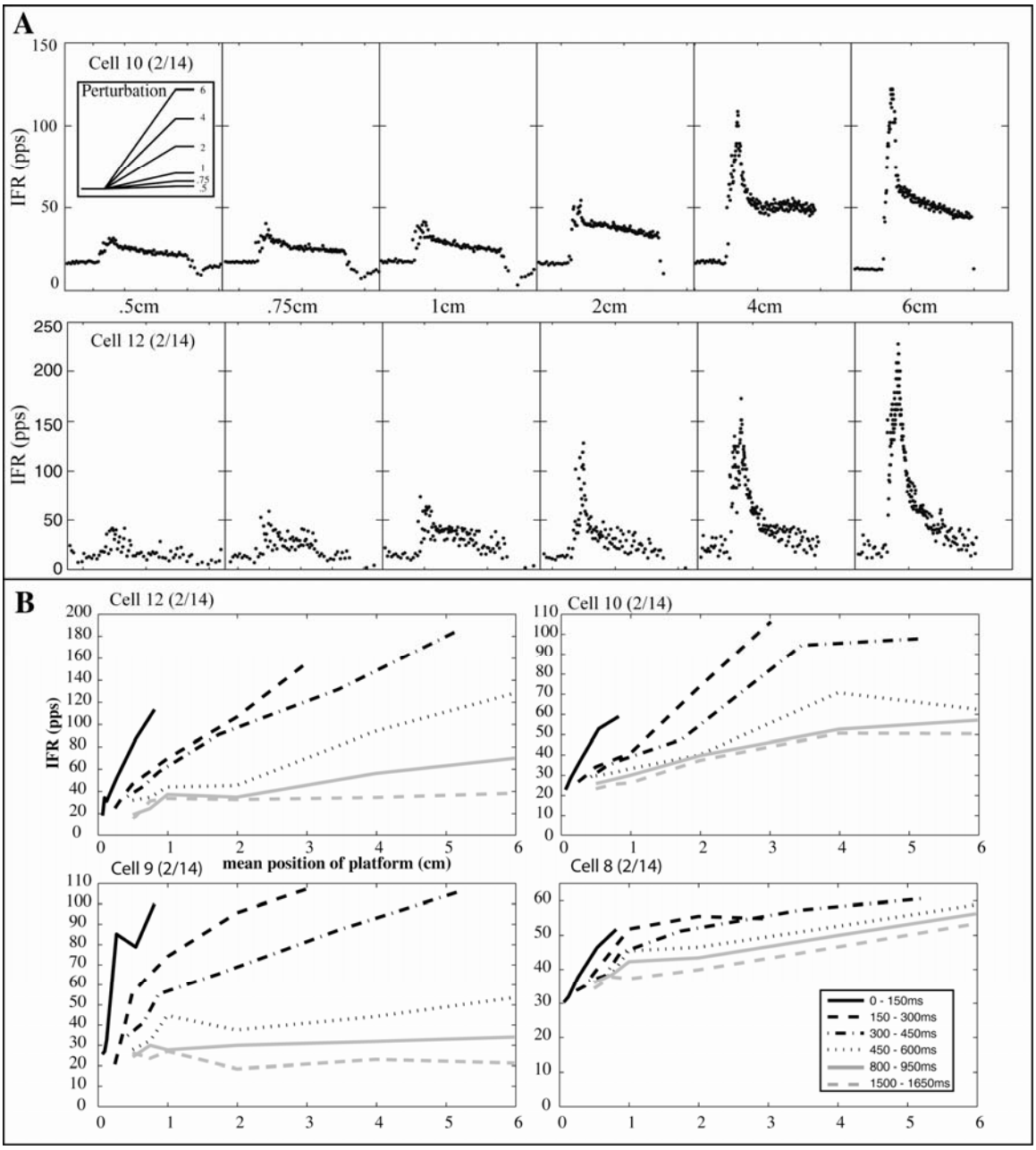

Figure 6.6: Quantification of MG muscle spindle responses to increasing amplitude constant duration. .Figure 6.6A depicts a Type 1 (Cell 12) and Type 2 (Cell 10) afferent response to ramp and hold perturbations of increasing amplitude (.5 – 6cm) over the same duration of 400ms. Six different time periods were evaluated, which correspond to the initial dynamic (0-150ms), middle dynamic (150-300ms), last dynamic/early steady-state (300-450ms), early steady-state (450-600ms), middle steady-state (800-950), and late steady-state (1500-1650ms) phases. The mean IFR during each of these time periods was then graphed against the mean position of the platform during the same time period (B). A steep slope indicates a high sensitivity to the position of the platform. It is noted that MG muscle spindle afferents appear highly sensitive to perturbations that occur within the first 150ms when the platform has been displaced on average less than 10mm.

6.3.4 Varying Velocity constant Amplitude

MG muscle spindle afferents produce increasing afferent firing as the velocity of perturbation is increased. Figure 6.7A illustrates a Type 1 (Cell 12) and Type 2 (Cell 5) afferent response to perturbations of increasing velocity (.1 - .8mm/ms) constant amplitude (4cm). Quantification of the short latency (0 – 80ms) firing (Figure 6.7B: left) indicates that all afferents produce increases in firing as velocity increases. Noticeable short latency firing (similar to initial bursting) is first present when velocities greater than .15mm/ms are achieved. In addition to the increased short latency firing, afferents produce larger dynamic responses as velocity is increased. Mean IFR was calculated at perturbation termination, when all afferents were at the same amplitude of 4cm but had been subjected to different velocities before achieving that amplitude. Despite being at the same amplitude, afferents showed increased firing correlated to increasing velocity of perturbation (Figure 6.7B: Right).

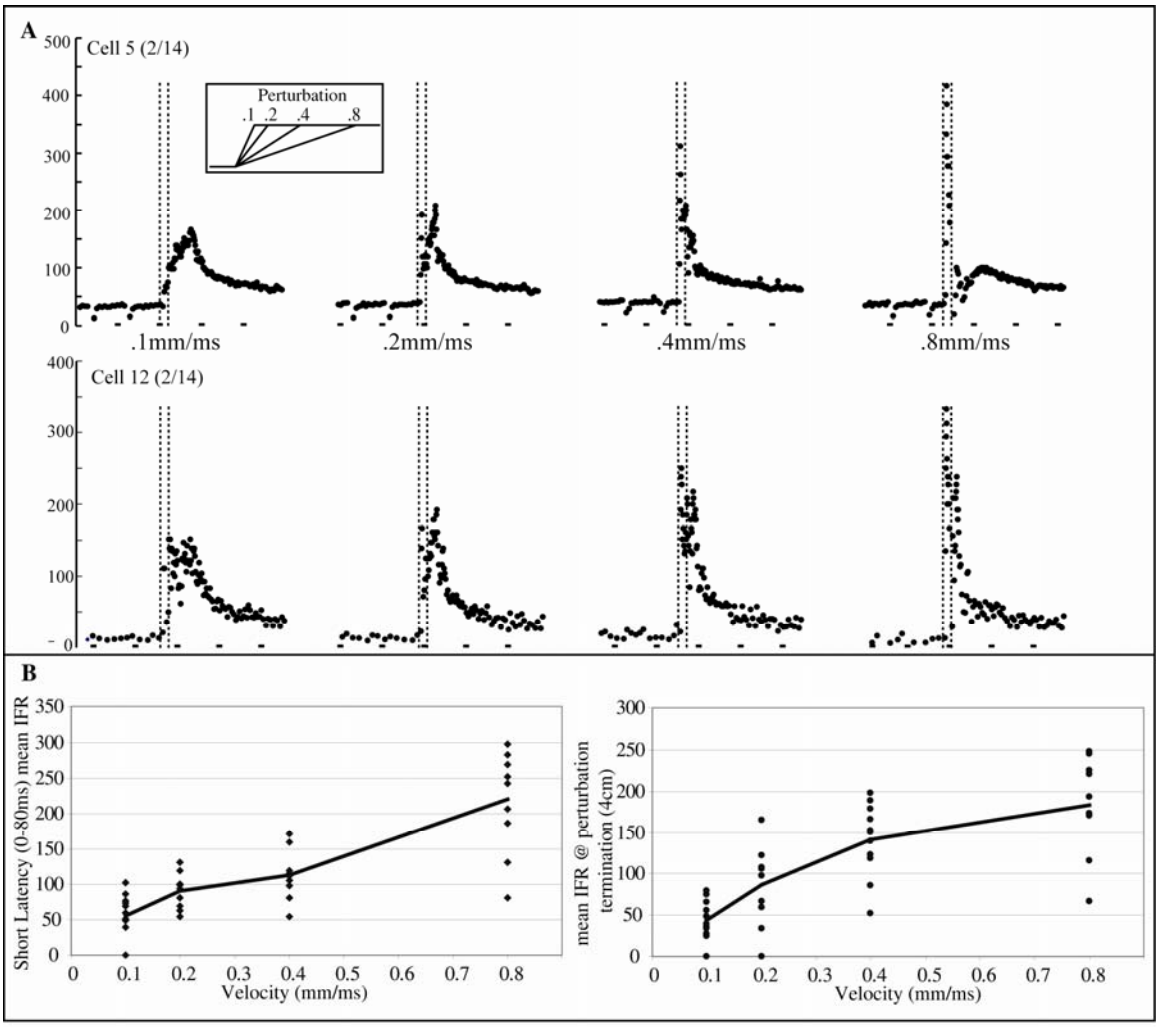

Figure 6.7: Response of MG muscle spindles to increasing velocity. Illustrates a Type 1 (Cell 12) and Type 2 (Cell 5) afferent response to perturbations of increasing velocity (.1 - .8mm/ms) constant amplitude (4cm) (A). Short latency (0-80ms) mean IFR was quantified (B: left) along with the mean IFR that occurred at perturbation termination (B: right). The heavy black line indicates the average response of all afferents evaluated. Both quantification techniques (short latency and perturbation termination) showed that all afferents exhibit increasing mean IFR as velocity increased.

6.4 Discussion

6.4.1 *Summary*

All muscle spindle afferents studied in the MG and BF muscles generated broadly tuned activation patterns. While individual afferents portrayed unique firing patterns, tuning curves were found to be almost identical in principal direction and breadth within an experiment. Although two distinct afferent populations were distinguishable based upon

their level of adaptation during steady-state firing, spindles generated the hypothesized amplitude changes with stance condition and velocity. Finally, muscle spindle afferents exhibit a trend towards increased sensitivity at small perturbations.

6.4.2 Comparison to isolated muscle responses

We hypothesized that the heightened sensitivity to small perturbations observed in isolated muscle will also be present in situ. Results from the intact limb indicate that during the initial dynamic phase (0-150ms) there is an increased sensitivity to perturbation, illustrated by the steep slopes observed during this time period (Figure 6.6). As the platform has been displaced only a short distance (25mm or less), this demonstrates a heightened sensitivity to these small perturbations. However, only half of the afferents demonstrate a shift from this high sensitivity to lower sensitivity at later time periods (Figure 6.6: Bottom cells). The other half of cells appear to have a graded shift in sensitivity as time progresses (Figure 6.6: Top cells). Cell type (1 or 2) does not appear to be a factor. Therefore these afferents do behave like those in isolated muscle demonstrating increased sensitivity during smaller length changes; however they differ because this sensitivity is not as readily apparent at later time periods. It is important to note that we are not directly comparing muscle spindle firing to muscle length. Rather we are comparing muscle spindle firing to the position of the support surface. Soft structures of the limb like ligament, tendons, and fascia probably affect muscle length during latter phases of the perturbation. Still, it appears that muscle spindles within the intact limb remain highly sensitive to smaller perturbations during the initial dynamic phase of the perturbation.

6.4.2 Population identification

Interestingly, we found two types of afferent populations that either had (Type 1) or did not have (Type 2) adaptation during the hold phase of the perturbation. Behaving similarly otherwise, Type 2 afferents fired at different rates during the hold phase corresponding to different muscle lengths. Conversely, Type 1 afferents demonstrated strong adaptation during the steady-state hold period showing little to no sensitivity to amplitude during this time period. This is graphically illustrated in the left cells of Figure 6.6, which showed a slope approximating zero during the steady-state response (time periods greater than 500ms). It was found that the Type 2 afferents had, on average, .3ms longer conduction times than Type 1s. Based upon their response properties and the conduction time differences, we believe that these Type 1 and Type 2 afferents correspond to Group I and Group II muscle spindle afferents, respectively. To further justify this conclusion, we compared the response properties of our Type 2 afferents to the responses of Group II afferent responses in the isolated muscle (Hasan and Houk 1975) and found them to be similar.

6.4.3 Comparison of muscle spindle responses to muscular responses

The tuning curves generated from muscle spindles (Group I and II) were similar in both direction and breadth to muscle tuning curves collected in the intact (Macpherson 1988b) and decerebrate cat (Chapter 2). Quantification of muscular activation tuning curves in the decerebrate cat (right leg) indicate that the MG muscle has an average principal direction of 105 degrees, while the BF muscle has regional differences producing

principal directions at 112 and 91 degrees in the anterior and posterior portions respectively (Chapter 2). The MG muscle spindle tuning curves generated principal directions ranging from 96 – 111 degrees. If the principal direction data from the 2/14 experiment, completed in the left leg, are reflected across the vertical axes, the 110 degree principal direction also closely resembles the 105 average principal direction in the decerebrate cat. The BF muscle spindle afferents ranged from 89 – 90 degrees, well within the ranges reported for the posterior portion of the BF muscle. Generally, the breadths of both the MG and BF afferents were lower than those reported in the decerebrate animal.

Additionally, the behavior of muscle spindles when subjected to perturbations from different stance conditions and velocities mimic muscular responses seen in the intact animal (Diener et al. 1988; Henry et al. 2001; Torres-Oviedo et al. 2006). MG muscle spindle afferents generally generate increases in background and max IFR firing rate as stance condition is shortened (longer muscle lengths). Reports from the intact animal demonstrate that amplitude of muscular activation generally increases at shorter stance conditions as well (Henry et al. 2001; Torres-Oviedo et al. 2006). MG muscle spindles also were sensitive to velocity increases. Muscular responses from humans have been shown to demonstrate short latency (0-80ms) increases in activation with respect to velocity (Diener et al. 1988). We found that short latency firing dramatically increased with velocity. To ensure this was a velocity effect and not due to differences in amplitude during this initial time period, we further evaluated the afferent firing at the end of the perturbation when the amplitudes were equivalent. End of the perturbation

afferent firing, demonstrated the same trend with similar slopes (see Figure 6.7). All muscle spindles evaluated generated this trend.

6.4.4 Implications for postural control

These data indicate that muscle spindle feedback strongly contributes to the directionally sensitive muscular activation patterns. Furthermore, these spindles appear capable of mediating many of the amplitude changes seen in the intact animal with regard to stance condition and velocity. Extending the arguments discussed in Chapter 4, these afferents likely deliver information about the internal changes of muscle that influence its ability to oppose a perturbation. When a muscle is lengthened as a result of perturbation, that same muscle is capable of generating an opposing force if contracted. Furthermore, the high sensitivity of these afferents to only small perturbations occurs at very short latencies. This indicates that muscle spindle afferents are tailor made to quickly deliver the necessary information to drive muscular activation in response to support surface perturbations.

6.5 Acknowledgments

Special thanks to Timothy Cope who provided his laboratory and scientific expertise for the completion of these experiments. Further thanks to Paul Nardelli and the rest of the Cope lab who were instrumental in the data collection and assisted with data processing techniques.

CHAPTER 7

DISCUSSION AND CONCLUSIONS

The generation of appropriate muscle activation patterns in the lower limbs certainly requires complex integration of many sensory sources, which is likely performed within all layers of the central nervous system. However, it is plausible that this integration exists within a hierarchical neural framework where each unit is responsible for increasingly complex integration of sensory and environmental information. We propose that the sensory feedback that drives the directionally specific muscle activation is located within the lowest level of this neural hierarchy, the spinal cord.

Central mechanisms

The cortex has been implicated to participate dynamically in control of complex motor tasks including integration of information about global parameters, limb position, and environmental conditions (Dietz et al. 1984). This notion is corroborated by pyramidal tract (primary descending cortical neurons) recordings demonstrating that these cells are excited by contralateral limb movements (Beloozerova et al. 2005; Beloozerova et al. 2003). Additionally, reports showing that cortical suppression can inhibit the longer latency muscle stretch responses to simulated postural disturbances (Taube et al. 2006) indicate that the cortex plays a role in scaling muscle responses at a longer latency. While these longer latency responses are likely not under exclusive control of the cortex (Schieppati and Nardone 1995), it is reasonable to assume that the longer latency responses are influenced by the cortex, in particular the somatosensory cortex (Miller and

Brooks 1981). Therefore, the cortex and other supra-spinal structures plausibly are responsible for scaling and in some cases elimination of directionally inappropriate responses (Nashner 1976).

In contrast, our data show that the cerebral cortices are not required for directionally appropriate muscle activation. This result argues for a critical role for both the spinal cord and brainstem; however we support the notion that the brainstem is primarily playing a permissive role or providing support to the spinal circuitry (Chapter 2). The spinalized animal generates directionally appropriate muscle activation indicating that the spinal cord alone is capable of driving directional tuning (Macpherson and Fung 1999). Still, authors also reported that the spinal animal has considerable difficulty in maintaining its balance and does not appear capable of delivering ground reaction forces of sufficient strength to oppose the perturbation. It is possible that the spinal animal's inability to generate functional forces occurs as a result of the significant injury to the cord resulting from the spinalization (Bonasera et al. 1994; Edgerton et al. 2001; Nichols et al. 1999; Potluri et al. 2008); however an alternative hypothesis is that the presence of the brainstem may be required for appropriate spinal cord excitability.

A role for the brainstem in providing the required excitability, is supported by our evidence that a higher brainstem transection (modified premammillary decerebration), which preserves the rostral brainstem, more frequently generates muscle responses to support surface perturbations than a lower transection (intercollicular decerebration) implies that the rostral brainstem structures can modulate the excitability of the lower

circuitry (Chapter 2,3). This notion that supra-spinal structures provide a supportive role to the spinal circuitry has been previously suggested in the literature (Lyalka et al. 2005; Nichols et al. 2002). Lyalka and coworkers note that spinal cord hemi-sectioned animals show a significant recovery of postural responses when supra-spinal support is present. We know that brainstem regions such as the ventral and dorsal tegmental fields can adjust postural tone through excitatory or inhibitory influences on the spinal cord (Mori 1987; Mori et al. 1989). Removing those regions may alter the excitability of the spinal circuitry inhibiting its ability to respond. The lower transected and spinalized animals that produced muscle responses also reported diminished amplitude additionally indicating that the brainstem may regulate excitability. Based upon these observations and earlier suggestions (Nichols et al. 2002), we propose that the spinal cord houses the appropriate circuitry to produce some of the key elements of postural control including directionally appropriate muscle activation.

The spinal cord is known to mediate diverse motor tasks including wiping reflexes (Poppele and Bosco 2003; Stein and Daniels-McQueen 2004) and locomotion (Edgerton et al. 2001). The wiping reflex is a goal-directed task that requires integration of limb position and desired endpoint information (Poppele et al. 2003). The isolated spinal circuits of the frog and turtle are capable of control and programming of many unique wiping actions, including choosing to use the contralateral limb when the ipsilateral limb is inappropriate (Stein 2008; Stein and Daniels-McQueen 2004). These spinalized animals can achieve the appropriate endpoint destination from unique limb configurations (Fukson et al. 1980) as well, indicating that the isolated cord has access to feedback about

limb kinematics and muscle actions. In addition to wiping actions, the isolated cord can mediate locomotion patterns (Edgerton et al. 2001) even demonstrating control by adjusting these patterns when external stimuli (such as loads during swing) are present (Timoszyk et al. 2002). Therefore knowing that spinal circuits can negotiate such a variety of motor tasks and sensory integration leads us to believe that these same circuits also mediate some aspects of postural control, most specifically the directional components of appropriate muscle activation. The spinalized cat has significant balance insufficiencies and does not show responses in all muscles, yet they are able to generate appropriately directed tuning curves in the aBF, aSart, Glut, RF, and VM (Ni) muscles (Macpherson and Fung 1999). Additionally, we know that spinal circuits participate in a variety of postural functions including stiffness regulation of muscle, joints, and limb (Nichols 1989; Nichols and Houk 1976). Therefore, we propose that the spinal cord is capable of generating the necessary integration to generate appropriate directional tuning during postural perturbations.

Sensory contributions

The critical sensory sources that contribute to the excitatory and inhibitory muscle responses remain poorly understood. Hypotheses about the most critical sensory systems are profuse and diverse; however, there exists little experimental evidence to support these wide ranging hypotheses. We propose that sensory integration exists within a hierachical neural framework. We hypothesize that a central circuit, located within the spinal cord, makes up the foundation from which most postural corrections are made. This foundational circuit utilizes feedback from autogenic and heterogenic sources to

generate appropriately directed muscle activation and inhibition in response to support surface perturbations. We further propose that this foundational circuit is modulated by other sources of feedback such as cutaneous, vestibular, and joint along with feedback from other limbs and supra-spinal sources.

Autogenic and heterogenic feedback is generated through primary and secondary sensory fibers whose length and velocity sensitivities are sophisticatedly controlled through three types of intrafusal muscle fibers: dynamic bag, static bag, and nuclear chain. Each intrafusal fiber type has different actions on primary and secondary muscle spindles generating a complex system by which each muscle spindle's sensitivity is closely controlled. Dynamic bag fibers are effective at increasing length sensitivity of primary muscle spindles during movement, which additionally translates to some increases in velocity sensitivity. However dynamic bag fibers have little effect on secondary endings. Static bag fibers increase the discharge of primary endings regardless of muscle length and do so without influencing amplitude and velocity sensitivity. Nuclear chain fibers, unlike both types of bag fibers, have the most dramatic impact on secondary endings increasing their firing along with their length sensitivity as stretch is increased. Nuclear chain firing does appear to diminish the dynamic response of secondary endings. All of these intrafusal fibers are further modulated through the fusimotor system can regulate the "gain" of intrafusal fibers such that they are extremely sensitive to stretch during movement. This system is primed to generate important feedback about the internal conditions of a muscle. Additionally, the sophisticated and complex innervation of this system implies that it can be equally complexly controlled to direct muscle activation.

Therefore, this thesis investigated if these primary and secondary sensory fibers could generate appropriate feedback to drive muscle activation. (Boyd 1980)

Our data demonstrate that autogenic feedback from muscle spindles drives the direction and breadth of excitatory muscle activation patterns in response to support surface perturbations. We found that all muscle spindles evaluated generated broadly tuned activation patterns that were similarly directed (Chapter 6). Furthermore, we observed other features of excitatory muscle response that are evoked in intact subjects (stance condition and velocity sensitivities) were also observed in muscle spindle responses (Chapter 6). This clearly shows that the muscle spindle can generate all the necessary feedback to drive the direction and breadth of the excitatory muscle response. However, it still was not certain that autogenic feedback was contributing strongly to the excitatory muscle response until we showed that absence of autogenic feedback severely disrupts the excitatory muscle response (Appendix B). As the reinnervation surgery eliminates all autogenic feedback, it is also likely that autogenic positive force feedback contributes to the generation of strong excitatory response. Our reinnervation data is even more powerful in light of the knowledge that no other experimental manipulation of sensory systems has resulted in a complete elimination of the excitatory response evoked by support surface perturbations (Macpherson and Inglis 1993; Stapley et al. 2002). The combination of these observations argue strongly that autogenic feedback, which is not limited to the monosynaptic stretch reflex, drives the direction and breadth of excitatory muscle responses. Therefore, autogenic feedback is at the core of our foundational circuit.

The results reported in this thesis show further that excitatory muscle activation likely is not exclusively driven autogenically. While we would argue that the autogenic response is the strongest contributor, heterogenic excitatory pathways have well documented excitatory effects that could shape the excitatory muscle response (Eccles et al. 1957; Nichols 1989; 1999; Nichols et al. 1999; Ross and Nichols 2009). Excitatory heterogenic feedback has been seen most prevalently in synergist muscles but has also been observed in muscles that span joints such as the excitatory feedback from the vastus intermedialis muscle to the soleus muscle (Nichols et al. 1999). The impact of excitatory heterogenic feedback on the direction and breadth of excitatory muscle responses in uncertain; however we have observed an instance where this type of feedback might contribute. In Chapter 4, we observe that the direction of the LG excitatory tuning curve does not correspond to its expected direction based upon its IM stimulation forces, while the MG muscle shows a very close association with its IM stimulation forces. While there are a few possible explanations (Chapter 4), it is plausible that the LG muscle tuning curve is rotated as a result of synergistic excitatory feedback from the MG muscle. The LG muscle, which has relatively few muscle spindles (Chin et al. 1962), receives strong excitatory feedback from the MG muscle (Eccles et al. 1957; Nichols 1999). Therefore, heterogenic excitatory feedback is also part of our foundational circuit.

Our preliminary data from the reinnervation experiment (Appendix B) demonstrating that the inhibitory muscle response remains strongly intact despite no autogenic feedback indicates that the inhibitory responses are not exclusively autogenically driven. While

there are several potential sensory sources that could be driving these responses, we hypothesize that the inhibitory muscle response is shaped both by 1) the dysfacilitation that occurs as muscle spindles are subjected to perturbations that shorten the muscle and 2) heterogenic inhibitory feedback: specifically from reciprocal inhibition, although heterogenic force feedback likely would also contribute.

We believe that heterogenic inhibitory feedback is the strongest contributor to the inhibitory response. Muscle spindles are asymmetric in their responses showing more sensitive to increases in length than decreases (Houk et al. 1981a). Thus, it is plausible to assume that the dysfacilitation signal is not as strong as the signal from reciprocal inhibition generated from a large increase in firing from antagonist muscle spindles. Ancillary evidence comes from our observation that the excitatory and inhibitory EMG tuning curves are rarely a perfect 180 degrees rotated from one another (Chapter 2). Indeed, we noted that inhibitory tuning curves, while generally directed oppositely to excitatory tuning curves, could be as much as 30 degrees off from complete numerical opposition (180 degrees). If the inhibitory tuning curves were primarily driven through autogenic muscle spindle dysfacilitation, the inhibitory tuning curves would be mirror images of the excitatory responses (Chapter 6). Regardless dysfacillitation and heterogenic inhibitory feedback are both represented in our foundational circuit diagram.

Finally, it was noted that the EMG generated during the steady-state hold in the decerebrate cat (Chapter 2) is often variable in its expression. Due to their quick adaptation, primary muscle spindle afferents are likely not strongly contributing during

this phase of the response. Secondary muscle spindle afferents do have a steady state firing response; however this alone likely does not fully explain the strong EMG response. We would suggest that longer latency heterogenic pathways like positive force feedback along with bistable behavior (Hultborn 1999) also contribute at longer latencies to the expression of muscular activation in the decerebrate animal.

Foundational circuit

Our foundational circuit is therefore composed of feedback from 1) autogenic, 2) heterogenic excitatory, and 3) heterogenic inhibitory sources. We propose that these three are important sources of feedback that drive the direction and breadth of both the excitatory and inhibitory muscle responses to support surface perturbations. As previously stated, we hypothesize that the spinal cord alone houses the circuitry to mediate directional tuning. All the circuitry described is known to be present within the spinal cord. While it is likely that this feedback is also integrated on higher levels in the neural hierarchy, our data along with that collected in the spinal cat suggests that these higher structures are not required for directionally appropriate muscle activation.

Experimental evidence that appears to refute our notion of a foundational circuit driven by autogenic and hetereogenic feedback comes from EMG collected during rotations of the support surface. Authors noted that muscles generated similarly directed excitatory muscle activation patterns in directions where muscle spindle feedback would theoretically be inappropriate (Ting and Macpherson 2004). However, this conclusion arises from the assumption that muscle spindle firing can be elucidated from kinematic

measurements of muscular length. Muscle spindle recordings during locomotion in the intact cat demonstrate that muscle spindle firing does not always correlate to whole muscle length particularly during active contractions (Prochazka 77). Furthermore, more recent evaluation of muscle fascicle length in humans during volitional sway indicates that fascicle length does not match the kinematically assessed muscle length (Loram et al. 2006). Finally, as the autogenic feedback occurs throughout the muscular response and is not limited to the monosynaptic stretch reflex, without further information about the muscle spindle response throughout the duration of the rotation, one cannot conclude that muscle spindle feedback is inappropriate.

Still, it is likely that other sources of sensory feedback are required to modulate our foundational circuit to generate an appropriate response. For example, our data suggests that cutaneous feedback generates a biasing effect on the muscular activity (Chapter 5). It has also been shown that a loss of vestibular feedback causes subjects to generate hypermetric responses (Macpherson and Inglis 1993), indicating that vestibular influences the scale of muscle responses. Vestibular feedback may induce these scaling effects by utilizing our foundational circuit. Joint afferents that innervate the intra-articular structures of the limb demonstrate diverse responses to joint movements which may relay feedback about the position of the limb (Proske et al. 1988; Zimmy 1988). However little known about these receptors as their identification and study is challenging. Most of the joint afferents that have been studied fired very little during mid-range joint movement (Burgess and Clark 1969; Clark and Burgess 1975; Ferrell 1980). This was particularly the case in joints of the lower limb where only 2 percent of

the knee join afferents were found to fire during mid-range movements (Grigg and Greenspan 1977) suggesting that these receptors are more appropriate for signaling extreme joint angle configurations that might lead to injury. Still, as some of the studies found that joints afferents do respond to mid-range movements (Burgess and Clark 1969), particularly in the fingers of the human, we can not exclude them as contributing to muscular activation during postural tasks. Finally, we know that supraspinal circuits can suppress the excitability of reflexes, such as the monosynaptic stretch reflex, mediated by the spinal cord circuitry (Kandel et al. 2000; Nashner 1976). Thus it is also likely that supraspinal circuits modulate our foundational circuit. Therefore all of these sensory sources are depicted as generating input onto our foundation circuit in Figure 7.1.

Finally, our observation that four-limb perturbations "rescue" the excitatory responses of the reinnervated limb implies an important role for inter-limb feedback (Appendix B). This rescue effect also appears to diminish the responses of the untreated limb. This suggests an important relationship between the two limbs in generating appropriate tuning. It is unclear if this inter-limb connection is a result of an adaptation to the reinnervation itself or if these connections exist under normal conditions. It is logical to assume that inter-limb feedback integration is necessary to generate appropriate muscle responses. A subject would respond differently if only one limb was perturbed as opposed to a whole body perturbation. These pathways, along with those of our foundational circuit, are members of a distributive neural network in the spinal cord that could provide the foundation for the postural response. As this distributive network receives inputs from many sensory systems that provide feedback about the many joints

and limbs of the musculoskeletal system, it may provide representation of the key global variables required for postural control.

Conclusions

It is clear that postural regulation is complex and involves many sensory systems and levels of neural integration. Appropriately directed muscle activation is only one aspect of this complex motor task. Full expression of postural control relies not only on appropriate directional tuning but biasing, scaling, and modulation of muscle responses requiring integration of several types of feedback. Therefore it is plausible that the structures critical to postural control exist within a hierarchical framework in which each unit is responsible for increasingly complex integration of sensory and environmental information. Autogenic and heterogenic circuits, known to be located within the spinal cord, appear sufficient to determine directional tuning of postural responses; however, these muscle activation patterns are likely biased through cutaneous or scaled through vestibular feedback or signals from supraspinal structures. Complex tasks such as managing terrain adjustments during locomotion or anticipatory adjustments prior to volitional movements are likely mediated by the cortex which presumably makes use of sensory information from the lower structures. While it is certain that many brain structures actively participate in postural control, we believe the spinal cord and the foundational circuit described in Figure 7.1 contribute the critical elements of directional tuning in order to produce appropriate postural responses.

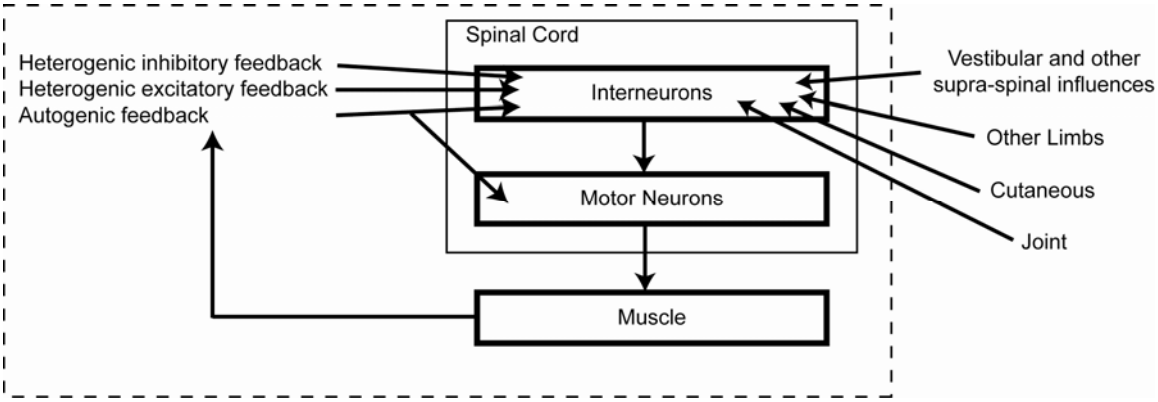

Figure 7.1: Foundational Circuit. Depicts the foundation circuits (in dashed box) described in the above text. We propose that autogenic and heterogenic feedback from muscle are among the most critical forms of feedback driving the directional tuning of excitatory and inhibitory muscle activation patterns. We further propose that integration of this feedback is completed from within the spinal cord. Finally, we propose that other sources of sensory feedback along with supra-spinal influences act to modulate our foundational circuit.

APPENDIX A

THE MODIFIED PREMAMMILLARY DECEREBRATION TECHNIQUE

A.1 Rationale

The development of the modified premammillary decerebrate preparation was critical to the success of Chapter 2, 3, and 5. We know that animals decerebrated at the precollicular level are able to generate directionally appropriate muscle activation patterns (see Chapter 2). However, they did so infrequency (4 out of 28 animals) and rarely for longer than a few minutes such that systematic investigation of the muscle responses was almost impossible. The spontaneous locomotion generated by the premammillary decerebrate animal made analysis of specific postural adjustments very challenging. Animals decerebrated with the modified premammillary technique generated muscular responses to support surface perturbations that were larger in amplitude, in a more diverse set of muscles, and for longer than any of the intercollicular preparations (see Chapter 2). Our main objective was to quantify our new decerebration technique such that we could 1) develop a systematic protocol and 2) evaluate the role of the upper brainstem (rostral to the colliculi) in achieving robust muscular responses to support surface perturbations.

A.2 Methods

Animals were decerebrated using two alterations from the traditional premammillary decerebration: 1) a slightly steeper premammillary transection and 2) a second vertical transection. Before the transections were completed, the large sections of cortex

surrounding the brainstem (left, right, and dorsal) were removed. The first transection is completed at a 45 degree angle from 1.5cm to 3cm rostral of the tentorium. A traditional premammillary decerebration is around 50 degrees (Grillner and Shik 1973). The 1.5cm corresponds to the rostral boundary of the superior colliculus. The 3cm corresponds to the rostral boundary of the mamillary bodies. All brain material rostral to the first transection was removed. The second, vertical transection was made 2-3mm caudally from the first. Brain material rostral to the second transection was preserved to dissipate the additional injury of removal. Figure 1 shows these transections along with the traditional precollicular and premammillary decerebration transections. The 10/8/2007, 1/22/08, 1/24/08, and 1/29/08 experiments required no further transections. However, occasionally preparations still exhibited locomotion and further transections were required. One additional vertical transection was performed in the 9/28/07, 10/16/07, 12/4/07, 12/6/07, and 12/20/07 and two more were performed in the 12/18/07 experiment.

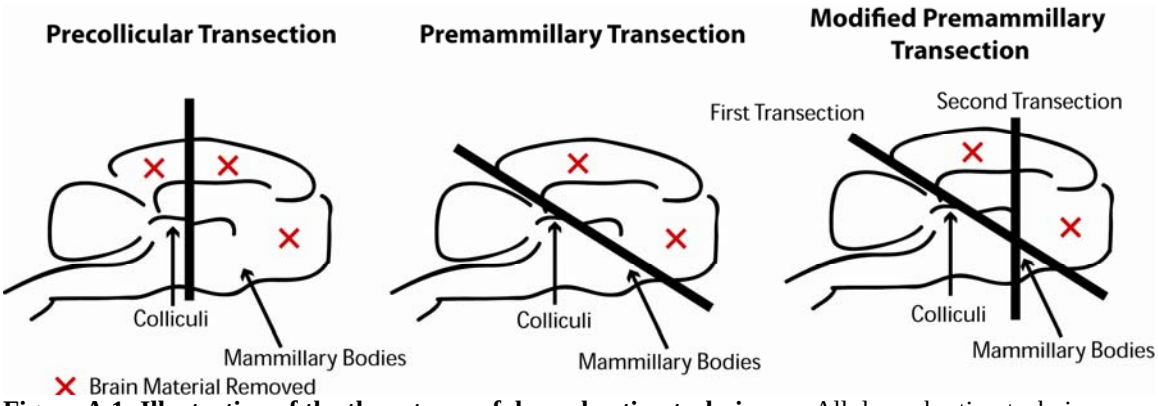

Figure A.1: Illustration of the three types of decerebration techniques. All decerebration techniques begin with full removal of the cerebral cortices. The precollicular decerebration is following by one vertical transection at the rostral boundary of the superior colliculus (Left). The premammillary decerebration includes a 50 degree transection starting at the rostral boundary of the superior colliculus and continuing forward just rostral to the mammillary bodies (Center). Our technique adds a vertical transection 2-3mm caudally from the front edge of the premammillary decerebration (Right).

After the decerebration, the animals were positioned for support surface perturbations and data were collected as previously described in Chapters 2 and 3. After data collection

and administration of euthisol, the brainstem was carefully removed and immediately placed in formaldehyde. After approximately a week, the brainstem was removed from the formaldehyde and placed in sucrose for storage. Half of each brainstem was then sliced into 50 micrometer sections every .8 mm of brainstem. Three sections were collected and one section was mounted for staining and imaging. A traditional nissle stain was performed for ease of structure identification. Finally, an imaging microscope was used to take images that could be enlarged for analysis. Structures rostral to the superior colliculus were identified from each of the most medial brainstem transections. They were identified as being present, absent or marginally present.

A.3 Results and Discussion

The best experiments were defined as those that exhibited muscle responses in the most diverse set of muscles and did so for over 30minutes. Table A.1 shows the list of muscles that generated at least one tuning curve in each experiment. Three of the best experiments (10/8, 12/18, and 1/22) are further described in chapters 2 and 3 while the last of the best experiments (1/29) is further described in Appendix B. Three of the four best experiments required no further retransections; however the 12/18 experiment required 2 retransections to eliminate locomotion. A few of the poor experiments (12/20, 12/6) initially exhibited strong locomotion but after the retransection not only did not exhibit locomotion but showed poor postural performances as well.

We found that the best experiments had a clear vertical transection along the rostral border of the thalamus. The brainstems associated with the best experiments are seen in

Figure A.2, while those associated with the poor experiments are seen in Figure A.3. Detailed structures lists are located in Table A.2. The brainstems of Figure A.2 clearly contain the colliculi (C), the thalamus (T), and all structures located ventrally to these structures. All of the brainstems associated with poor experiments (with one exception: 1/24) have damage to the thalamic or hypothalamic regions (Figure A.3). Marked with an asterisk the 12/6 and 9/28 experiments have damage to the hypothalamic region located ventrally to the thalamus while the 12/20 and 10/16 experiments exhibit a transection through the middle of the thalamus and hypothalamus. Finally, the 12/4 experiment initially exhibited strong locomotion and therefore was retransected at a point that appears precollicular in nature (asterisk). The only poor experiment that did not have obvious damage to these regions was the 1/24 experiment. This preparation is classified as a poor experiment due to the small number of muscles that exhibited responses. However, the muscle responses that were attained were exhibited for an extended period of time (greater than 30minutes). We suspect that while the thalamus and hypothalamus structures are present, they may have significant death. Further analysis of vitality of the brainstem structures is necessary to verify that hypothesis.

While further study is required, it appears that the presence of the thalamus and hypothalamus greatly enhances the robustness of the muscle responses to support surface perturbations. Before we can establish which structures are contributing to the robustness of these responses, we must know 1) which regions are still alive and 2) how these preparations differ from the locomotion preparations. Flurojade staining will allow us to quantify which regions were still living at the time of the animal's death and will help us

determine which regions may be contributing. Detailing the difference between the locomotion preparation and the postural preparation will be more challenging. The traditional premammillary decerebration described in the literature (Grillner and Shik 1973) eliminates the thalamus. However all of our preparations that exhibit strong locomotion, including those evaluated but not reported in this Appendix, had a fully intact thalamus. Therefore, it is necessary to perform this same type analysis on the brainstems of the preparations that exhibit robust locomotion for specific comparison.

Table A.1: List of muscles that generated tuning curves.

Best Experiments	Muscles demonstrating tuning
1/29/2008	R LG, R Sol, L MG, L LG, L Sol, R Glut
12/18/2007	MG, aSart, ST, cSM, pBF, aBF, VM, Grac
1/22/2008	R LG, L MG, L sol, L Glut, R Glut, L aBF
10/8/2007	Glut, pBF, aBF, VM, VL, ST, SM, Ilio, Grac

Poor Experiments	Muscles demonstrating tuning
9/28/2007	Glut, Grac, L Sol, R LG, R Sol
1/24/2008	R LG, L Sol, L LG,
12/4/2007	L sol, R sol
12/6/2007	Glut, L Sol,
12/20/2007	Ilio
10/16/2007	Before mechanical failure EMG data present in Grac, ST

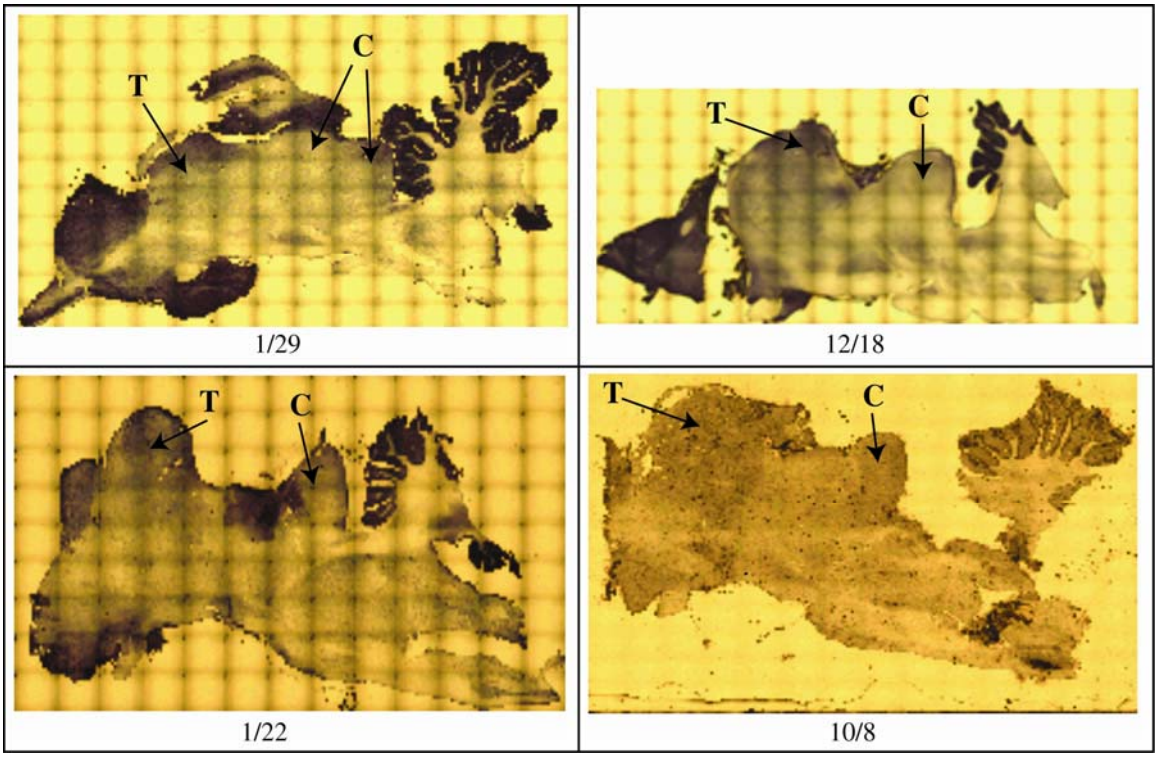

Figure A.2: Brainstems from experiments exhibiting the best muscular responses to support surface perturbations. The colliculi (C) and thalamus (T) are labeled in each of the four best experiments. It is noted that all of these experiments contain the full thalamus and exhibit no obvious damage to either the thalamus or hypothalamus (ventral to T) structures.

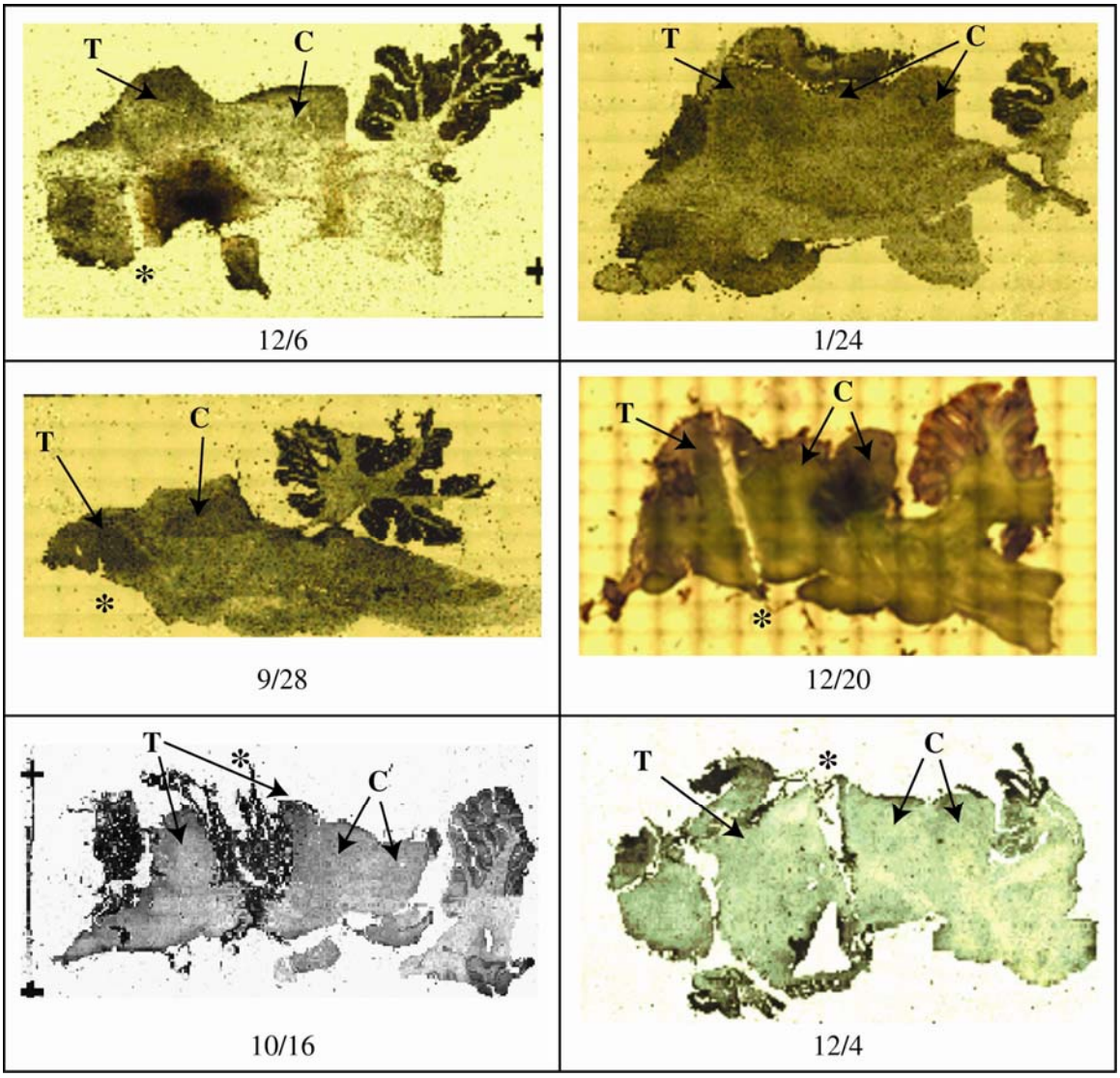

Figure A.3: Brainstems from the experiments that generated poor responses to support surface perturbations. The colliculi (C) and thalamus (T) are labeled in each of the brainstems presented above. An asterisk marks regions were damage was observed in each of these experiments. The only experiment that did not have clear damage was the 1/24 experiment.

Table A.2: List of present (black), absent (white) or marginally present (dashed) brainstem structures is each experiment.

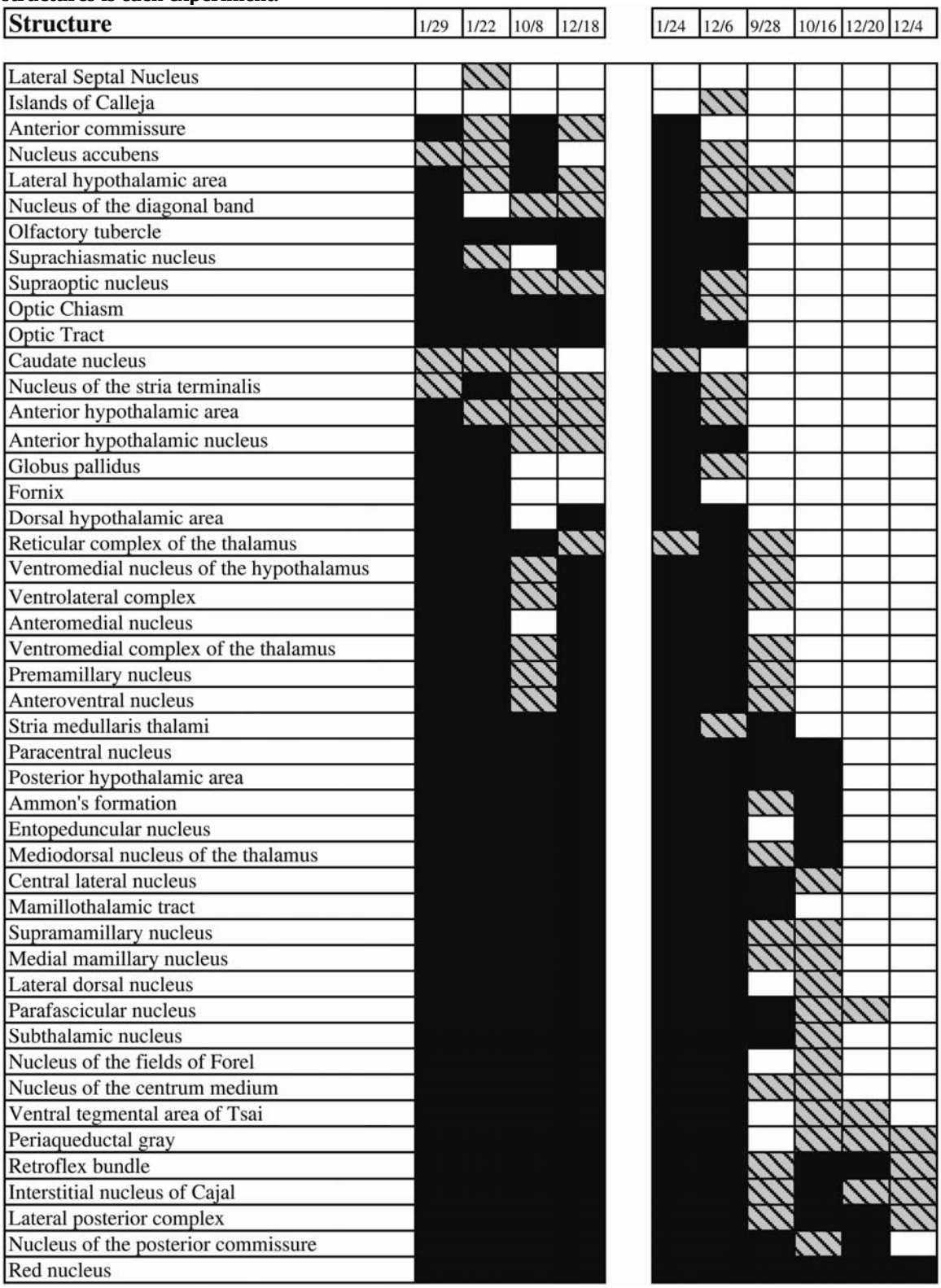

Best experiments are located in the first four columns.

A.4 Acknowledgments

Special thanks to Shawn Hochman who provided his expertise, lab space, and supplies for this venture. Thanks also to Mike Sawchuk and Tejal Patel who performed the slicing, mounting, staining, and imaging. Finally, thanks to Constance Harrell who assisted with the slicing and imaging and performed the analysis.

APPENDIX B

LOSS OF PROPRIOCEPTIVE FEEDBACK FROM MUSCLE SIGNIFICANTLY DISRUPTS THE EXCITATORY MUSCULAR RESPONSE TO SUPPORT SURFACE PERTURBATIONS IN THE DECEREBRATE CAT

B.1 Rational

As discussed in detail in the preceding chapters, we hypothesize that feedback from muscle receptors, specifically muscle spindles, drives the directional tuning of muscle responses to support surface perturbations. We have demonstrated that muscle spindle afferents generate similarly tuned activation patterns to support surface perturbations. Furthermore, muscle spindle responses scale with stance condition and show attributes of velocity dependence seen in the intact animal. Finally, we have demonstrated that loss of cutaneous feedback from the pads of the feet does not alter the directional tuning of muscle responses in the decerebrate cat. As this preparation does not have feedback from the visual or vestibular systems, a strong role for muscle receptor feedback in driving directional tuning is implied. Therefore, our objective was to evaluate what, if any, muscle activation was possible after a surgically induced loss of muscle receptor feedback. If a significant disruption of the muscle activation patterns is present, this would strongly support our primary hypothesis.

B.2 Methods

A reinnervation surgery was performed on the entire triceps surae group of the right hindlimb in two animals. The reinnervation technique disrupts feedback to the reinnervated muscle while preserving motor function (Cope and Clark 1993). After two years of recovery, the animals were decerebrated using a modified premammillary

decerebration, which allows for robust postural responses similar to that of the intact animal, and the animals were subjected to support surface perturbations like those previously described (Chapter 2). EMG data was collected from the triceps surae muscles on both the right (reinnervated) and left (untreated) legs. The untreated muscles from the 1/24 experiment did not generate strong responses. Therefore, it was impossible to determine if the disruption of EMG in the reinnervated muscles was due to a poor preparation or due to the reinnervation intervention. Therefore, all results discussed will be from the 1/29 experiment.

B.3 Results and Discussion

While individual trials from the untreated muscles always gave excitatory tuning curves, the reinnervated muscles generated small and fragmented excitatory responses. Therefore, 3 trials were averaged to pull out consistent activity changes. Figure B.1 shows the averaged raw EMG trials of both the reinnervated and untreated sides and Figure B.2 shows the tuning curves associated with those EMG traces. When averaged, a brief excitatory response was present approximately 50-100ms delayed from the untreated side. These responses were extremely small in amplitude and duration consisting of a brief burst of activity. However they appear to be in the appropriate directions (see Figure B.2). Interestingly, the inhibitory response remained mostly intact.

When all four limbs were perturbed together, the reinnervated limb was able to elicit a more pronounced excitatory response (Figure B.3). While the response of the reinnervated limb was not nearly as robust or defined as a typical response, it was able to

generate a quantifiable response in the appropriate directions. These same trials showed a disruption of the untreated side's excitatory responses. The raw EMG demonstrates diminished amplitude and the tuning curves appear more fragmented. As four limb trials were performed first, this observation is likely not the result of preparation deterioration. While this inter-limb interaction may result from the chronic animal's compensation for the autogenic feedback loss, we suspect that these inter-limb interactions exist under normal, control conditions.

These results confirm our hypothesis that muscle receptors are critically important to generating directionally appropriate muscle activation patterns. Furthermore as cutaneous feedback is not affected by the reinnervation, this data demonstrates that cutaneous feedback alone is not sufficient to generate excitatory muscle responses in the decerebrate cat. However, these studies also indicate that an individual muscle's response is likely influenced by other musculature even from within the contra-lateral limb. In the future, we will further confirm this result with additional animals. Additionally, we plan to investigate the inter-limb feedback driving the rescue of the reinnervated side. After completing the necessary controls, we will evaluate the length driven feedback between the limbs using muscle pullers.

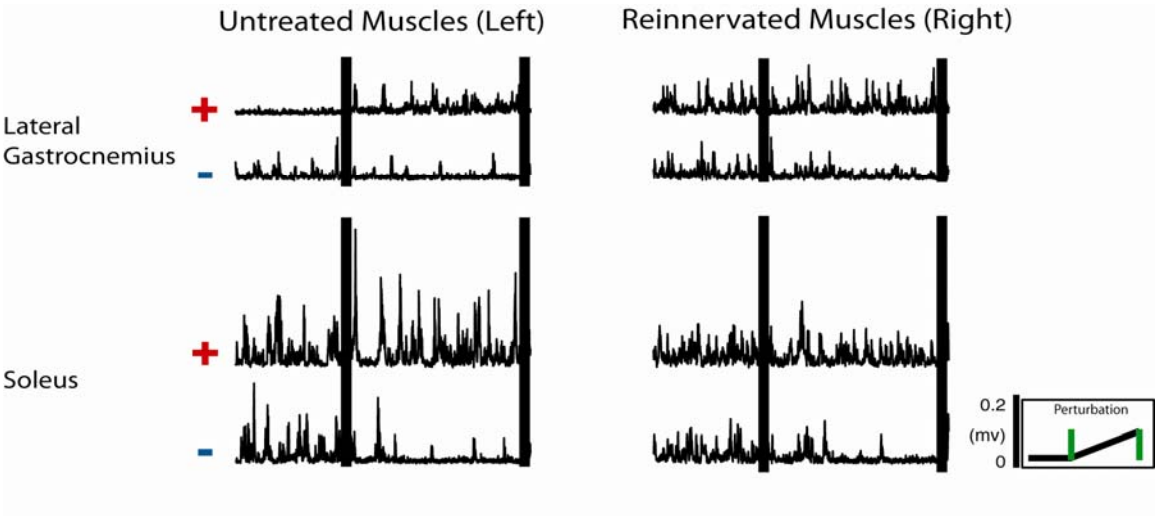

Figure B.1: Raw EMG traces from reinnervated and untreated muscles. Raw EMG from the LG and Sol muscles from both the reinnervated and untreated limbs during support surface perturbations of 1 leg. The untreated muscles show the typical increase in activation within 25-30ms after perturbation initiation (Left). The reinnervated muscles, however, show a significant disruption in the excitatory response.

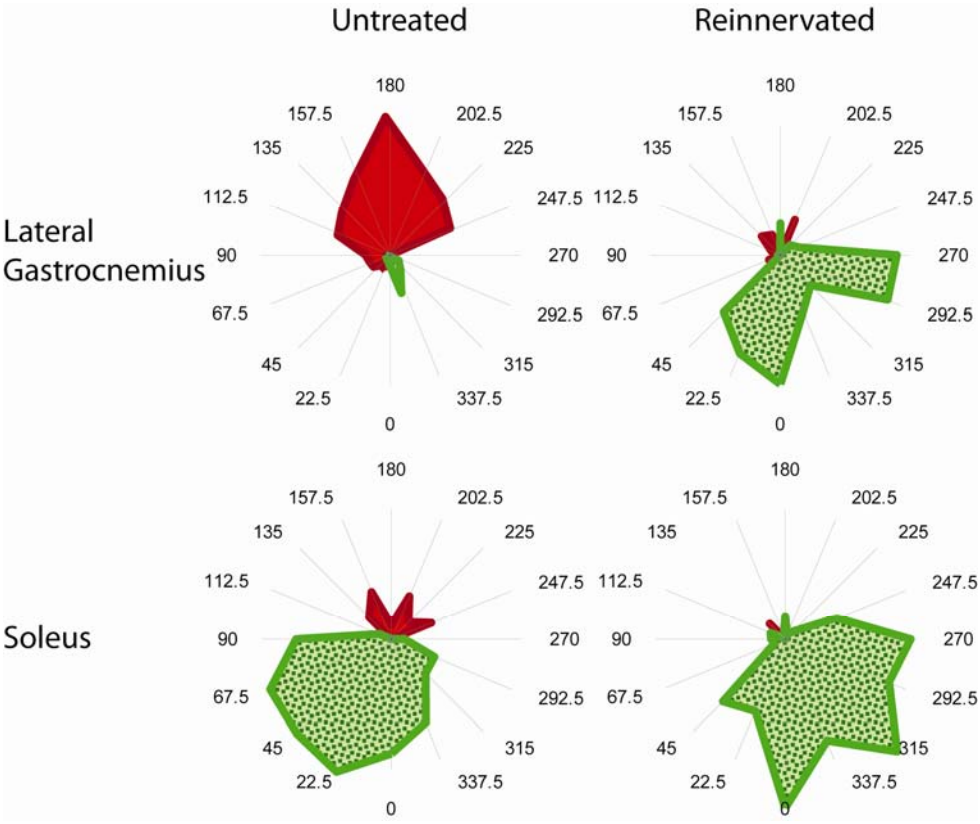

Figure B.2: Tuning curves of the reinnervated and untreated limbs during 1 limb perturbations. The reinnervated muscles have a very poor excitatory response, while the untreated limb generates typical tuning curves. Interestingly, the inhibitory response of the reinnervated muscles remains intact.

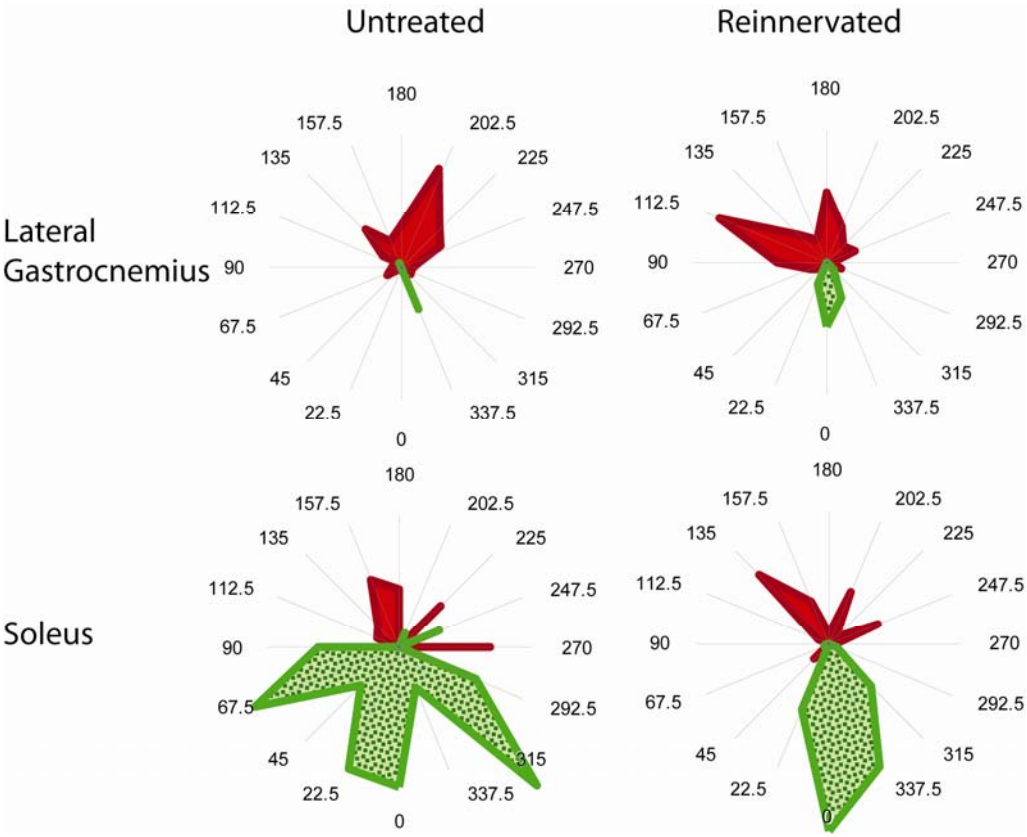

Figure B.3: Tuning curves of the reinnervated and untreated limbs during 4 limb perturbations. Perturbation of the untreated limb appears to "rescue" the reinnervated limb. However, the responses seen in the reinnervated limb are still not typical tuning curves. Furthermore, the tuning curves of the untreated limbs are diminished as a result of the "rescue."

REFERENCES:

Abelew TA, Miller MD, Cope TC, and Nichols TR. Local loss of proprioception results in disruption of interjoint coordination during locomotion in the cat. *J Neurophysiol* 84: 2709-2714, 2000.

Adkin AL, Quant S, Maki BE, and McIlroy WE. Cortical responses associated with predictable and unpredictable compensatory balance reactions. *Exp Brain Res* 172: 85-93, 2006.

Allum JH, Bloem BR, Carpenter MG, Hulliger M, and Hadders-Algra M. Proprioceptive control of posture: a review of new concepts. *Gait Posture* 8: 214-242, 1998.

Beloozerova IN, Sirota MG, Orlovsky GN, and Deliagina TG. Activity of pyramidal tract neurons in the cat during postural corrections. *J Neurophysiol* 93: 1831-1844, 2005.

Beloozerova IN, Sirota MG, Swadlow HA, Orlovsky GN, Popova LB, and Deliagina TG. Activity of different classes of neurons of the motor cortex during postural corrections. *J Neurosci* 23: 7844-7853, 2003a.

Beloozerova IN, Zelenin PV, Popova LB, Orlovsky GN, Grillner S, and Deliagina TG. Postural control in the rabbit maintaining balance on the tilting platform. *J Neurophysiol* 90: 3783-3793, 2003b.

Bloem BR, Allum JH, Carpenter MG, and Honegger F. Is lower leg proprioception essential for triggering human automatic postural responses? *Exp Brain Res* 130: 375-391, 2000.

Bolton DAE, and Misiaszek JE. The role of hind paw cutaneous information in lateral stability during walking in the cat. In: *Society for Neuroscience*. San Diego: 2007.

Bonasera SJ, and Nichols TR. Mechanical actions of heterogenic reflexes among ankle stabilizers and their interactions with plantarflexors of the cat hindlimb. *J Neurophysiol* 75: 2050-2070, 1996.

Bonasera SJ, and Nichols TR. Mechanical actions of heterogenic reflexes linking long toe flexors with ankle and knee extensors of the cat hindlimb. *J Neurophysiol* 71: 1096-1110, 1994.

Bonasera SJ, Pratt CA, Price CMJI, Cope TC, and Nichols TR. Stance training preserves intermuscular reflexes and muscle properties in chronic spinal cats. In: *Society for Neuroscience*1994, p. 572.

Bosco G, and Poppele RE. Proprioception from a spinocerebellar perspective. *Physiol Rev* 81: 539-568, 2001.

Buchanan TS, Almdale DP, Lewis JL, and Rymer WZ. Characteristics of synergic relations during isometric contractions of human elbow muscles. *J Neurophysiol* 56: 1225-1241, 1986.

Burkholder TJ, and Nichols TR. Three-dimensional model of the feline hindlimb. *J Morphol* 261: 118-129, 2004.

Chanaud CM, and Macpherson JM. Functionally complex muscles of the cat hindlimb. III. Differential activation within biceps femoris during postural perturbations. *Exp Brain Res* 85: 271-280, 1991.

Cope TC, and Clark BD. Motor-unit recruitment in self-reinnervated muscle. *J Neurophysiol* 70: 1787-1796, 1993.

Cope TC, and Clark BD. Motor-unit recruitment in the decerebrate cat: several unit properties are equally good predictors of order. *J Neurophysiol* 66: 1127-1138, 1991.

Cope TC, Sokoloff AJ, Dacko SM, Huot R, and Feingold E. Stability of motor-unit force thresholds in the decerebrate cat. *J Neurophysiol* 78: 3077-3082, 1997.

Crouch JE. *Text-Atlas of Cat Anatomy*. Philadelphia: Lea & Febiger, 1969.

Degtyarenko AM, Simon ES, and Burke RE. Differential modulation of disynaptic cutaneous inhibition and excitation in ankle flexor motoneurons during fictive locomotion. *J Neurophysiol* 76: 2972-2985, 1996.

Deliagina TG, Beloozerova IN, Zelenin PV, and Orlovsky GN. Spinal and supraspinal postural networks. *Brain Res Rev* 57: 212-221, 2008.

Deliagina TG, Orlovsky GN, Zelenin PV, and Beloozerova IN. Neural bases of postural control. *Physiology (Bethesda)* 21: 216-225, 2006.

Diener HC, Horak FB, and Nashner LM. Influence of stimulus parameters on human postural responses. *J Neurophysiol* 59: 1888-1905, 1988.

Dietz V, Quintern J, and Berger W. Cerebral evoked potentials associated with the compensatory reactions following stance and gait perturbation. *Neurosci Lett* 50: 181-186, 1984.

Eccles JC, Eccles RM, and Lundberg A. The convergence of monosynaptic excitatory afferents on to many different species of alpha motoneurones. *J Physiol* 137: 22-50, 1957.

Edgerton VR, Leon RD, Harkema SJ, Hodgson JA, London N, Reinkensmeyer DJ, Roy RR, Talmadge RJ, Tillakaratne NJ, Timoszyk W, and Tobin A. Retraining the injured spinal cord. *J Physiol* 533: 15-22, 2001.

Everaert DG, Ting LH, Stapley PJ, Chen K, and Stein RB. Postural responses to pitch and roll rotations in cats with vestibular loss. In: *Society for Neuroscience*. Washington D.C.: 2005.

Fagg AH, Shah A, and Barto AG. A computational model of muscle recruitment for wrist movements. *J Neurophysiol* 88: 3348-3358, 2002.

Fallon JB, Bent LR, McNulty PA, and Macefield VG. Evidence for strong synaptic coupling between single tactile afferents from the sole of the foot and motoneurons supplying leg muscles. *J Neurophysiol* 94: 3795-3804, 2005.

Fukson OI, Berkinblit MB, and Feldman AG. The spinal frog takes into account the scheme of its body during the wiping reflex. *Science* 209: 1261-1263, 1980.

Fung J, and Macpherson JM. Attributes of quiet stance in the chronic spinal cat. *J Neurophysiol* 82: 3056-3065, 1999.

Fung J, and Macpherson JM. Determinants of postural orientation in quadrupedal stance. *J Neurosci* 15: 1121-1131, 1995.

Gottschall JS, and Nichols TR. Head pitch affects muscle activity in the decerebrate cat hindlimb during walking. *Exp Brain Res* 182: 131-135, 2007.

Grillner S, and Shik ML. On the descending control of the lumbosacral spinal cord from the "mesencephalic locomotor region". *Acta Physiol Scand* 87: 320-333, 1973.

Haftel VK, Bichler EK, Wang QB, Prather JF, Pinter MJ, and Cope TC. Central suppression of regenerated proprioceptive afferents. *J Neurosci* 25: 4733-4742, 2005.

Hasan Z, and Houk JC. Transition in sensitivity of spindle receptors that occurs when muscle is stretched more than a fraction of a millimeter. *J Neurophysiol* 38: 673-689, 1975.

Henry SM, Fung J, and Horak FB. Effect of stance width on multidirectional postural responses. *J Neurophysiol* 85: 559-570, 2001.

Henry SM, Fung J, and Horak FB. EMG responses to maintain stance during multidirectional surface translations. *J Neurophysiol* 80: 1939-1950, 1998.

Hoffman DS, and Strick PL. Step-tracking movements of the wrist. IV. Muscle activity associated with movements in different directions. *J Neurophysiol* 81: 319-333, 1999.

Honeycutt CF, Nardelli P, Cope TC, and Nichols TR. Autogenic spindle pathways mediate the postural response during horizontal support surface perturbations. In: *Society for Neuroscience*. San Deigo, CA: 2007.

Honeycutt CF, and Nichols TR. Contribution of cutaneous and proprioceptive feedback on muscle activation patterns during postural perturbation in decerebrate cats. In: *Society for Neuroscience*. Washington, D.C.: 2005.

Honeycutt CF, and Nichols TR. Force responses of the postural strategy in the decerebrate cat. In: *Society for Neuroscience*. Atlanta, GA: 2006.

Honeycutt CF, Stahl VA, and Nichols TR. Loss of proprioceptive feedback from muscle disrupts the excitatory postural response to support surface perturbations. In: *Society for Neuroscience*. Washington, D.C.: 2008.

Houk JC. Regulation of stiffness by skeletomotor reflexes. *Annu Rev Physiol* 41: 99-114, 1979.

Houk JC, Rymer WZ, and Crago PE. Dependence of dynamic response of spindle receptors on muscle length and velocity. *J Neurophysiol* 46: 143-166, 1981a.

Houk JC, Rymer WZ, and Crago PE. Nature of the dynamic response and its relation to the high sensitivity of muscle spindles to small changes in length. In: *Muscle receptors and movement*, edited by Taylor A, and Prochazka A. London: MacMillan, 1981b.

Jacobs JV, and Horak FB. Cortical control of postural responses. *J Neural Transm* 114: 1339-1348, 2007.

Kandel ER, Schwartz JH, and Jessel TM. *Principals of Neural Science*. McGraw-Hill, 2000.

Kavounoudias A, Roll R, and Roll JP. Foot sole and ankle muscle inputs contribute jointly to human erect posture regulation. *J Physiol* 532: 869-878, 2001.

Kavounoudias A, Roll R, and Roll JP. The plantar sole is a 'dynamometric map' for human balance control. *Neuroreport* 9: 3247-3252, 1998.

Kaya M, Leonard TR, and Herzog W. Control of ground reaction forces by hindlimb muscles during cat locomotion. *J Biomech* 39: 2752-2766, 2006.

Kutch JJ, Kuo AD, Bloch AM, and Rymer WZ. Endpoint force fluctuations reveal flexible rather than synergistic patterns of muscle cooperation. *J Neurophysiol* 100: 2455-2471, 2008.

Lawrence JH, 3rd, Nichols TR, and English AW. Cat hindlimb muscles exert substantial torques outside the sagittal plane. *J Neurophysiol* 69: 282-285, 1993.

Lawrence JH, 3rd; Nichols, T. R.;. A three-dimensional biomechanical analysis of the cat ankle joint complex: I. Active and passive postural mechanics. *Journal of Applied Biomechanics* 15: 95-105, 1999.

Leonard JA, Brown RH, and Stapley PJ. Reaching to multiple targets when standing: The spatial organization of feed-forward postural adjustments. Montreal, Quebec, Canada: McGill University, 2009.

Lockhart DB, and Ting LH. Optimal sensorimotor transformations for balance. *Nat Neurosci* 10: 1329-1336, 2007.

Lyalka VF, Zelenin PV, Karayannidou A, Orlovsky GN, Grillner S, and Deliagina TG. Impairment and recovery of postural control in rabbits with spinal cord lesions. *J Neurophysiol* 94: 3677-3690, 2005.

Macpherson JM. Changes in postural strategy with inter-paw distance. *J Neurophysiol* 71: 931-940, 1994a.

Macpherson JM. The force constraint strategy for stance is independent of prior experience. *Exp Brain Res* 101: 397-405, 1994b.

Macpherson JM. Strategies that simplify the control of quadrupedal stance. I. Forces at the ground. *J Neurophysiol* 60: 204-217, 1988a.

Macpherson JM. Strategies that simplify the control of quadrupedal stance. II. Electromyographic activity. *J Neurophysiol* 60: 218-231, 1988b.

Macpherson JM, and Fung J. Weight support and balance during perturbed stance in the chronic spinal cat. *J Neurophysiol* 82: 3066-3081, 1999a.

Macpherson JM, and Fung J. Weight support and balance during perturbed stance in the chronic spinal cat. *J Neurophysiol* 82: 3066-3081, 1999b.

Macpherson JM, and Inglis JT. Stance and balance following bilateral labyrinthectomy. *Prog Brain Res* 97: 219-228, 1993.

Magnus R. Physiology of Posture. *Lancet* 11: 531-581, 1926.

Martin RS, Cope TC, Nakanishi ST, and Nichols TR. Differential Dynamic and Steady State Responses of Muscle Proprioceptors
in response to Postural Disturbances. In: *Society for Neuroscience*. Washington, D.C.: 2005.

Maurer C, Mergner T, Bolha B, and Hlavacka F. Human balance control during cutaneous stimulation of the plantar soles. *Neurosci Lett* 302: 45-48, 2001.

Maurer C, Mergner T, and Peterka RJ. Multisensory control of human upright stance. *Exp Brain Res* 171: 231-250, 2006.

McCrea DA, Shefchyk SJ, Stephens MJ, and Pearson KG. Disynaptic group I excitation of synergist ankle extensor motoneurones during fictive locomotion in the cat. *J Physiol* 487 (Pt 2): 527-539, 1995.

McKay JL, Burkholder TJ, and Ting LH. Biomechanical capabilities influence postural control strategies in the cat hindlimb. *J Biomech* 40: 2254-2260, 2007.

McKay JL, and Ting LH. Functional muscle synergies constrain force production during postural tasks. *J Biomech* 41: 299-306, 2008.

Mergner T, Maurer C, and Peterka RJ. A multisensory posture control model of human upright stance. *Prog Brain Res* 142: 189-201, 2003.

Meyer PF, Oddsson LI, and De Luca CJ. The role of plantar cutaneous sensation in unperturbed stance. *Exp Brain Res* 156: 505-512, 2004.

Miller AD, and Brooks VB. Late muscular responses to arm perturbations persist during supraspinal dysfunctions in monkeys. *Exp Brain Res* 41: 146-158, 1981.

Mori S. Integration of posture and locomotion in acute decerebrate cats and in awake, freely moving cats. *Prog Neurobiol* 28: 161-195, 1987.

Mori S, Sakamoto T, Ohta Y, Takakusaki K, and Matsuyama K. Site-specific postural and locomotor changes evoked in awake, freely moving intact cats by stimulating the brainstem. *Brain Res* 505: 66-74, 1989.

Murinas KI. Transformation of Muscular Actions into Endpoint Forces in the Cat Hindlimb during Stance. In: *Biomedical Engineering*. Atlanta, GA: Georgia Institute of Technology, 2003.

Musienko PE, Zelenin PV, Lyalka VF, Orlovsky GN, and Deliagina TG. Postural performance in decerebrated rabbit. *Behav Brain Res* 190: 124-134, 2008.

Nashner LM. Adapting reflexes controlling the human posture. *Exp Brain Res* 26: 59-72, 1976.

Nichols TR. The organization of heterogenic reflexes among muscles crossing the ankle joint in the decerebrate cat. *J Physiol* 410: 463-477, 1989.

Nichols TR. Receptor mechanisms underlying heterogenic reflexes among the triceps surae muscles of the cat. *J Neurophysiol* 81: 467-478, 1999.

Nichols TR, and Cope TC. The organization of distributed proprioceptive feedback in the chronic spinal cat. In: *Motor neurobiology of the spinal cord*, edited by Cope TC2001, p. 305-326.

Nichols TR, Cope TC, and Abelew TA. Rapid spinal mechanisms of motor coordination. *Exerc Sport Sci Rev* 27: 255-284, 1999.

Nichols TR, and Houk JC. Improvement in linearity and regulation of stiffness that results from actions of stretch reflex. *J Neurophysiol* 39: 119-142, 1976.

Nozaki D, Nakazawa K, and Akai M. Muscle activity determined by cosine tuning with a nontrivial preferred direction during isometric force exertion by lower limb. *J Neurophysiol* 93: 2614-2624, 2005.

Pearson KG. Proprioceptive regulation of locomotion. *Curr Opin Neurobiol* 5: 786-791, 1995.

Poppele R, and Bosco G. Sophisticated spinal contributions to motor control. *Trends Neurosci* 26: 269-276, 2003.

Poppele RE, Rankin A, and Eian J. Dorsal spinocerebellar tract neurons respond to contralateral limb stepping. *Exp Brain Res* 149: 361-370, 2003.

Potluri S, Himes TB, Hyun J, Tessler A, and Son YJ. Selective vulnerability of neuromuscular junctions in ankle flexors to the paralysis elicited by spinal cord injury. In: *Society for Neuroscience*. Washington D.C.: 2008.

Pratt CA. Evidence of positive force feedback among hindlimb extensors in the intact standing cat. *J Neurophysiol* 73: 2578-2583, 1995.

Pratt CA, Fung J, and Macpherson JM. Stance control in the chronic spinal cat. *J Neurophysiol* 71: 1981-1985, 1994.

Roll R, Kavounoudias A, and Roll JP. Cutaneous afferents from human plantar sole contribute to body posture awareness. *Neuroreport* 13: 1957-1961, 2002.

Ross KT. Quantitative Analysis of Feedback During Locomotion. In: *Department of Biomedical Engineering*. Atlanta, GA: Georgia Institute of Technology/ Emory University, 2006.

Schieppati M, and Nardone A. Time course of 'set'-related changes in muscle responses to stance perturbation in humans. *J Physiol* 487 (Pt 3): 787-796, 1995.

Sherrington CS. Decerebrate rigidity and reflex co-ordination of movements. *J Physiology* 22: 319-332, 1898.

Shik ML, Orlovskii GN, and Severin FV. [Locomotion of the mesencephalic cat evoked by pyramidal stimulation]. *Biofizika* 13: 127-135, 1968.

Stal F, Fransson PA, Magnusson M, and Karlberg M. Effects of hypothermic anesthesia of the feet on vibration-induced body sway and adaptation. *J Vestib Res* 13: 39-52, 2003.

Stapley PJ, Ting LH, Hulliger M, and Macpherson JM. Automatic postural responses are delayed by pyridoxine-induced somatosensory loss. *J Neurosci* 22: 5803-5807, 2002.

Stein PS. Motor pattern deletions and modular organization of turtle spinal cord. *Brain Res Rev* 57: 118-124, 2008.

Stein PS, and Daniels-McQueen S. Variations in motor patterns during fictive rostral scratching in the turtle: knee-related deletions. *J Neurophysiol* 91: 2380-2384, 2004.

Stein RB, Aoyagi Y, Weber DJ, Shoham S, and Normann RA. Encoding mechanisms for sensory neurons studied with a multielectrode array in the cat dorsal root ganglion. *Can J Physiol Pharmacol* 82: 757-768, 2004a.

Stein RB, Weber DJ, Aoyagi Y, Prochazka A, Wagenaar JB, Shoham S, and Normann RA. Coding of position by simultaneously recorded sensory neurones in the cat dorsal root ganglion. *J Physiol* 560: 883-896, 2004b.

Taube W, Schubert M, Gruber M, Beck S, Faist M, and Gollhofer A. Direct corticospinal pathways contribute to neuromuscular control of perturbed stance. *J Appl Physiol* 101: 420-429, 2006.

Thomson DB, Inglis JT, Schor RH, and Macpherson JM. Bilateral labyrinthectomy in the cat: motor behaviour and quiet stance parameters. *Exp Brain Res* 85: 364-372, 1991.

Timoszyk WK, De Leon RD, London N, Roy RR, Edgerton VR, and Reinkensmeyer DJ. The rat lumbosacral spinal cord adapts to robotic loading applied during stance. *J Neurophysiol* 88: 3108-3117, 2002.

Ting LH, and Macpherson JM. A limited set of muscle synergies for force control during a postural task. *J Neurophysiol* 93: 609-613, 2005.

Ting LH, and Macpherson JM. Ratio of shear to load ground-reaction force may underlie the directional tuning of the automatic postural response to rotation and translation. *J Neurophysiol* 92: 808-823, 2004.

Torres-Oviedo G, Macpherson JM, and Ting LH. Muscle synergy organization is robust across a variety of postural perturbations. *J Neurophysiol* 96: 1530-1546, 2006.

Wilmink RJ, and Nichols TR. Distribution of heterogenic reflexes among the quadriceps and triceps surae muscles of the cat hind limb. *J Neurophysiol* 90: 2310-2324, 2003.

Wilson VJ, Ezure K, and Timerick SJ. Tonic neck reflex of the decerebrate cat: response of spinal interneurons to natural stimulation of neck and vestibular receptors. *J Neurophysiol* 51: 567-577, 1984.

Wilson VJ, Schor RH, Suzuki I, and Park BR. Spatial organization of neck and vestibular reflexes acting on the forelimbs of the decerebrate cat. *J Neurophysiol* 55: 514-526, 1986.

Zehr EP, and Stein RB. What functions do reflexes serve during human locomotion? *Prog Neurobiol* 58: 185-205, 1999.